C 10

THE GEOLOGY AND VOLCANIC HISTORY OF THE BIG SOUTHERN BUTTE - EAST BUTTE AREA, EASTERN SNAKE RIVER PLAIN, IDAHO

by

DALLAS B. SPEAR

A dissertation submitted to the
faculty of the Graduate School of the State
University of New York at Buffalo in partial
fulfillment of the requirements for the degree of
Doctor of Philosophy

September, 1979

ABSTRACT

Three prominent buttes rise above the relatively flat accumulations of Quaternary basalt flows of the eastern Snake River Plain between Arco and the Idaho Falls-Blackfoot area. These are Big Southern Butte, Middle Butte, and East Butte in their order from southwest to northeast. Big Southern Butte and East Butte are rhyolitic domes and Middle Butte is an elevated block of basalt flows. Approximately 775 km^2 of volcanic terrain around and including the buttes was mapped in order to document the geology and to investigate the origin and localization of these features.

Big Southern Butte is the largest of the three buttes. It rises 760 m above the Plain and has a diameter of 6.5 km at its base; there is a slight NW-SE elongation. It is a 300,000 year old volcanic dome complex consisting of two coalesced cumulo domes and an elevated section of older basalt flows approximately 350 m thick. The basalt section covers most of the northern slope of the butte. The complex began its development as a laccolithic intrusion but because of its shallow emplacement broke through to the surface and continued its evolution by endogenous growth. The rhyolite is aphyric and chemically is mildly peralkaline. It originated by fractional crystallization of a silicic parent at depths in the range of 10 to 16 km.

East Butte is a 600,000 year old rhyolite dome located 28 km northeast of Big Southern Butte. It is 360 m high and has a diameter of 2.4 km. It is interpreted as a single cumulo dome which developed by endogenous growth. The rhyolite is porphyritic with phenocrysts of sanidine, quartz, and minor clinopyroxene. Within the rhyolite are

numerous reddish-brown inclusions. They have a phenocryst assemblage of plagioclase, sanidine, olivine, clinopyroxene, magnetite, and quartz rimmed with augite. The inclusions are interpreted to be hybrid in origin and resulted from the mechanical mixing of East Butte rhyolite magma and an evolved tholeiite magma. Major element mixing diagrams support the interpretation.

Middle Butte is an upraised block of basalt flows located 4 km west of East Butte. It has a diameter of 2 km and is 350 m high. The mechanism responsible for elevating the basalt is believed to be the intrusion of viscous silicic magma concealed beneath the butte.

Other features in the map area include a 1.42 m.y. old rhyolitic dome 1 km southwest of East Butte and a unique volcanic center, Cedar Butte, composed of a differentiated suite of evolved tholeiite lavas ranging from 54% SiO_2 to 67% SiO_2. This 400,000 year old volcano is located 7 km east of Big Southern Butte. Cedar Butte magma formed by fractional crystallization of olivine tholeiite magma emplaced at the base of the crust. A long crustal residence time is implied by its chemistry; the more evolved members of the suite are on mixing lines with rhyolites from the area.

Twenty-five olivine tholeiite basalt lava fields of varying areal extent have been delineated within the map area. The eruptive style of these flows characterizes basaltic plains volcanism, that is, extensive outpouring of very fluid lavas from low shield volcanoes. The dominant flow type is pahoehoe.

The volcanism of this part of the Snake River Plain is controlled by two major structural trends: one, NE-SW, paralleling the long axis of the Plain and the other, NW-SE, perpendicular to that. The NW-SE trend

reflects extension of Basin and Range structure onto the Plain and the axial trend reflects zones of weakness produced by the gentle arching of the Plain and/or a high thermal input concentrated along the axis at depth.

A model for the volcanic development within the map area is presented which incorporates the common occurrence of rhyolite and evolved tholeiite lavas with other data from the Sanke River Plain. The emplacement of hot basaltic magmas at the base of the crust and concentrated along the axis of the Plain raised the crustal geotherms sufficiently to induce partial melting of the overlying crustal rocks. The silica-rich melts thus produced collected to form large rhyolitic magma reservoirs which subsequently erupted as voluminous ash-flows. Basaltic magma trapped at the base of the crust differentiated to form evolved tholeiite magma and upon migration or emplacement to higher levels in the crust (in the range of 10 to 16 km depth) these magmas encountered residual silicic melts and/or induced additional melting of crustal rocks of granitic composition. Ultimately the rhyolite domes of the eastern Snake River Plain formed from these small magma chambers; their emplacement was concurrent with predominantly basaltic volcanism.

CONTENTS

	Page
Abstract	i
Contents	iv
Illustrations	vi
Plates	vi
Figures	vi
Tables	ix
Introduction	1
Purpose of study	1
Previous investigations	3
Methodology	4
Acknowledgements	5
Regional geologic framework	8
Big Southern Butte	13
Geology	15
Southeastern flow-layered dome	15
Northwestern massive rhyolite dome	25
Basalt section	27
Emplacement history of Big Southern Butte	34
Petrology	36
Petrography	36
Major element compositions	39
Origin of Big Southern Butte magma	41
East Butte	50
Geology	50

Page

East Butte - continued

Petrography 53

Rhyolite 56

Hybrid inclusions 56

Petrology 62

Origin of the hybrid inclusions 68

Middle Butte 70

Old rhyolite dome 73

Cedar Butte 76

Geology 76

Petrography 81

Petrology 86

Origin of Cedar Butte magma 93

Basaltic volcanism 95

Eruptive style 95

Lava flows 95

Volcanoes 98

Flow stratigraphy 102

Petrology 102

Petrography 102

Major element compositions 104

Structural control of volcanism 110

Volcanic history of the map area 114

Summary 120

References cited 123

Page

Appendix A. Precision and accuracy of chemical analyses 128

Appendix B. Location and description of samples from Big Southern Butte .....

Appendix C. Location and description of samples from Cedar Butte .....

Appendix D. Location and description of basalt samples chosen for chemical analysis .....

Appendix E. Trace element analyses for volcanic rocks within the study area .....

ILLUSTRATIONS

Plate 1. Geologic map of Big Southern Butte ..... in pocket

2. Geologic map of the East Butte - Middle Butte area ..... in pocket

3. Geologic map of the central eastern Snake River Plain from Big Southern Butte to East Butte .... in pocket

Figure 1. Sketch map of the eastern Snake River Plain showing location of study area 2

2. Geologic sketch map of southern Idaho 9

3. Photograph of Big Southern Butte 14

4. Aerial photograph of Big Southern Butte 14

5. Photograph of rhyolite flow layering 16

6. Generalized stratigraphic section of flow-layered dome 17

7. Photograph of autoclastic breccia 19

Page

Figure 8. Stratigraphic section of explosion breccia 20

9. Photograph of base of explosion breccia 21

10. Photograph of ash layer and lapilli 23

11. Photograph of rhyolite dike in flow-layered rhyolite 24

12. Photograph of erosion of sugary rhyolite 26

13. Photograph of northern slope of Big Southern Butte . 28

14. Photograph showing basalt layering on northern slope of Big Southern Butte 29

15. Photograph of contact breccia 30

16. Composite stratigraphic column of basalt section ... 32

17. Photograph of basaltic dikes at base of basalt section 33

18. Summary of the emplacement history of Big Southern Butte 37

19. Photomicrograph of flow-layered rhyolite 38

20. Photomicrograph of massive rhyolite 38

21. Rare earth element plot of Snake River Plain volcanic rocks 45

22. Plot of normative quartz, albite, and orthoclase for Big Southern Butte rhyolite 47

23. Melting of granite and geothermal gradients in the Snake River Plain 49

24. Photograph of East Butte 51

25. Aerial photograph of East Butte 51

26. Photograph of platy layering in rhyolite of East Butte 52

27. Photograph of concentric flow planes 54

28. Reyer's experimentally produced flow planes 55

29. Photomicrographs of East Butte rhyolite 57

Page

Figure 30. Photomicrograph of micropegmatitic intergrowths 58

31. Photomicrograph of hybrid inclusion showing quartz rimmed with augite 60

32. Photograph of globular inclusion 61

33. Comparison of East Butte rhyolite with Big Southern Butte rhyolite 64

34. Rare earth element plot of East Butte rhyolite, hybrid inclusion, and basalt 66

35. Mixing diagram for East Butte rhyolite and inclusions 67

36. Model for the origin of hybrid inclusions 69

37. Photograph of Middle Butte 71

38. Aerial photograph of Middle Butte 71

39. Photograph of old rhyolite dome 73

40. Photomicrograph of old dome rhyolite 74

41. Geologic sketch map of Cedar Butte 77

42. Aerial photograph of Cedar Butte 78

43. Photograph of dike at Cedar Butte 80

44. Photograph of dike rock - rhyolite contact 80

45. Phenocryst assemblages of Cedar Butte lavas 83

46. Photomicrographs of Cedar Butte lavas 84, 85

47. Variation diagram for Cedar Butte lavas 88

48. AFM diagram for Cedar Butte lavas 89

49. Rare earth element plot for Cedar Butte lavas 92

50. Diagram illustrating the hypothetical development of the Snake River Plain 96

51. Photograph of ropy pahoehoe lava 97

Page

Figure 52. Photograph of collapse depressions 99

53. Photograph of pressure ridge 99

54. Aerial photograph of South Robbers Flow 100

55. Topographic profiles of volcanoes 101

56. AFM diagram for basalts in the study area 108

57. Olivine - plagioclase control diagram 109

58. Map of the area showing dominant structural trends . 111

59. Rift zones of the central eastern Snake River Plain as identified by Kuntz 112

60. Summary of the volcanic development of the Snake River Plain within the map area 116-119

TABLES

Page

Table 1. Radiometric age data for Big Southern Butte 15

2. Major element analyses and CIPW norms for Big Southern Butte samples 40

3. Rare earth element contents of samples from Big Big Southern Butte 43

4. Major element analyses and CIPW norms for East Butte samples 63

5. Major element analyses and CIPW norms for Middle Butte samples 72

6. Comparison of major element compositions of East Butte and rhyolite of old dome 75

7. Major element analyses and CIPW norms for Cedar Butte samples 87

8. Fractionation calculations for Cedar Butte 90

Page

Table 9. Rare earth element contents of samples from Cedar Butte 91

10. Criteria used to establish relative stratigraphy ... 103

11. Summary of the mineralogy of Snake River Plain olivine tholeiite lavas 105

12. Major element analyses and CIPW norms for basalts in study area 106

INTRODUCTION

Volcanism of the eastern Snake River Plain, Idaho is dominated by extensive Pleistocene-Holocene basalt lava flows originating from numerous low shield volcanoes. The resulting physiographic province is a lava plain of low relief. Between Arco and the Idaho Falls-Blackfoot area three prominent buttes are exceptions to this generalization. These conspicuous landmarks are known as Big Southern Butte, Middle Butte, and East Butte respectively from southwest to northeast (Fig. 1).

Big Southern Butte, the largest of the three buttes, rises 760 m above the lava plain and has a diameter at its base of 6.5 km. Middle Butte is located 24 km east-northeast of Big Southern Butte; it is 350 m high and has a diameter of 2 km. East Butte, 4 km east of Middle Butte, rises 360 m above the surrounding basalt flows and has a diameter of 2.4 km at its base. Big Southern Butte and East Butte are rhyolitic domes whereas Middle Butte is an upraised block of stratified basalt.

These unique features have provoked much speculation concerning their origin and relationship, both structurally and petrologically, to the basaltic volcanism of the Snake River Plain. However, up to now, no detailed investigations have been conducted on these features. Therefore, a study was undertaken to map and describe the geology of Big Southern, Middle, and East Buttes and the surrounding area, and to evaluate hypotheses for the origin and localization of the buttes. The study area covers approximately 775 km^2 and includes ten 7 1/2 minute

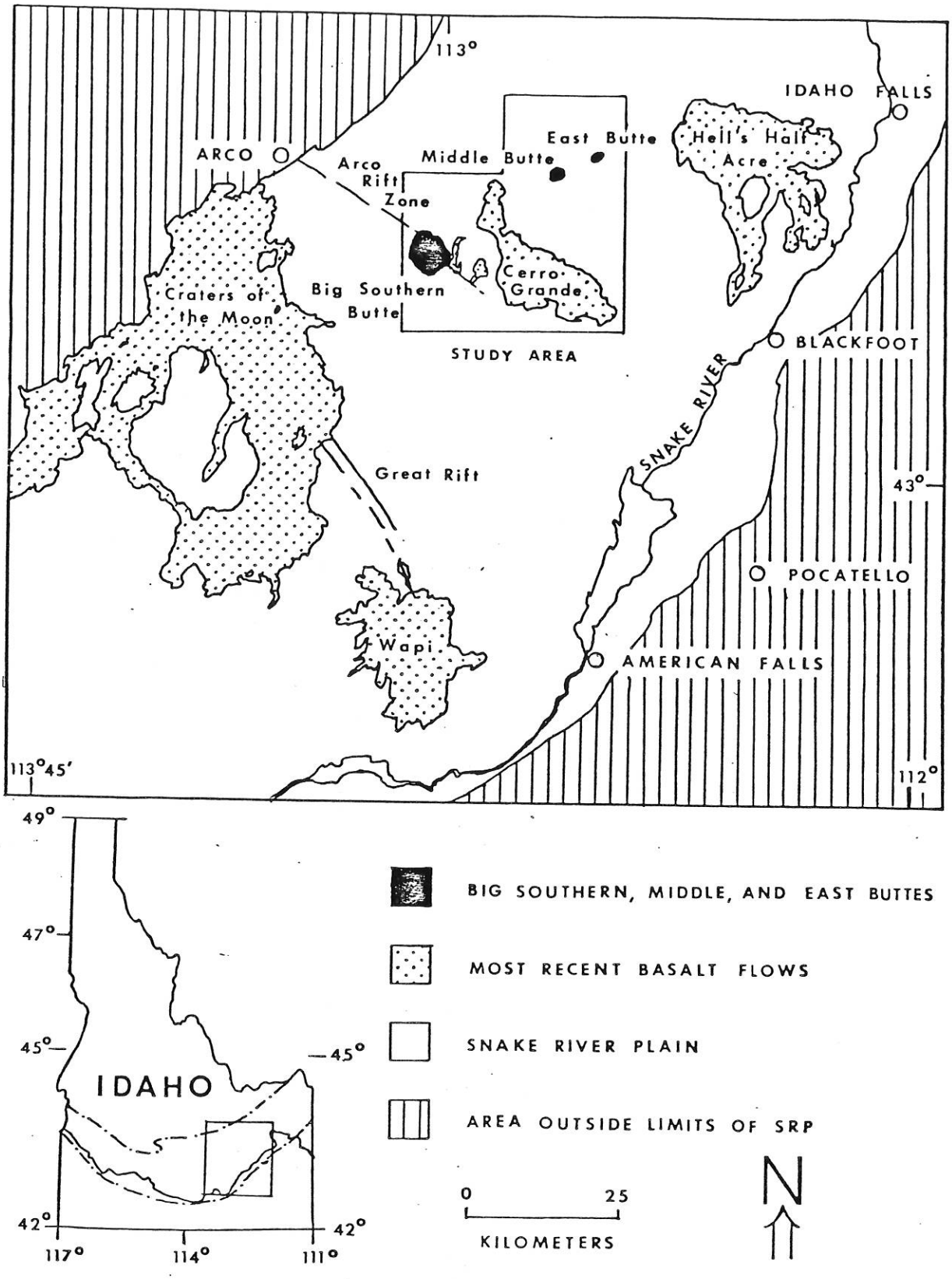


FIGURE 1. Central eastern Snake River Plain showing location of study area.

topographic quadrangles. Within the study area rock types are dominated by basalt but include rhyolite and an intermediate differentiated suite of evolved tholeiite lavas.

Previous Investigations

Russell (1902) was the first geologist to visit the buttes and offer an interpretation of their origin. He proposed that Big Southern Butte and East Butte are steptoes - ancient rhyolitic volcanoes surrounded by a sea of basalt. He interpreted Middle Butte to be a fault block of older lavas but did not speculate to the process for its elevation.

Stearns and others (1938) suggested that the buttes are the result of differential erosion of a mountain range of acid and basic lavas. They also suggested that faulting may have been important in the development of East and Middle Buttes. Subsequent eruptions of basalt left the buttes as steptoes.

Hamilton (1965), in a report of the geology of the Island Park Caldera, was the first to acknowledge that Big Southern Butte and East Butte are rhyolitic domes.

Schoen (1974) interpreted the silicic buttes to be relatively young rocks emplaced as viscous plugs and domes. His interpretation was based on evidence from well logs, gravity and resistivity studies, and K-Ar dates. He speculated that the source of the rhyolitic magmas was remobilized rhyolitic basement which underlies the basalt.

Armstrong and others (1975) report K-Ar dates of 0.30 ± 0.02 m.y. and 0.60 ± 0.01 m.y. for Big Southern and East Buttes respectively.

They attempted to date the basalt of Middle Butte but, because of contamination by atmospheric argon, report that it was not precisely dated; they give the date for Middle Butte as 1.9 ± 1.2 m.y. Both Schoen (1974) and Armstrong and others (1975) suspect that the basalt of Middle Butte was pushed up by a younger still concealed rhyolitic dome.

The basalt flows in most of the area around the buttes have not been studied in detail. LaPoint (1977) published a reconnaissance photogeologic map of the entire eastern Snake River Plain at a scale of 1:250,000 which shows some subdivision of flows within the study area. Kuntz (1978a,b) published a report on the Arco-Big Southern Butte area and an open-file map at a scale of 1:48,000 which included the area around Big Southern Butte.

Methodology

This study is based on field work conducted during parts of the summers of 1976, 1977, and 1978. Reconnaissance photogeologic mapping of the area was done on aerial photographs at scales of 1:60,000, 1:30,000, and 1:20,000 prior to field work. Data was transferred to 1:24,000 topographic quadrangle maps primarily by inspection and with the aid of a Saltzman projector and a radial planimetric plotter. Individual maps were field checked for accuracy and improved where necessary. Sample locations were plotted on the field maps and that information was used for verification of contacts, descriptions of the flows, and comparison between flows after petrographic data was available. All pertinent information was transferred to a mylar topo-

graphic base at a scale of 1:48,000 for final compilation.

Big Southern Butte and East Butte were mapped in detail on topographic bases at scales of 1:8,000 and 1:7,200 respectively. Final compilation is at 1:12,000.

Petrographic descriptions and interpretations are based on the study of approximately 200 thin sections of samples collected within the study area and supplemented by inspection of several hundred others from flows located outside the area. Plagioclase and olivine compositions were determined with the 4-axis universal stage. Slemmons' (1962) curves were used for the plagioclase determinations and 2V measurements of olivines were compared with the curves of Poldervaart (1950) to estimate the percent Fo.

Major element analyses were obtained by the rapid methods of Shapiro (1975) or by XRF using the method of Norrish and Hutton (1969). For samples analyzed by XRF, Na_2O and MgO were determined by atomic absorption and P_2O_5 by spectrophotometer. Precision and accuracy of the methods, determined by replicate analyses of a known sample, are reported in Appendix A. Unless noted otherwise analyses are by the author.

Acknowledgements

I would like to acknowledge and sincerely thank the many individuals, faculty, and fellow students who have contributed to this project and who have been a part of my development as a student and individual over the past few years.

In particular, I want to thank John S. King, my major advisor,

whose council and support made this investigation a reality. John C. Fountain provided invaluable help in the acquisition and interpretation of geochemical data; his discussions of geologic problems have been both informative and enjoyable. Charles V. Clemency served as a member of the doctoral committee; his help during the course of this study and in reviewing this dissertation are appreciated. Mel A. Kuntz of the U.S. Geological Survey first showed me around Big Southern Butte, supplied base maps for my use and shared much information on the area. His critical review of this dissertation as the outside reader provided the basis for improvement and clarification of many points; his efforts are greatly appreciated.

Steven S. Oriel of the U.S. Geological Survey first suggested this project and supplied topographic maps and loaned aerial photos to help me get started. Jack Barraclough, also of the U.S. Geological Survey, assisted in obtaining clearance to work on the restricted areas of the Idaho National Engineering Laboratory and in supplying subsurface geologic information.

Adrian Spear assisted in the field in 1976 and 1978; Peter Carr helped during 1977. Their assistance substantially reduced the amount of time I would have otherwise been required to spend. I thank them both for their help and company. Thanks to Dave Borden for his time and expert help with the analytical procedures for wet chemical analysis.

Financial support for most of this project was covered by National Aeronautics and Space Adminstration Planetology Office Grant NGR 33-014-108 awarded to John S. King. The U.S. Geological Survey provided topographic maps, mylar base maps, and loaned some of the photos used.

A grant from the State University of New York at Buffalo Graduate Student Association defrayed the cost of some drafting and photographic supplies.

REGIONAL GEOLOGIC FRAMEWORK

The Snake River Plain is an enigmatic volcano-tectonic feature in the western United States. It extends across southern Idaho as a 65 to 100 km wide arcuate depression from Yellowstone National Park in the east to the Idaho-Oregon border in the west (Fig. 2). The Plain is characterized by low relief. Elevations decrease from 1600 m in the east to 800 m in the west; this contrasts with elevations in excess of 3800 m in the bordering ranges. Most of the Plain is covered by basalt and interbedded fluvial, lacustrine, and aeolian sediments.

Thw Snake River Plain began to develop as an active tectonic and volcanic province during the Miocene with rapid subsidence and volcanism within a depression which formed during the Oligocene; this activity was concurrent with the uplifting of bordering ranges (Axelrod, 1968). The associated volcanism began with the eruption of voluminous ash-flows which were subsequently covered by basalt flows.

Malde and Powers (1962) developed a stratigraphy for the western part of the Plain and divided the rocks into three principal groups: the upper Miocene to middle Pliocene Idavada Group, consisting predominantly of rhyolitc ash-flows with minor basalt; the upper Pliocene to middle Pleistocene Idaho Gruop, composed of olivine tholeiite basalt flows intercalated with continental sediments; and the Snake River Group, also olivine tholeiite basalt flows and minor intercalated sediments. Armstrong and others (1975) established a K-Ar chronology for these groups and documented a systematic eastward shift with time in the rhyolitic volcanic centers. Ages of the rhyolites vary from 9 to 13 m.y. in western Idaho, 8 to 10 m.y. in central Idaho, and 4 to 5 m.y.

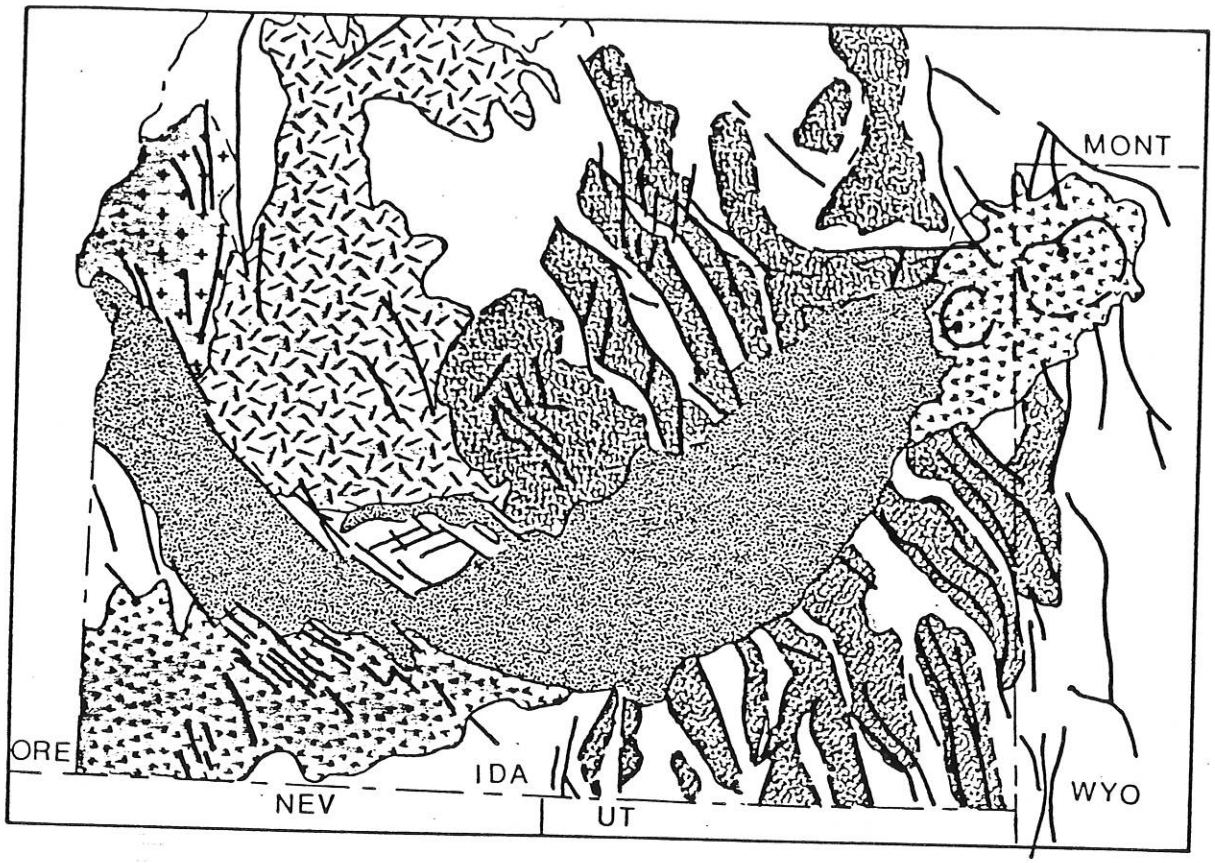


FIGURE 2. Geologic sketch map of southern Idaho.

in eastern Idaho. K-Ar dates from ash-flows of the Yellowstone National Park-Island Park area range from 2.6 to 0.56 m.y. (Eaton and others, 1975).

Although the Sanke River Plain is a continouos physiographic feature, there are fundamental differences in the structural and geophysical characteristics of its western and eastern parts which join at approximately 115° longitude. The western Snake River Plain (WSRP) is a northwest-trending graben averaging 65 km in width. Its northeastern boundary is defined by Cretaceous plutonic rocks of the Idaho batholith in contact along faults with Plio-Pleistocene basalts and sediments of the Plain. Malde (1959) estimated a total displacement of at least 2750 m on the northwest-trending normal faults. The southern and southwestern boundary is more complex with both faulting and downwarping (McIntyre, 1972). However, numerous en echelon faults parallel to the trend of the WSRP shown on the map of Malde and others (1963) suggest that faulting has had the dominant role.

The eastern Snake River Plain (ESRP) trends northeastward and is somewhat wider than the WSRP, averaging approximately 100 km. It is generally described as a downwarp, an interpretation suggested by Kirkham (1931). He noted the plainsward dip of Tertiary volcanic and lacustrine rocks and an increase in the amount of dip with age of those rocks as supporting evidence. North and south of the ESRP are mountain ranges of Paleozoic and Mesozoic miogeosynclinal rocks deformed during Basin and Range tectonism. Although bounding faults have not been identified, the abrupt termination of these ranges at the margin of the Plain implies that faulting has contributed to the development of the ESRP.

Mabey (1976) showed that the WSRP has relatively simple gravity and magnetic anomalies, with a large elongate positive Bouguer anomaly situated along its axis. The overall magnetic anomaly is the highest along the southwestern edge of the Plain and lowest along the northeastern margin. Based on studies by Hill (1963), Hill and Pakiser (1967), and Mabey and others (1974), Mabey (1976) proposed a crustal model to account for the measured anomalies in which there is a very thin or completely rifted upper crust with a large volume of dense magnetic rock high in the crust.

The ESRP is an area of more complex gravity and magnetic anomalies consisting of alternating highs and lows reflecting differences in the thickness of Cenozoic rocks (Mabey, 1978). Mabey also noted that the amplitude of the regional Bouguer gravity high is about half that of the WSRP and could be produced by a thinning of the crust under the ESRP by 4.5 to 7 km.

The basaltic rocks of the Snake River Plain have been studied by Powers (1960), Stone (1967), Tilley and Thompson (1970), Thompson (1972), Leeman (1974), Leeman and Vitaliano (1976), Leeman and others (1976), Stout (1975), and Stout and Nicholls (1977). They have shown that the mafic lavas can be broadly grouped into two suites, the voluminous olivine tholeiites of limited compositional range and the evolved tholeiits which form differentiated suites. The evolved tholeiites occur in only a few localities and range in composition from andesine-normative ferrobasalts to ferrolatites; they have been designated Craters of the Moon-type lavas by Leeman (1974) because of their widespread occurrence at Craters of the Moon National Monument.

The compositional variation within the olivine tholeiites is minor

and, for the most part, can be accounted for by low-pressure fractionation of olivine and plagioclase, which are the phenocryst phases. However, some compositional differences may be related to variations in the degree of partial melting of the source rocks (Leeman, 1974). The evolved tholeiites are distinctive both for their high iron enrichment and high alkali content. Experimental work by Tilley and Thompson (1970) demonstrated that these features are due to fractionation of apatite, magnetite, olivine, plagioclase, and in the latter stages, clinopyroxene. Anomalous Sr and Pb isotopic compositions suggest that the evolved tholeiites have experienced some crustal contamination (Leeman and others, 1976).

BIG SOUTHERN BUTTE

Big Southern Butte is the most prominent feature of the eastern Snake River Plain. Rising to an elevation of 2304 m, 760 m above its base, its rugged outline contrasts dramatically with the relatively flat accumulation of basalt flows which comprise most of the surrounding terrain (Fig. 3). Big Southern Butte has an average diameter of 6.5 km at its base with a slight northwest-southeast elongation (Fig. 4).

The slopes of Big Southern Butte are steep, commonly greater than 30^{o}, and are dissected by ravines and canyons which contribute debris to the broad apron of talus surrounding the butte. On the northwest side there is a deep canyon which allows access up the butte and from which extends a broad alluvial fan.

Detailed mapping at a scale of 1:12,000 has revealed that Big Southern Butte is a volcanic dome complex consisting of two coalesced cumulo domes and a 350 m thick section of older basalt flows uplifted and tilted during the development of the domes (Plate 1). The basalt section covers most of the northern slope of the butte.

The contact between the two domes is not sharp and their division is based on overall morphology and minor, but characteristic, differences in respective lithologies. Unconformable relationships of the two rock types in a roadcut near the top of Big Southern Butte allows relative ages to be established. The two domes are aligned along a N 45^{o} W trend causing the slight elongation of the entire complex in that orientation. The southeastern dome was the first to develop. Although relative ages are inferred, evidence discussed in the following sections suggests that the evolution of the complex was more or

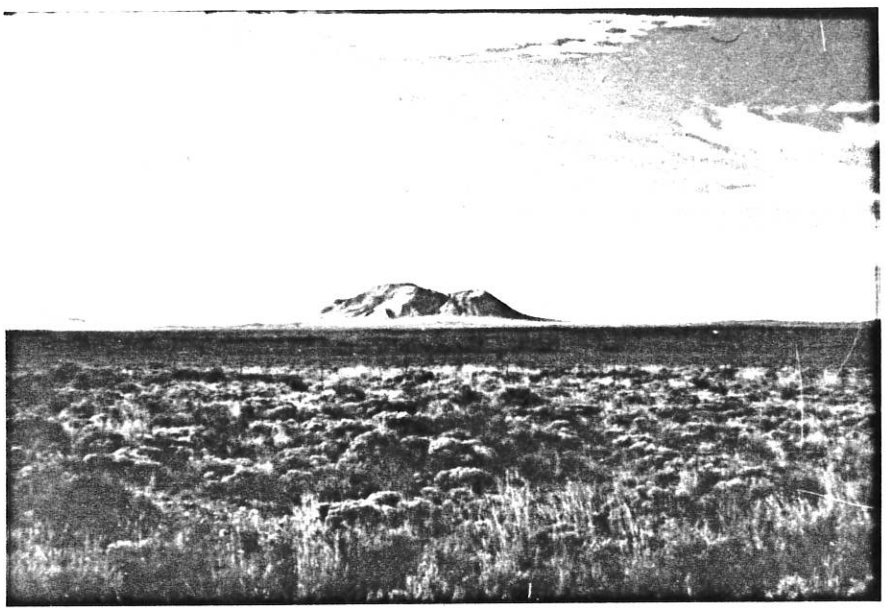


FIGURE 3. Big Southern Butte, 30 km in the distance, rises 760 m above the eastern Snake River Plain between Arco and the Idaho Falls-Blackfoot area in southern Idaho.

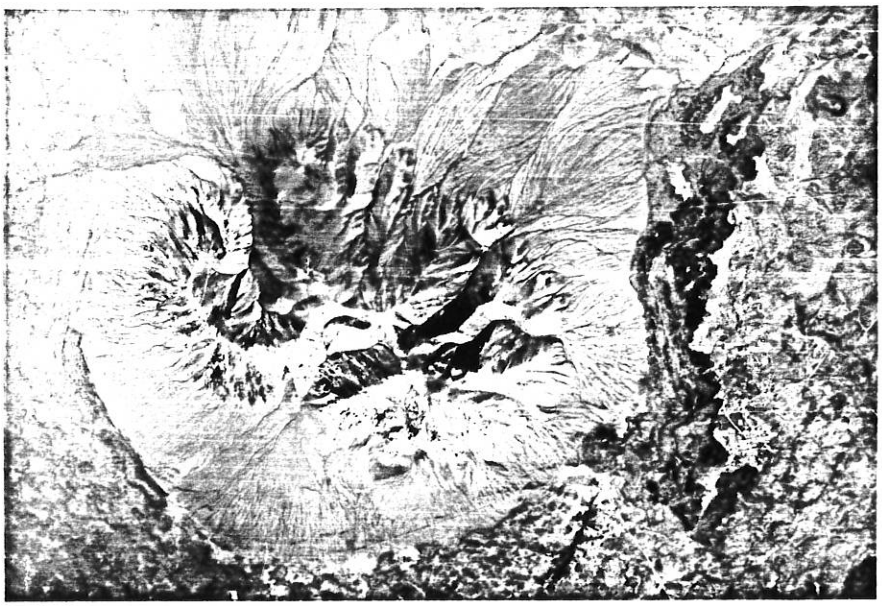


FIGURE 4. Aerial view of Big Southern Butte volcanic dome complex. North is at top of photo and the east-west diameter of Big Southern Butte is approximately 6.5 km.

less a continuous process. Based on the available age data (Table 1), Big Southern Butte developed approximately 300,000 years ago.

SAMPLE	LOCATION	AGE	METHOD	REFERENCE
Obsidian	SW1/4 NW1/4 Sec. 23, T.1N., R.29E.	0.26 ± 0.05 m.y.	Fission-Track	Glenn Izett, in Kuntz, 1978
Obsidian	SW1/4 NW1/4 Sec. 23, T.1N., R.29E.	0.312 ± 0.011 m.y.	K-Ar whole rock	G.B. Dalrymple, in Kuntz, 1978
Rhyolite	NW1/4 SE1/4 Sec. 22, T.1N., R.29E.	0.296 ± 0.015 m.y.	K-Ar whole rock	G.B. Dalrymple, in Kuntz, 1978
Rhyolite	exact location unknown	0.30 ± 0.020 m.y.	K-Ar whole rock	Armstrong and others, 1975

TABLE 1. Radiometric age data for Big Southern Butte, Idaho.

Geology

Southeastern Flow-layered Dome. The first dome to develop at Big Southern Butte is characterized by lavender-gray, flow-layered rhyolite. The rock is aphyric and contains abundant spherulites. Flow-layering is on the order of a few centimeters or less and attitudes of the layering are generally tangential to the flanks of the dome (Fig. 5). The flow-layered rhyolite grades into a white sugary rhyolite in upper parts of the generalized stratigraphic section (Fig. 6). The transition can be observed particularly well in the deep canyons on the southern slope. Although the sugary rhyolite is more susceptible to



FIGURE 5. Flow layering in rhyolite at Big Southern Butte. Flow was from upper left to lower right. Hammer for scale is 33 cm long.

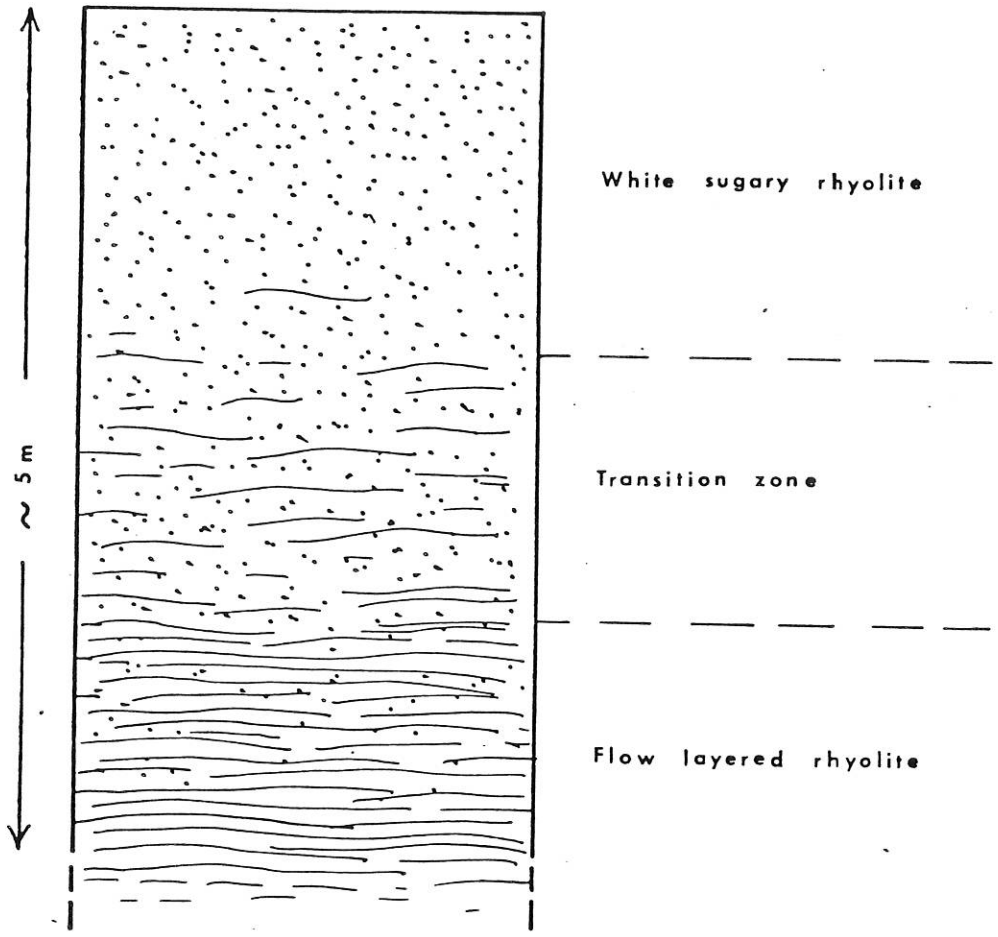


FIGURE 6. Generalized stratigraphic section of flow-layered dome (as seen on the southern slope) illustrating the transition from flow-layered rhyolite to sugary rhyolite.



FIGURE 14. Northern slope of Big Southern Butte; view to the northwest. Note the steeply dipping (~45° to the NE) layers of basalt.

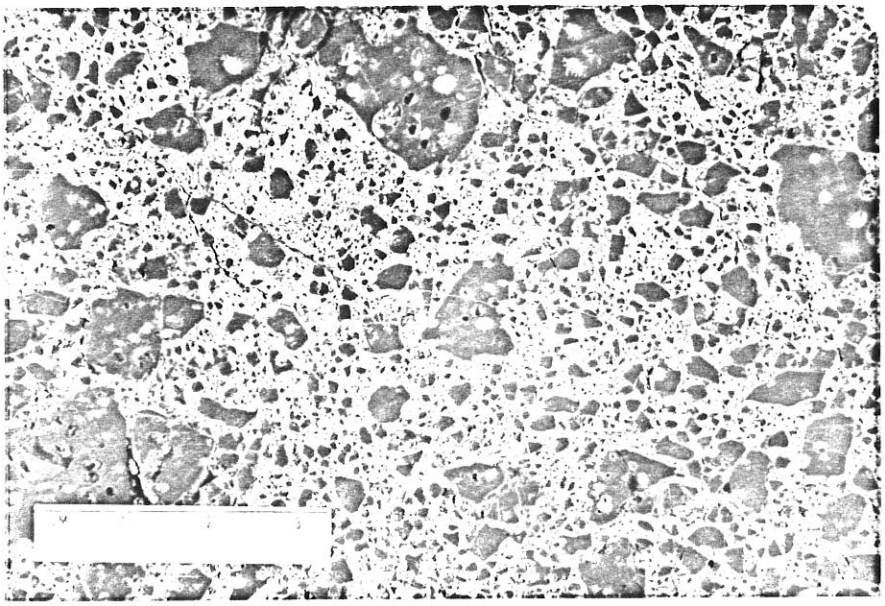


FIGURE 15. Example of contact breccia found in a narrow zone at the basalt-rhyolite contact. Light-colored groundmass is rhyolite and dark fragments are from the basaltic lavas.

The section of older lavas is composed of 15 to 20 flows which dip an average of 45° to the northeast. A generalized composite stratigraphic column is shown in Figure 16. The oldest part of the section is exposed in the deep canyon on the northwestern side of Big Southern Butte. The oldest, lowermost rocks have been extensively altered and cut by small basaltic dikes, which are also altered (Fig. 17). At least some, if not all, of the alteration is believed to be a direct result of the action of hydrothermal fluids which accompanied the intrusion of the rhyolite. This interpretation is supported by the occurrence of rocks higher in the stratigraphic section which are altered near the basalt-rhyolite contact but are unaltered some distance away from it.

One of the significant features of the basalt section is a sequence of evolved tholeiite lava intercalated between the typical Snake River Plain olivine tholeiite flows. It occurs near the base of the section and forms a prominent ridge extending up the eastern slope of the canyon. Features in outcrop such as welded spatter and a glassy layer suggest that the source vent for this flow(s) may have been close by. Cedar Butte, a large volcanic shield composed of a differentiated suite of evolved tholeiite lavas, is located 7 km to the east of Big Southern Butte. Lavas erupted from Cedar Butte, however, are believed to be much younger than the evolved tholeiite sequence. As shown in Figure 16 a ferrolatite flow from Cedar Butte caps the entire basalt section and at least ten olivine tholeiite flows separate it from the evolved tholeiite sequence. Because evolved tholeiite lavas are not common throughout most of the Snake River Plain , their occurrence at

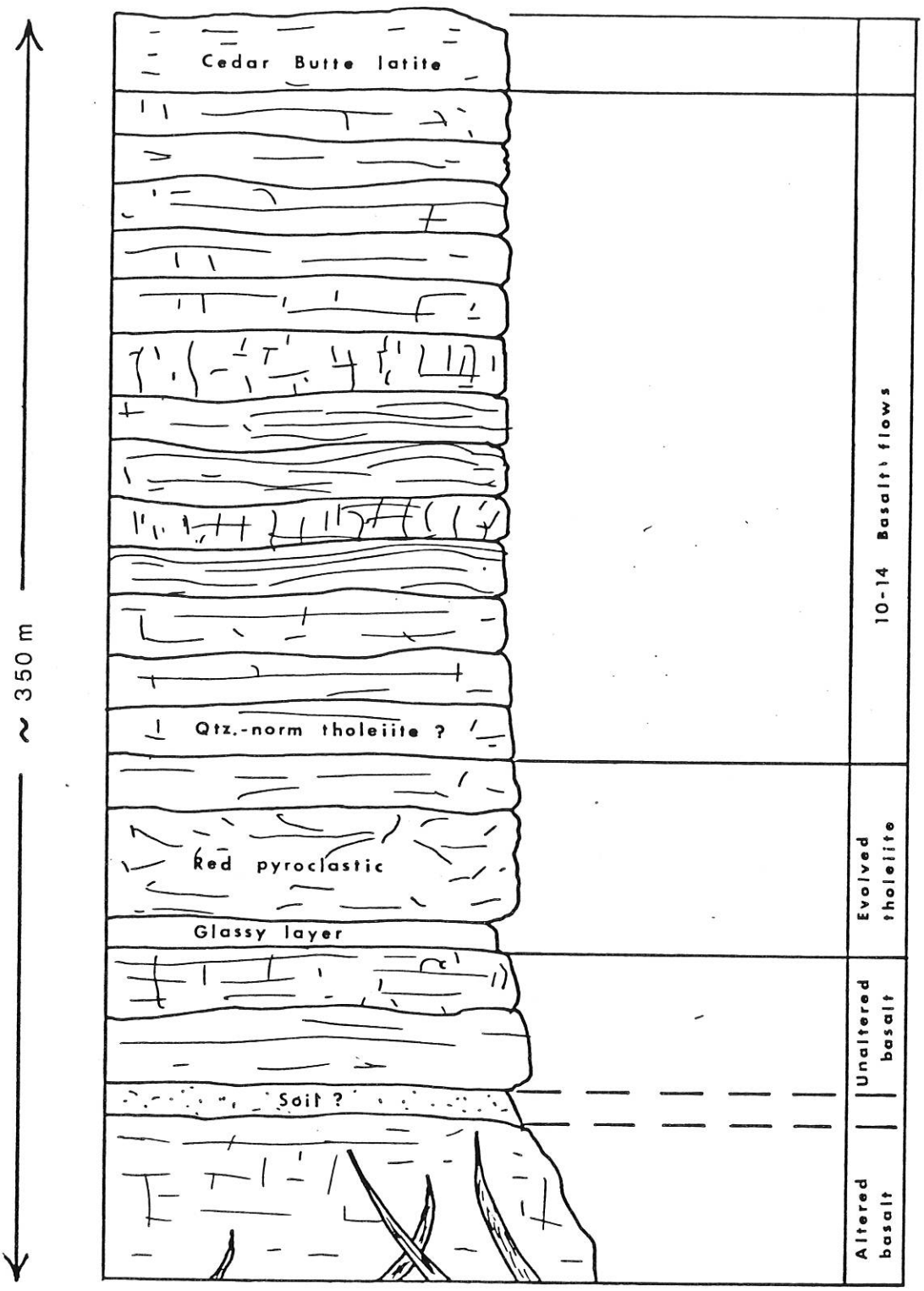


FIGURE 16. Diagrammatic composite stratigraphic section of older basalt flows on the northern slope of Big Southern Butte (not to scale).

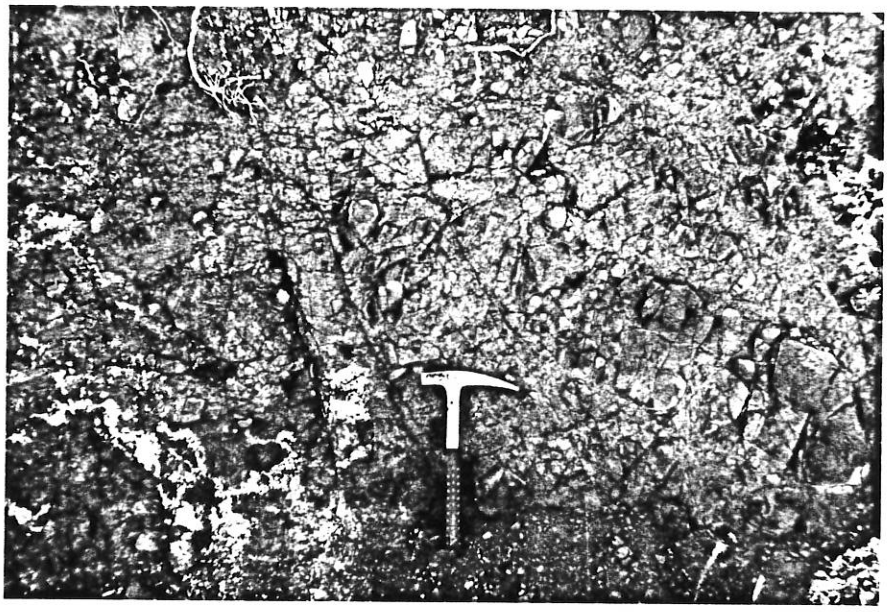


FIGURE 17. Basaltic dikes intruding basalt at base of the basalt section on Big Southern Butte. Hammer for scale is 33 cm long.

Big Southern Butte is intriguing; further discussion on this rock type is given in a subsequent section.

Hamilton (1965) stated that the upper 100 m of the basalt section at Big Southern Butte was interlayered basalt and rhyolite. No such interlayering was observed. There is, however, a small massive rhyolite dike within the basalt section near the top of Big Southern Butte; this may have been interpreted as interlayering.

The basalt section covering the northern slope does not extend completely to the base of Big Southern Butte. Near the base apophyses of rhyolite were extruded from beneath the basalt. The transition from basalt to rhyolite is marked by a distinct break in slope with the basalt section forming the steeper slope.

At the base of Big Southern Butte on the northern side are three large mounds (Plate 1). Their overall morphology is consistent with an interpretation that they represent an old basaltic volcano. However, the surface of the mounds is covered by basaltic rubble of several lithologies, not one predominant lithology as would be expected. In addition, there is a large outcrop of flow-layered rhyolite at the base of the mounds on their eastern side. In light of these observations another interpretation of these mounds can be offered: they are domal intrusions of rhyolite concealed beneath basaltic rubble.

Emplacement History of Big Southern Butte

A combination of two physical processes, intrusion and extrusion, acting contemporaneously contributed to the development of Big Southern Butte. The large tilted block of older lavas covering most of the

northern slope attests to the fact that Big Southern Butte began as a laccolithic-type intrusion. Throughout the latter part of its evolution, however, extrusion was the dominant process. This section will attempt to reconstruct the sequence of events for the emplacement of magma at Big Southern Butte.

Initially magma ascended along a fracture and intruded at a depth approximately equal to the thickness of the basalt section to form an elliptical sill-like intrusion. The depth of the intrusion is believed to be related to the total thickness of basalt overlying the pre-existing rhyolite topography at the time of intrusion. Stanley and others (1977) estimate that the total thickness of basalt in the area now is about one kilometer, therefore a thickness of 400 m 300,000 years ago might be reasonable.

After a period of lateral growth the intrusion began to dome the overlying basalt flows. This laccolithic stage continued until the yield strength of the overburden was exceeded. When this occurred it marked the transition from intrusive development to extrusive development.

During the early stages of extrusive growth the dome was mantled by blocky debris (crumble breccia) and a massive crust of white rhyolite. As the dome increased in size by endogenous growth, the crust was broken through, autoclastic breccias formed, and minor extrusions quickly chilled to form localized areas of obsidian. A violent vulcanian explosion formed the breccia and lapilli tuffs now exposed in the roadcut near the top of Big Southern Butte.

After these events the intrusive center shifted to the northwest and another endogenous dome began to grow. The cessation of the supply

of magma caused the top of the dome to sag slightly producing the basined depression. This ended the volcanic development of Big Southern Butte. Figure 18 summarizes the sequence of events.

Petrology

The rhyolite of Big Southern Butte is mineralogically and chemically homogeneous. The macroscopic characteristics, such as color variations and flow-layering, which were used for purposes of mapping are not related to any significant compositional variations. Approximately 70 samples of rhyolite collected from all areas of Big Southern Butte were studied by binocular microscope and from these 37 were chosen for thin sections and 10 were chosen for chemical analysis.

Petrography. In thin section the rhyolite appears as fine-grained intergrowths of microcrystalline quartz and alkali feldspar. Small (less than 1 mm) anhedral phenocrysts (?) of quartz are rare. Mafic minerals are also rare; magnetite is present as small equant grains and microphenocrysts of variably altered fayalite and a dark green, pleochroic clinopyroxene are very rare. Devitrification spherulites are common in the flow-layered variety (Fig. 19). The mineral aggregates of the spherulites cannot be identified by the microscope but Ross and Smith (1961) report that x-ray studies of samples of rhyolite glasses from many different localities in the world show that the devitrification products are always cristobalite and alkali feldspar. The massive rhyolite is holocrystalline and has a "snowflake" texture (Fig. 20) due to the slightly larger anhedral crystals of quartz distributed throughout the microcrystalline groundmass. A few, small irregular

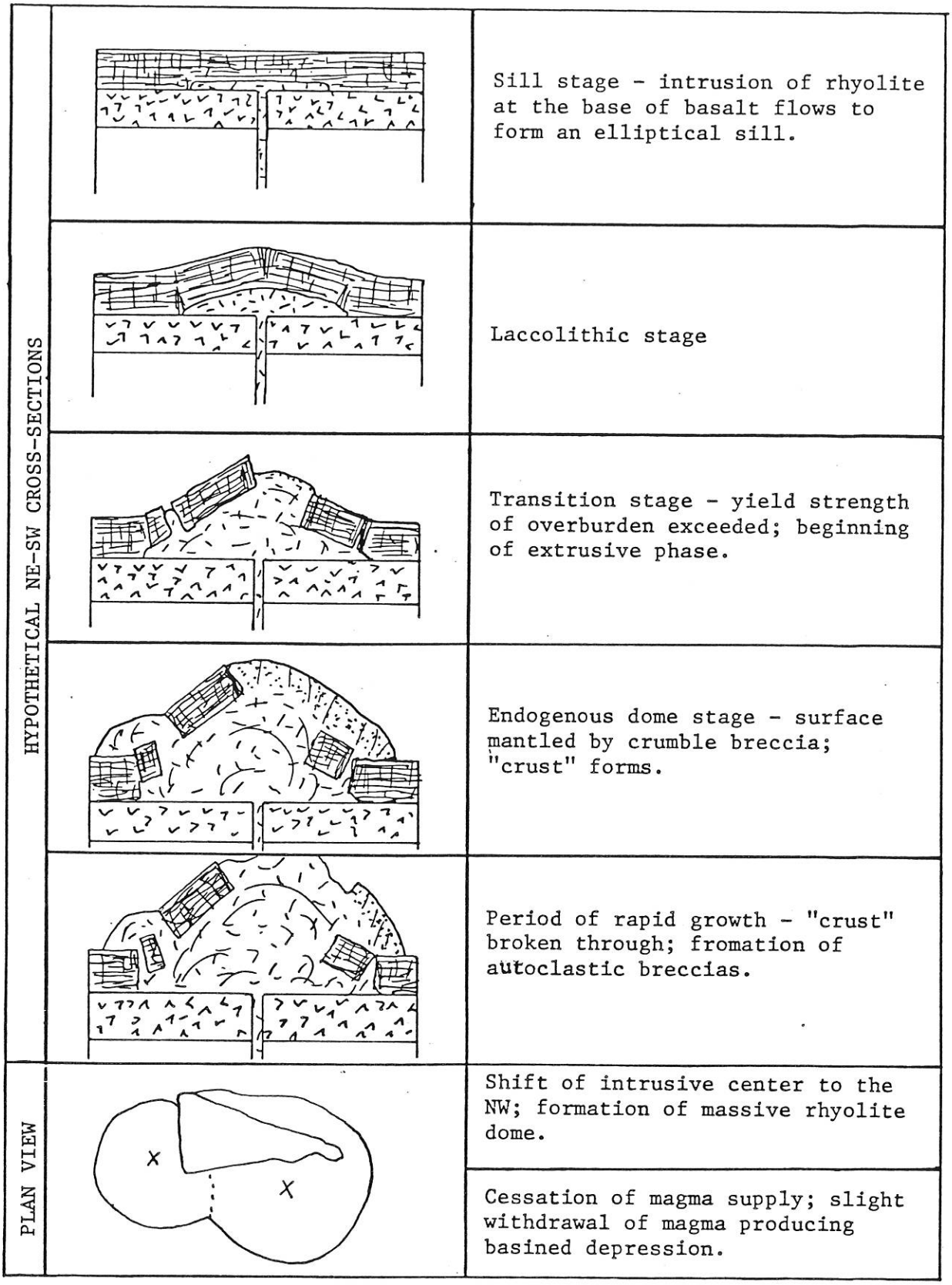


FIGURE 20. Summary of emplacement history of Big Southern Butte.

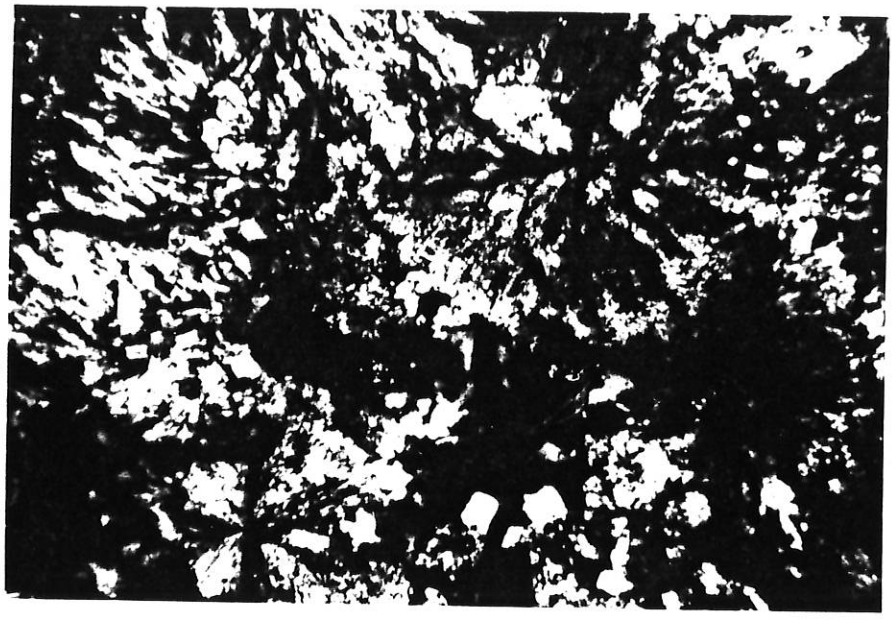


FIGURE 19. Photomicrograph of flow-layered rhyolite showing devitrification spherulites. Field of view is 2.50 mm by 1.62 mm.

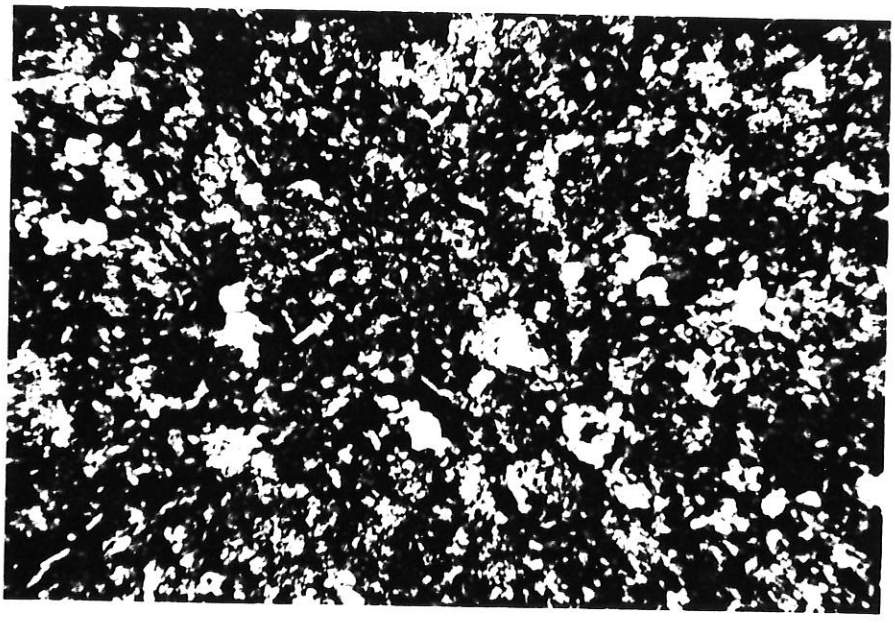


FIGURE 20. Photomicrograph of massive rhyolite showing "snowflake" texture due to slightly larger anhedral crystals of quartz. Field of view is 2.50 mm by 1.62 mm.

cavities were observed in some samples.

Major Element Compositions. Major element data and CIPW norms for 13 samples of rhyolite, 2 basaltic inclusions, and 4 mafic flows from Big Southern Butte are presented in Table 2. Sample locations and brief petrographic descriptions are reported in Appendix B. The rhyolite analyses (excluding BS-10) document the relative homogeneity throughout the dome complex. Chemically the rhyolite is mildly peralkaline (molecular excess of $Na_2O + K_2O$ over Al_2O_3) and is classified as comendite based on the criteria of Nicholls and Carmichael (1969).

Sample BS-10 was collected from the base of the Butte near the large mounds previously mentioned. Its chemistry differs from the other rhyolites, particularly in the lower silica and higher magnesium and calcium. Two interpretations are possible; either this represents a separate intrusion from a different magma source or it is an early or late eruptive phase of Big Southern Butte. Based on the available chemical and petrographic data it is tentatively considered to be an early eruptive phase.

Samples BS-13 through BS-15 are evolved lavas from the basalt section at Big Southern Butte. The analyses clearly show their distinct character: low silica and magnesium and high total iron, total alkalies, and phosphorous. Discussion on the origin of the evolved lavas is given in the section on Cedar Butte.

The basaltic inclusions, samples BS-11 and BS-12, have compositions which fall in the general range of Snake River Plain olivine tholeiites. The high volatile and alkali contents of these samples suggests that they have undergone some hydrothermal alteration. One of the inclusions

TABLE 2. Major element analyses and CIPW norms for Big Southern Butte samples.

	RHYOLITES													INCLUSIONS		EVOLVED LAVAS			Q-NRM
	BS-1[1]	BS-2	BS-3	BS-4	BS-5	BS-6	BS-7[1]	BS-8	BS-9[1]	BS-10	NOB[2]	KFB[3]	KS[3]	BS-11	BS-12	BS-13	BS-14	BS-15	BS-16
SiO_2	76.22	75.32	75.84	76.02	75.99	76.08	75.82	75.7	76.27	74.2	75.33	75.4	76.5	44.7	45.3	48.4	51.1	53.1	53.8
TiO_2	.09	.10	.10	.10	.10	.10	.09	.09	.10	.10	.10	.07	.06	2.40	3.05	2.75	2.46	2.21	1.73
Al_2O_3	12.22	12.18	12.12	12.28	12.22	12.14	12.09	12.2	12.13	12.2	12.29	12.3	12.5	14.6	14.6	13.2	13.2	13.2	14.6
Fe_2O_3	1.17	1.66	1.31	1.94	1.70	1.76	1.76	---	1.45	---	.59	1.7	1.7	---	---	---	---	---	---
FeO	.72	.13	.44	.03	.10	.04	.06	1.74*	.46	1.61*	1.09	.12	.04	15.6*	14.3*	16.5*	15.6*	15.9*	9.7*
MnO	.04	.05	.05	.03	.03	.03	.04	.05	.02	.01	.04	.02	.03	.28	.22	.31	.31	.31	.17
MgO	.00	.02	.03	.03	.03	.03	.01	.03	.00	.15	.00	.10	.00	5.98	7.09	3.00	2.77	2.04	6.42
CaO	.47	.44	.48	.40	.45	.48	1.03	.44	.35	2.33	.48	.57	.23	9.69	9.70	7.42	6.38	6.15	7.77
Na_2O	4.40	4.32	4.27	4.24	4.31	4.35	4.32	4.36	4.32	4.27	4.29	4.2	4.5	2.66	3.15	3.50	3.15	3.31	2.91
K_2O	4.76	4.76	4.66	4.69	4.68	4.72	4.67	4.57	4.57	4.40	4.98	4.5	4.7	1.81	.73	1.93	2.32	2.29	1.55
P_2O_5	.01	.03	.02	.02	.03	.03	.02	.01	.01	.07	.00	.00	.00	.70	.60	1.65	1.36	1.25	.31
H_2O^+	.30	.32	.27	---	---	---	.26	---	.27	---	.09	.32	.34	---	---	---	---	---	---
CO_2	.01	.04	.03	.08	.05	.05	.44	---	.00	---	.00	.01	.00	---	---	---	---	---	---
Loss on ignition	---	---	---	---	---	---	---	.71	---	1.36	---	---	---	.75	.61	1.43	2.11	1.14	.61
TOTALS	100.36	99.56	99.55	99.73	99.59	99.71	100.51	99.5	100.02	100.8	99.49	99.3	100.6	99.2	99.4	98.6	99.4	99.3	99.6
Q	31.22	31.41	32.15	32.34	32.04	31.79	31.56	31.84	32.04	29.23	30.48	32.30	31.29	---	---	---	3.45	5.21	3.39
Or	28.03	28.25	27.66	27.79	27.77	27.97	27.46	27.21	27.95	26.16	29.64	26.81	27.64	10.96	4.36	11.65	14.01	13.61	9.18
Ab	36.23	36.31	36.30	35.98	36.62	36.27	36.00	37.17	36.05	36.35	35.75	35.83	37.89	16.79	23.12	30.25	27.24	28.17	24.69
An	---	---	.14	.63	.18	---	---	.22	---	1.13	---	1.43	.03	23.10	23.78	14.92	15.35	14.48	22.25
Ne	---	---	---	---	---	---	---	---	---	---	---	---	---	3.40	2.06	---	---	---	---
Ac	.77	.36	---	---	---	.57	.32	---	.44	---	.72	---	---	---	---	---	---	---	---
Di Wo	.92	.73	.81	.30	.65	.78	.91	.80	.70	1.61	1.00	.57	.46	8.96	8.72	4.87	3.30	3.34	5.83
Di En	---	.03	.05	.02	.04	.04	.01	.04	---	.38	---	.09	---	4.02	4.40	1.43	.95	.73	3.23
Di Fs	1.04	.79	.86	.32	.69	.84	1.02	.85	.79	1.33	1.14	.52	.53	4.90	4.12	3.64	2.50	2.83	2.39
Hy En	---	.02	.03	.06	.04	.04	.01	.03	---	---	---	.16	---	---	---	4.78	6.10	4.38	12.80
Hy Fs	.72	.73	.57	1.19	.73	.75	.50	.71	.85	---	.48	.93	.87	---	---	12.11	15.98	16.88	9.49
Ol Fo	---	---	---	---	---	---	---	---	---	---	---	---	---	7.87	9.42	.99	---	---	---
Ol Fa	---	---	---	---	---	---	---	---	---	---	---	---	---	10.54	9.72	2.77	---	---	---
Mt	.57	.69	.87	.96	.87	.59	.72	.94	.72	.88	.52	.89	.84	3.13	3.05	3.33	3.14	3.25	2.05
Il	.17	.19	.19	.19	.19	.19	.19	.17	.17	.19	.19	.13	.11	4.67	5.85	5.34	4.77	4.22	3.29
Ap	.02	.07	.05	.05	.07	.07	.05	.02	.02	.17	---	---	---	1.70	1.44	3.99	3.29	2.98	.74

1,2, and 3 refer to analysts; see Appendix B.

* refers total iron determined as FeO

shows complete alteration of olivine and replacemnt of glass by a clay(?) mineral.

Sample BS-16 is a unique sample; compared with the averages of Nockolds (1954), it is a typical quartz-normative tholeiite basalt. Based on available analyses, this is one of only a few truly quartz-normative tholeiites described from the eastern Snake River Plain. Although the evolved lavas, BS-14 and BS-15, also have quartz in their norms, they differ considerably from BS-16, particularly in their much lower MgO and higher total iron.

Origin of Big Southern Butte Rhyolite

There are three possible origins which need to be considered for the rhyolite of Big Southern Butte: remobilization of rhyolitic basement, a magma generated through partial melting of crustal rocks, and fractional crystallization of an olivine tholeiite magma.

Remobilization of rhyolitic basement, suggested by Schoen (1974), is not considered a likely source. The strongest argument against remobilization is the absence of phenocrysts in the rhyolite. This implies that it was completely liquid at the time of emplacement. The rhyolitic basement is estimated to extend presently to a depth of no more than 2 km in the vicinity of Big Southern Butte (Stanley and others, 1977); it was probably a few hundred meters less than that 300,000 years ago. Considering this, then the geothermal gradient would have had to be abnormally high (400 to 500 ^{o}C/km) to mobilize an aphyric rhyolite - a highly unlikely situation.

The low abundance of Sr ($<$4 ppm) and Ba ($<$10 ppm) (Appendix E) as

well as a large negative Eu anomaly (Table 3) suggest that the rhyolite of Big Southern Butte was not a direct partial melt of crustal rocks. To produce such low abundances of Sr and Ba by partial melting would require a source very low in these components. It is not known what rocks underlie the Snake River Plain but it is generally believed that beneath the thin cover of volcanics (~2 km) and Paleozoic sedimentary rocks (a few kilometers of predominantly carbonate sediments) there is "normal" granitic crust. Gneissic xenoliths found in some of the Craters of the Moon lavas support this interpretation. Leeman (1974) analyzed three of the xenoliths and found that they had relatively high Ba and Sr contents (>700 ppm and > 70 ppm respectively). He found that a quartz monzonite from just north of the Plain had lower abundances, 68 ppm Ba and 42 ppm Sr, but these are still too high to be a source of the rhyolite if it is interpreted as a direct partial melt of crustal rocks. This can be verified by a simple calculation involving bulk crystal-liquid partition coefficients of Sr and Ba for the pertinent minerals of the source, namely potassium feldspar, sodium feldspar, and biotite. Feldspars have a partition coefficient of 3 to 5 for Sr; potassium feldspar and biotite are reported to have coefficients in the range of 6 to 10 for Ba (Arth, 1976). Bulk crystal-liquid partition coefficients (D_o) larger than ~3 for both components would characterize only extrodinarily feldspar-rich compositions; if appreciable quartz, hornblende, or (for Sr) biotite were present, values of D_o would be lower than 2.5 for both elements (Hildreth, 1979). Using the equations of Gast (1968) and Shaw (1970), calculations indicate that even for an extremely small amount of partial melting of such a source the melt would contain more than 40% of the intitial Ba and Sr concentrations.

	BS-1	BS-7	BS-10	BS-13	BS-15
Ce	174.8	164.9	129.5	302.7	424.3
Nd	91.5	91.2	68.8	234.8	315.5
Sm	80.3	80.1	67.7	158.4	205.4
Eu	4.0	4.1	5.7	129.1	155.9
Dy	99.2	99.0	65.6	80.6	114.7
Er	108.8	103.8	81.6	89.8	95.6
Yb	110.4	101.4	87.5	62.0	84.7

TABLE 3. Rare earth element contents of samples from Big Southern Butte (Fountain and Spear, in preparation).

Therefore, the rholite could not have originated directly from partial melting of granitic rocks which are inferred to underlie the Plain. Consequently, an origin by fractional crystallization is implied. Noble and others (1972) arrived at the same conclusion in their study of Glass Mountain, a composite rhyolite dome in east-central California which has a similar chemistry as that of Big Southern Butte. They demonstrated that the very low abundances of Sr (3 ppm) and Ba (20 ppm) could have only originated from removal of large amounts of phenocrystic feldspar.

The two magmas from which the rhyolite of Big Southern Butte could have evolved by fractional crystallization are an olivine tholeiite magma and a magma generated by partial melting of crustal rocks. The latter is considered the most likely parent. This conclusion was reached after eliminating the olivine tholeiite (or evolved tholeiite) parent magma through comparisons of rare earth element data. Figure 21 shows that for all available data on mafic lavas from the Snake River Plain, rare earth element abundances increase with differentiation. If the rhyolite of Big Southern Butte were related to the olivine tholeiite by fractional crystallization then either it should be greatly enriched in rare earths or there should be a phase of phases present which could effectively removed the rare earth elements. Neither is the case. The abundances of the rare earths in the rhyolite are much less than that of the evolved tholeiite (a presumed intermediate step in a differentiation process) and no phase or phases have been identified which preferentially incorporate the light rare earths relative to the heavy rare earths; a necessary requirement to produce the observed pattern. Therefore, it is tentatively concluded that the rhyolite of Big Southern

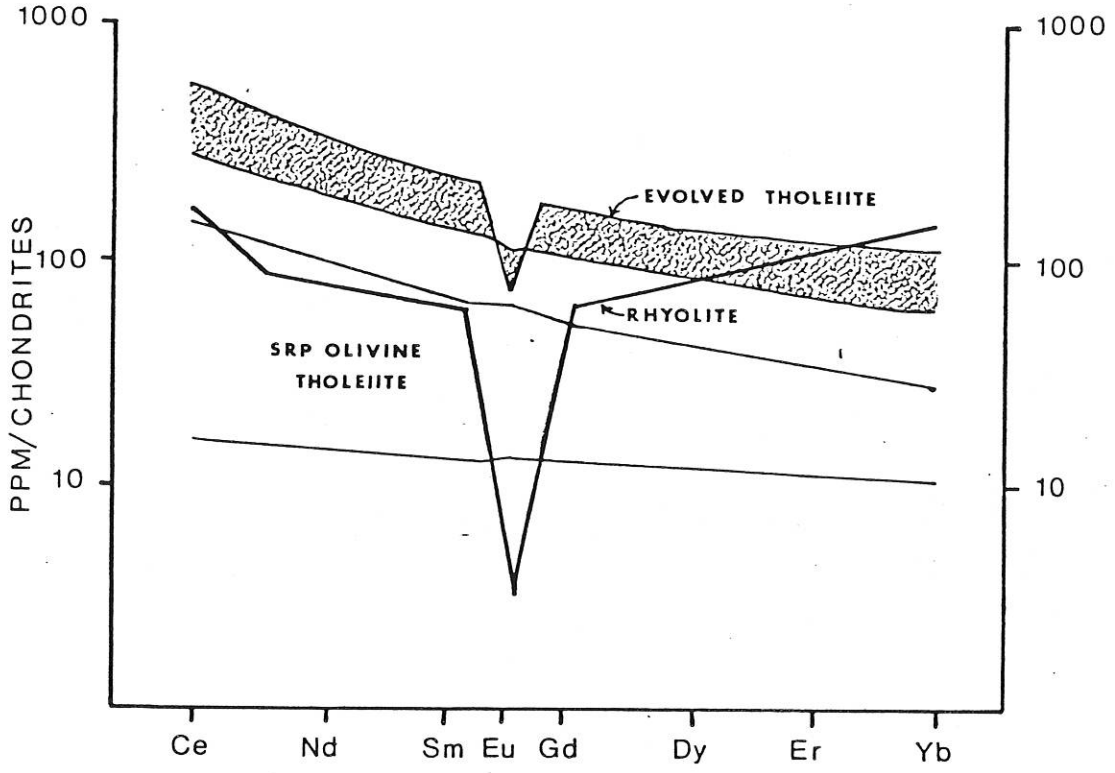


FIGURE 21. Rare earth element plot of Snake River Plain volcanic rocks within the boundaries of study area. Data from Fountain and Spear, unpublished analyses; range of basalts from Leeman (1974).

Butte originated by fractional crystallization of a magma generated by partial melting of crustal rocks, probably intermediate to granitic in composition. This conclusion is also inferred for all other rhyolites in the study area due to their chemical similarities with the rhyolite of Big Southern Butte.

The depth at which the rhyolite evolved can be approximated by comparing its bulk composition expressed as normative quartz, orthoclase, and albite with the experimentally determined system $KAlSi_3O_8$ - $NaAlSi_3O_8$ - SiO_2 - (H_2O). Although Steiner and others (1975) caution against this approach, it seems applicable in this case, at least for a rough estimation. The justification for this is based on two observations: 1) the experimental systems adequately model the bulk composition of the rhyolite (Q + Or + Ab comprise greater than 95% of the rock and there is no An component), and 2) the rhyolite has evolved through extensive crystal fractionation and therefore is theoretically moving toward (or has reached) the minimum of the system.

Figure 22 shows how the normative bulk composition of Big Southern Butte rhyolite plots relative to the experimentally determined 4 kbar minima for the water-saturated system of Tuttle and Bowen (1958) and the anhydrous system of Steiner and others (1975). Because the rhyolite contains some water (<1%) but is not saturated, neither of the experimental systems can be strictly applied. However, note that the bulk composition falls very near a unique fractionation curve (from Steiner and others, 1975) between the two systems. This suggests that 4 kbar might be a good approximation of the pressure. Even if this is not acurate it does indicate that moderate pressures (perhaps 3 to 5

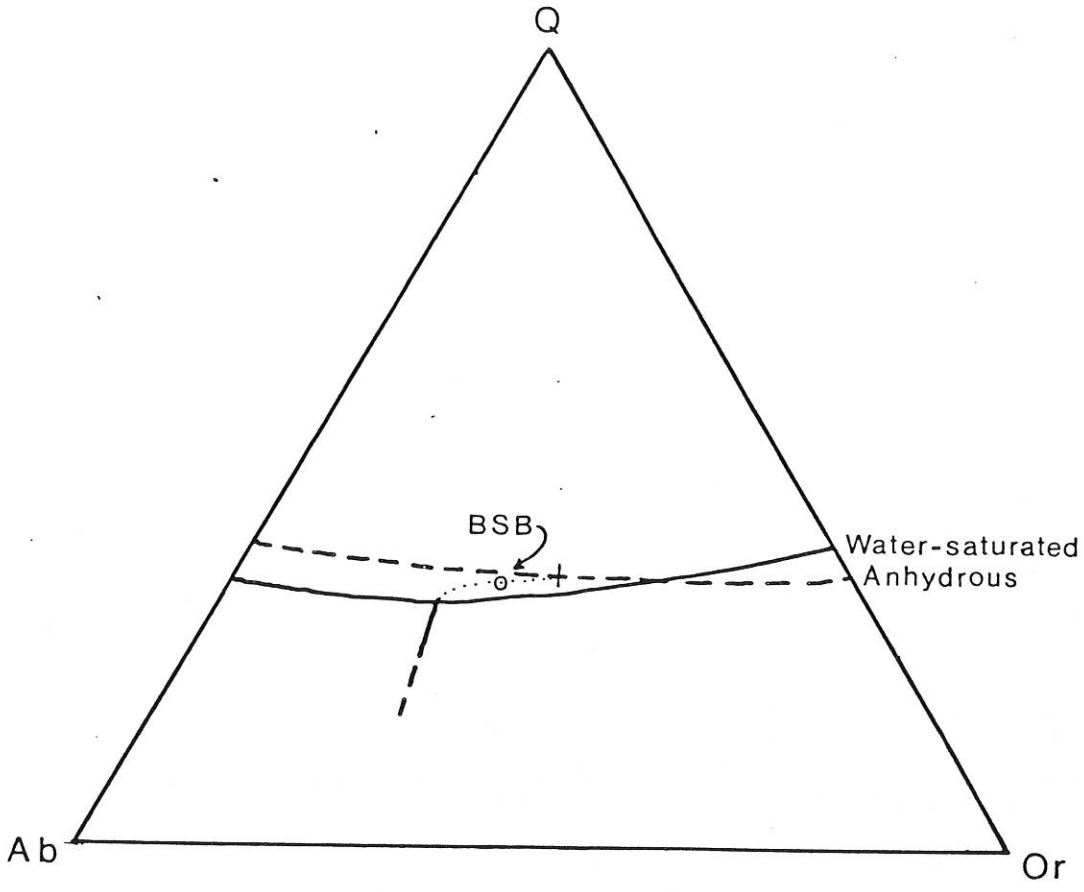


FIGURE 22. Bulk composition of Big Southern Butte (average of 9 analyses) plotted in terms of normative quartz, albite, and orthoclase. The solid line is the experimentally determined phase boundary for the water-saturated system at 4 kbar (Tuttle and Bowen, 1958); the dashed line represents the anhydrous phase boundary at 4 kbar (Steiner and others, 1975). The dotted line is a unique fractionation curve between the two systems (from Steiner and others, 1975).

kbar) were involved.

Stanley and others (1977) estimate an average geothermal gradient of approximately 69 ^{o}C/km in the Snake River Plain today. There is no reason to think that it was much different at the time Big Southern Butte formed. Figure 23 shows that if the geothermal gradient were 69 ^{o}C/km, melting of rocks of granitic composition would occur at depths ranging from 10 to 15 km (which is roughly equivalent to 3 to 5 kbar of pressure). This corresponds nicely with the pressures inferred above.

In conclusion, the rhyolite of Big Southern Butte formed by fractional crystallization in a silicic magma chamber at a depth of 10 to 15 km (3 to 5 kbar). The parent magma originated through partial melting of crustal rocks granitic in composition.

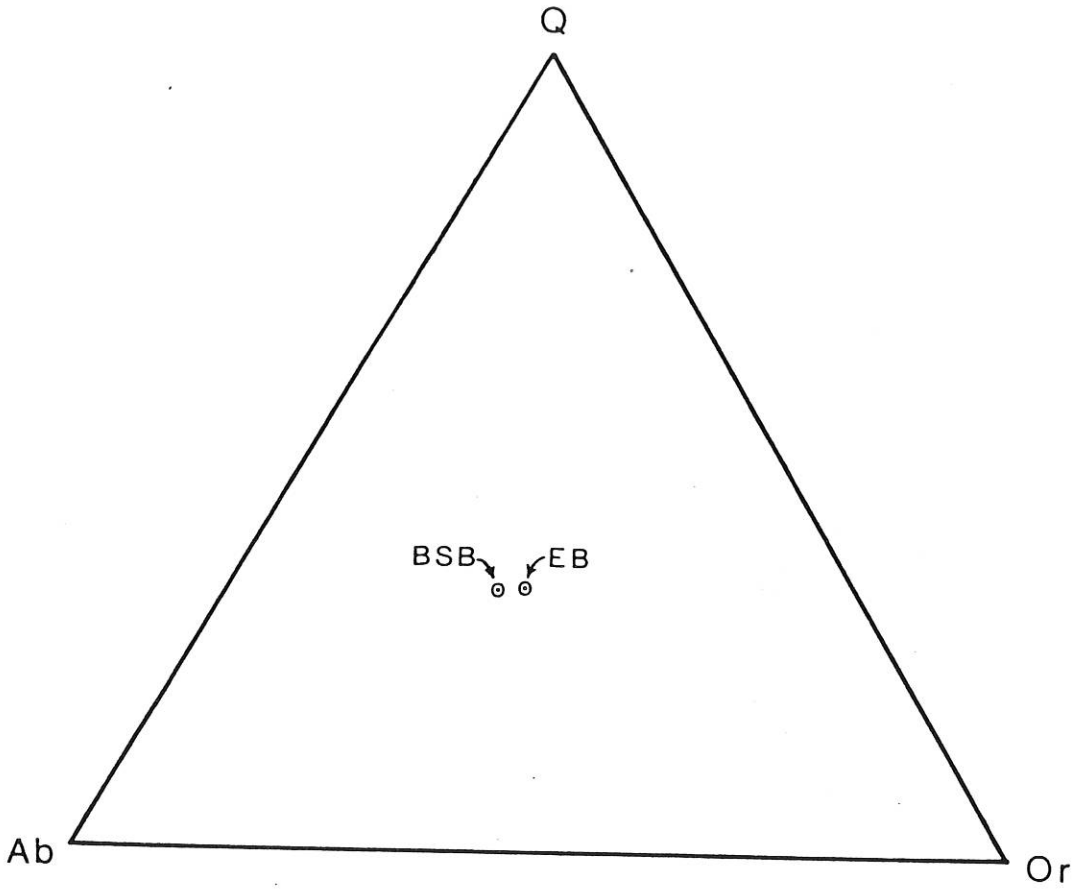


FIGURE 33. Comparison of the average bulk composition of East Butte rhyolite and Big Southern Butte rhyolite plotted in terms of normative quartz, albite, and orthoclase.

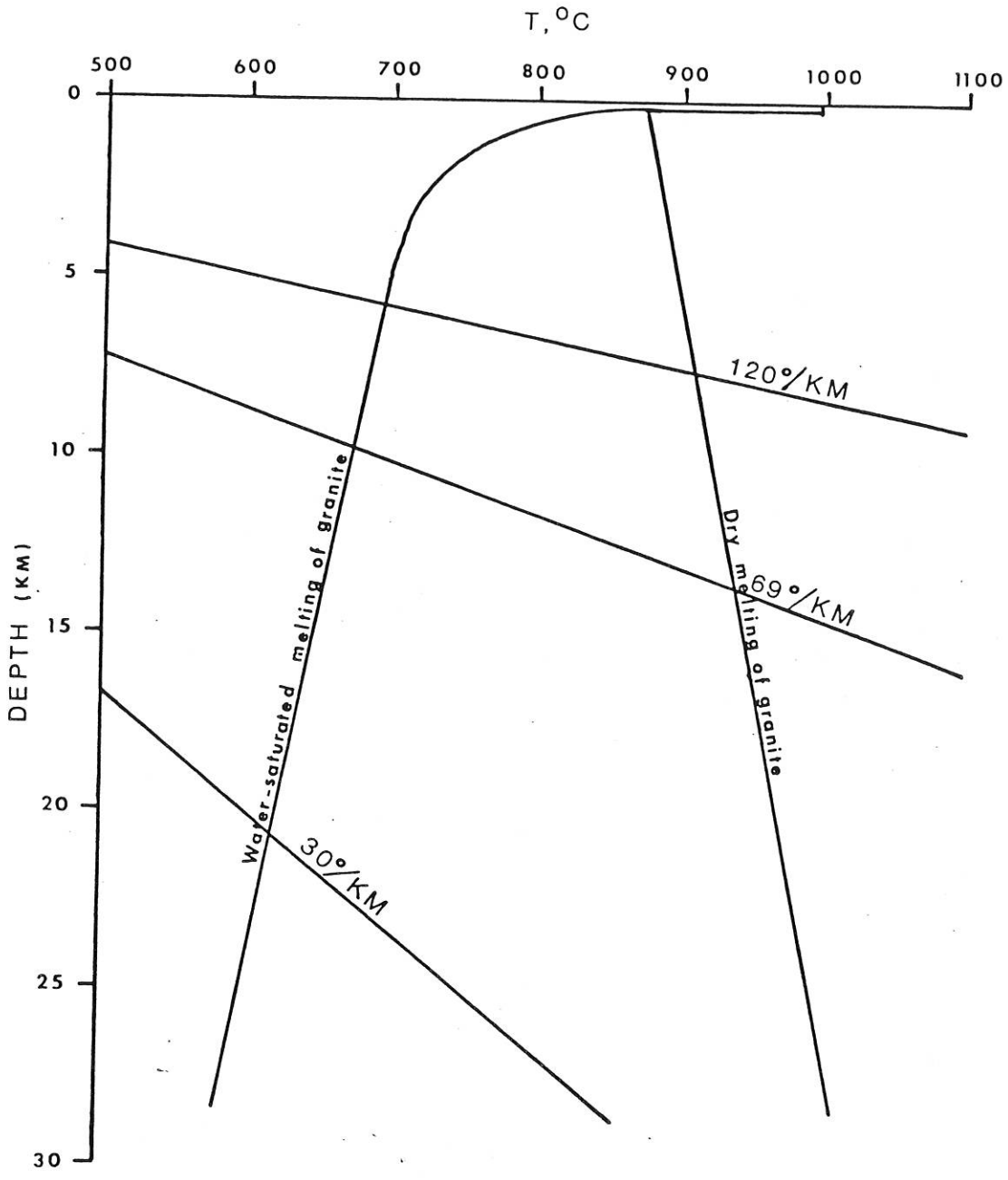


FIGURE 23. Selected geothermal gradients for the eastern Snake River Plain, Idaho. 69 °/km is average of Stanley and others (1977), 120 °/km is measured gradient in a geothermal prospect hole in the Raft River area (also from Stanley and others, 1977), and 30 °/km is normal continental geothermal gradient. Melting relations of granite are superimposed.

EAST BUTTE

East Butte is a 600,000 year old (Armstrong and others, 1975) cumulo dome located 28 km east-northeast of Big Southern Butte (Plate 2). It has a diameter of 2.4 km and rises to 2003 m, some 360 m above the surrounding basalt flows (Figs. 24, 25). The slopes of East Butte have not been dissected to any large degree by erosion and it lacks the conspicuous talus slopes and alluvial fans present at Big Southern Butte. This probably reflects differences in lithology and the smaller overall size and height of East Butte; it offers little surface area on which water can collect.

The dome is composed of light gray, buff, and pinkish-gray rhyolite. Dark reddish-brown to steel-gray porphyritic inclusions are common in the rhyolite. The rhyolite apparently does not grade into a sugary variety as was observed at Big Southern Butte. Also, autoclastic breccias are not present.

Flow-layering is conspicuous at East Butte. Dips vary but are generally steeply inclined away from the center. Some of the more massive parts of the Butte exhibit a platy appearance in outcrop (Fig. 26). Whether this feature is a direct result of flow or due to planar jointing after solidification is not known. Whatever the cause, the planar surfaces are generally parallel with the direction of flow.

In the center of East Butte is a shallow circular depression 275 m in diameter. No breccias of agglomerates are present in or around this depression to prove the existence of a crater. However, at two different locations on the rim are mounds of oxidized rhyolitic debris which are interpreted to be remnants of small viscous protrusions (spines).

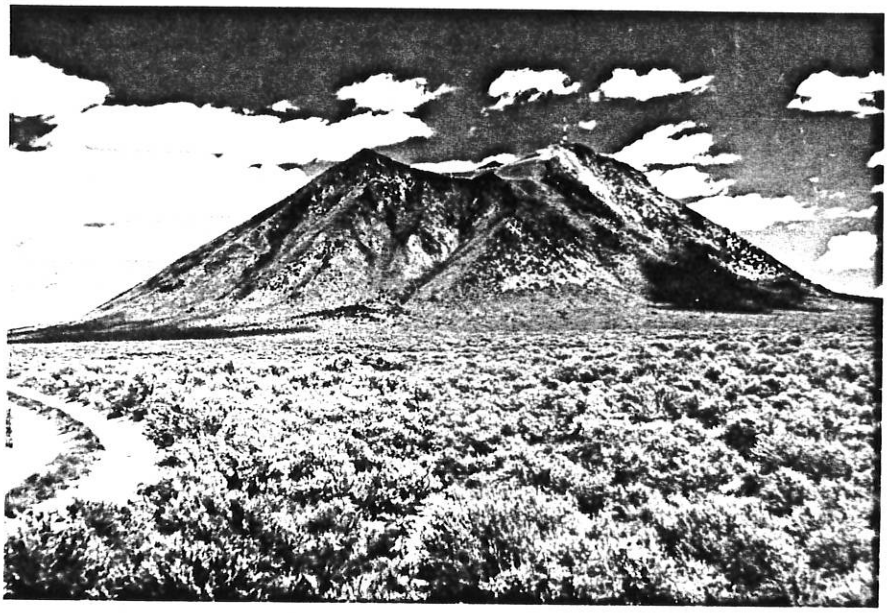


FIGURE 24. East Butte, 5 km away, rises 360 m above the surrounding basalt flows of the Snake River Plain. View to the southwest.

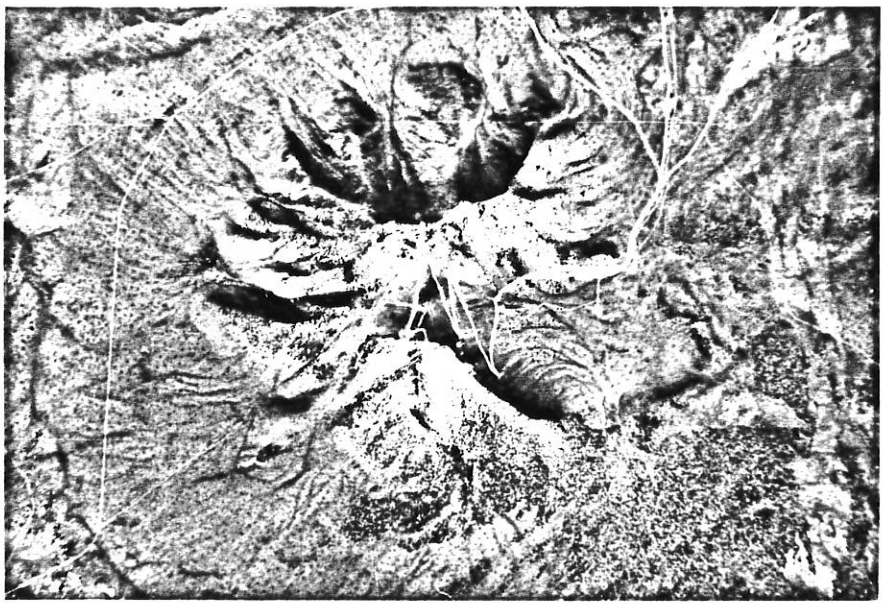


FIGURE 25. Aerial view of East Butte. Photo is 3 km wide and north is at the top.

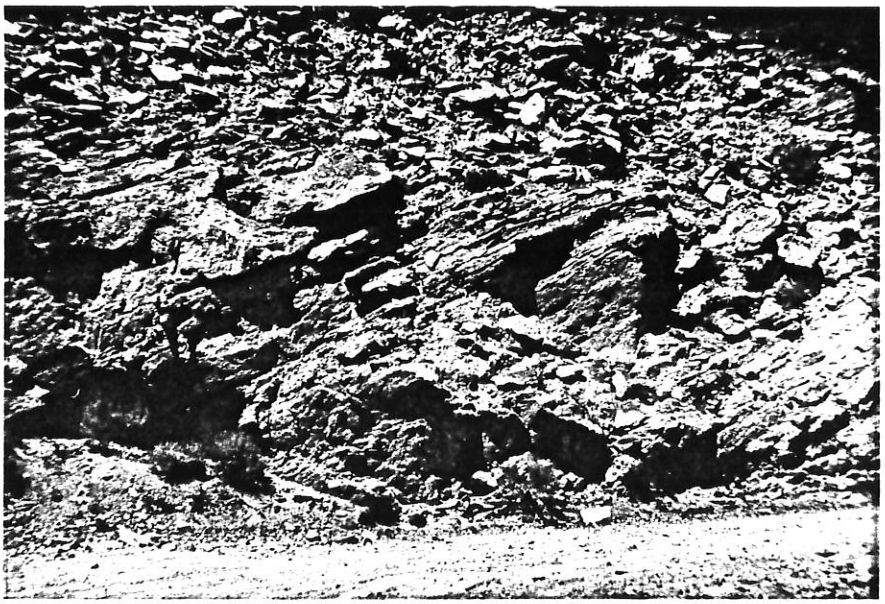


FIGURE 26. Platy layering in rhyolite of East Butte. Width of photo is about 8 m.

Whether or not an open crater existed is a matter for speculation but the general morphology of the depression and the flow-layering dipping steeply away on all sides document an intrusive center.

Based on the attitudes of flow-layering, absence of autoclastic breccias, and other field evidence, it is concluded that East Butte developed primarily by endogenous growth. Concentric flow-planes shown in Figure 27 also support the interpretation. Reyer (1888) experimentally produced concentric flow-planes in scale models of endogenous domes (Fig. 28). He called this Zwiebelstruktur (onion structure). Although this idealized picture is probably oversimplified for the development of East Butte, it does suggest the dominant mode of growth.

At the base of East Butte on its eastern side is a large basaltic crater, 350 m in diameter. This vent was the source of a large flow which covers 60 km^2 and almost completely encircles the butte. The basalt is distinctive in hand specimen when compared to other basalts in the area due to the large plagioclase laths (up to 3 cm in length) and large equant olivine crystals which occur together in glomeroporphyritic clusters.

Petrography

The rhyolite of East Butte varies in appearance in outcrop but is mineralogically and compositionally homogeneous. Most of the differences in hand specimen can be related to the amount of glass in the groundmass. The rock is porphyritic with phenocrysts of sanidine, quartz, and minor clinopyroxene and opaque minerals.

The porphyritic inclusions are present in most outcrops at East



FIGURE 27. Concentric flow planes in rhyolite of East Butte. Compare with Figure 28. Width of photo is about 4 m.

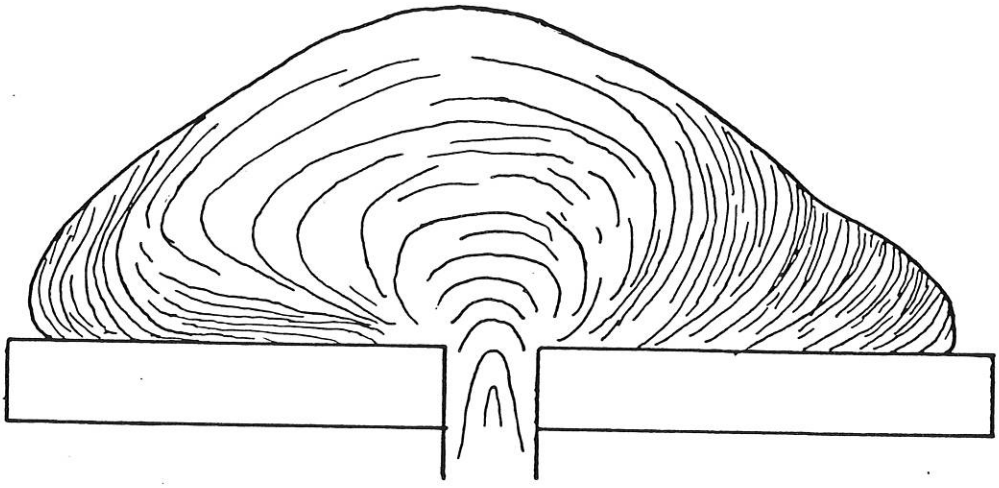


FIGURE 28. Flow planes produced by squeezing viscous substance through narrow aperture. (After Reyer, Theoretische Geologie, fig. 84, 1888, in Williams, 1932)

Butte but their volume is small, probably less than one percent. Most of the inclusions have phenocrysts of plagioclase, olivine, magnetite, clinopyroxene, quartz, and alkali feldspar. As will be discussed in the following sections, these inclusions are interpreted to be hybrid rocks produced by the mechanical mixing of two magmas of contrasting compositions.

Rhyolite. The rhyolite contains 10 to 20 percent phenocrysts set in a glassy to devitrified groundmass of alkali feldspar and quartz. The phenocryst assemblage is comprised of sanidine and quartz with minor amounts of green clinopyroxene, variably altered fayalite, and an Fe-Ti oxide mineral. Plagioclase is a rare component. Representative textures are shown in Figure 29.

Sanidine occurs as colorless euhedral crystals 1 to 5 mm long. It has a 2V of 19-23° indicating a composition of $Or_{61-65}Ab_{29-32}An_7$ according to Tröger (1956, p. 96). Quartz is present as anhedral to subhedral crystals as much as 2 mm long. Quartz also occurs with alkali feldspar as large micropegmatitic crystals up to 8 mm in length (Fig. 30).

Clinopyroxene is present as greenish-brown, weakly pleochroic, equant crystals. It is optically positive, has large extinction angles, and a 2V of approximately 75° indicating that it is an aegirine-augite. Small (<1 mm) equant grains of fayalite occur less frequently than the clinopyroxene and range from fresh to completely altered. A dark reddish-brown opaque mineral (aenigmatite ?) is also a minor constituent.

Hybrid Inclusions. The phenocrysts of the hybrid inclusions comprise about 10 percent of the rock and are set in a fine-grained groundmass of plagioclase, alkali feldspar, clinopyroxene, and Fe-Ti oxides.

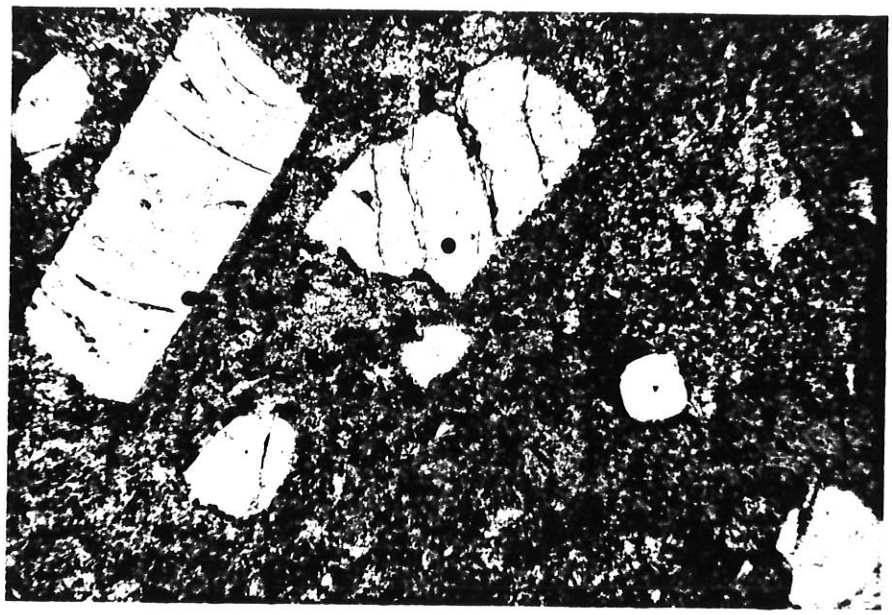


FIGURE 29a. Photomicrograph of East Butte rhyolite. Euhedral crystals of sanidine and rounded crystal of quartz (southeast portion of photo) set in a devitrified groundmass. Field of view is 2.50 mm by 1.62 mm.

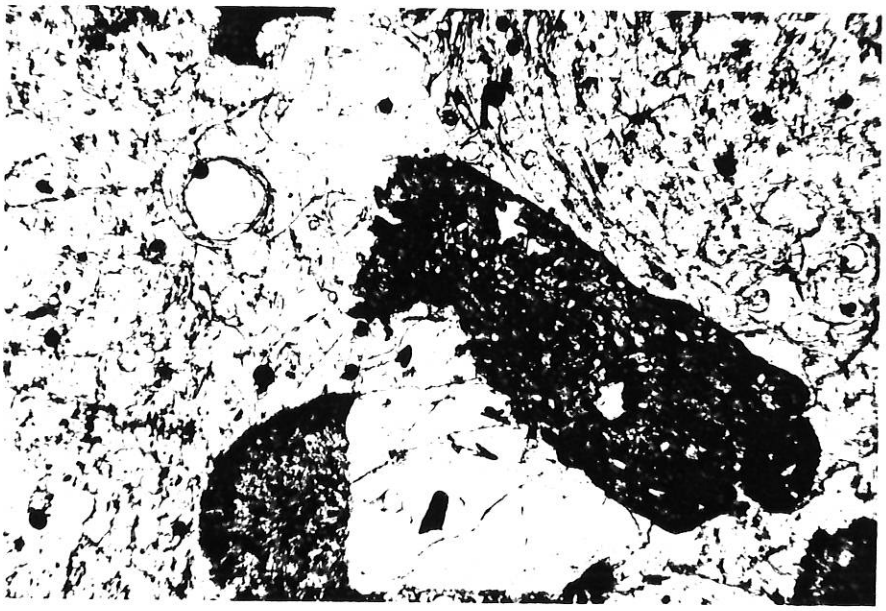


FIGURE 29b. Photomicrograph of East Butte rhyolite. Dark mineral is a clinopyroxene which is next to a sanidine crystal. Rounded quartz crystal is present in northwest part of photo. Groundmass is glassy. Field of view is 2.50 mm by 1.62 mm.

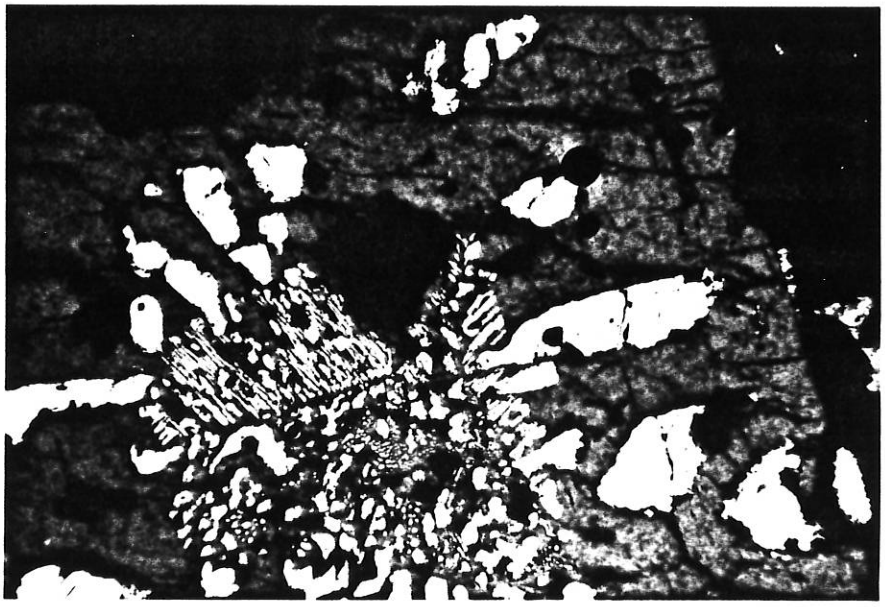


FIGURE 30. Micropegmatitic intergrowths of alkali feldspar and quartz in rhyolite of East Butte. Quartz is light-colored, feldspar is dark. Field of view is 2.50 mm by 1.62 mm.

Plagioclase makes up 70 to 80 percent of the phenocrysts and occurs as euhedral laths and fragments up to 3 cm long. Many are embayed and have strongly zoned overgrowths of sodic feldspar. Universal stage determinations of several relatively unzoned grains gave compositions of $An_{48} \pm 2$.

Clinopyroxene is present in two varieties: pale brown euhedral crystals (positive, $2V \approx 48$) and as reddish-brown grains in the groundmass. Reddish-brown clinopyroxene also completely rims the quartz phenocrysts (Fig. 31). Other phenocryst minerals include forsteritic olivine, generally exhibiting various stages of alteration, and magnetite granules which occur sporadically. A few sanidine crystals are also present; they have approximately the same composition as those in the rhyolite described above.

One of the inclusions studied was slightly different from the general description just given. The dark gray sample is fusiform in shape, approximately 10 cm in length and 4 cm in diameter. In cross-section it can be seen that the interior is vesicular and the other portions are not (Fig. 32). In thin section phenocrysts of large tabular to lath-shaped plagioclase (An_{48}), forsteritic olivine, magnetite, and light yellow clinopyroxene (aegirine-augite ?) occur in a fine-grained groundmass of feldspar, magnetite, clinopyroxene, and abundant muscovite; no quartz or alkali feldspar was observed. The phenocrysts comprise 20 percent of the sample.

The shape, texture, and mineralogy of this sample can best be explained as being the result of intrusion of a partially crystalline mafic magma into a rhyolitic magma. Eichelberger (1978) reports that basalt magma breaks into globules as it intrudes rhyolitic magma. He

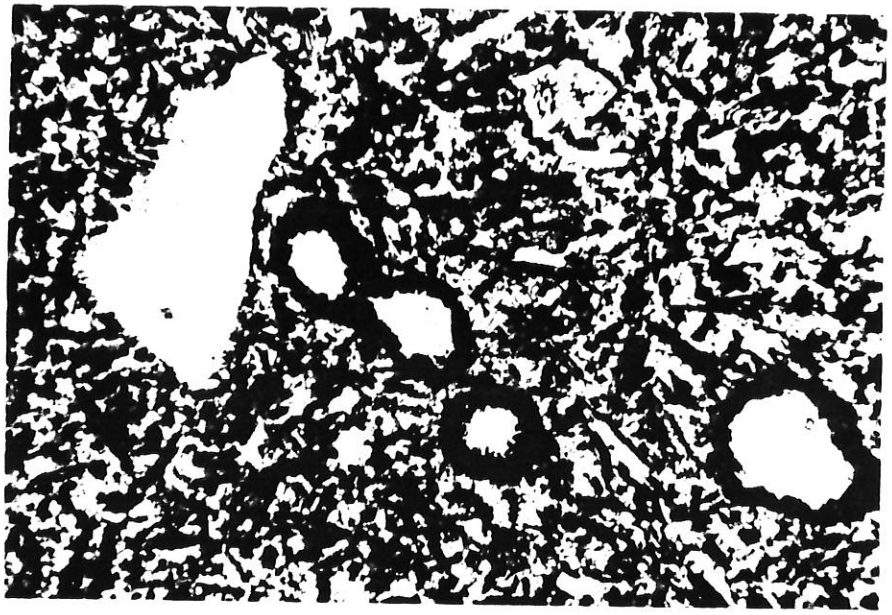


FIGURE 31. Photomicrograph of hybrid inclusion showing rounded quartz crystals completely rimmed by augite. Large crystal is a sanidine. Field of view is 2.50 mm by 1.62 mm.

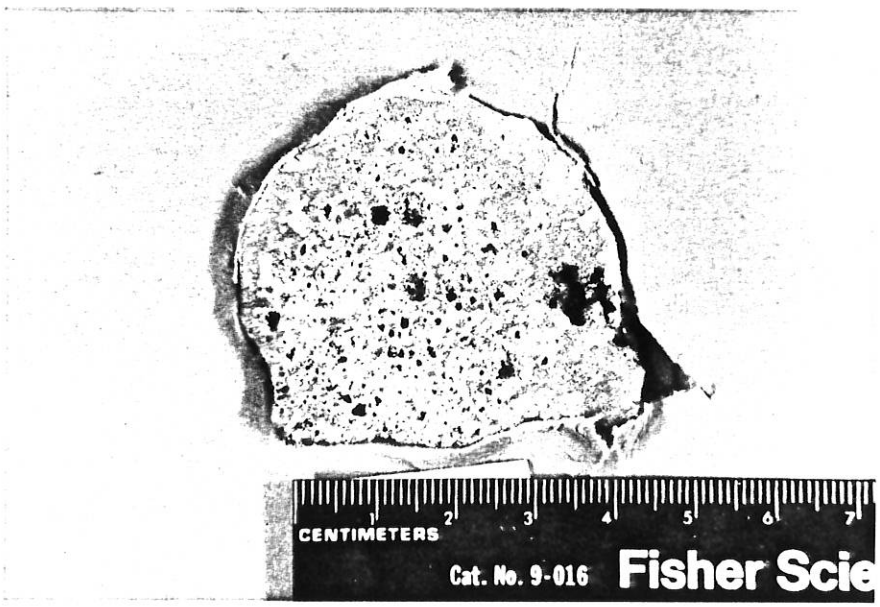


FIGURE 32. Cross-sectional view of globular inclusion (EB-7) showing vesicular center.

also states that the basalt globules are vesicular and the amount of mixing between the mafic and silicic magmas is minor because the globules are quickly crystallized. If this interpretation is correct, then this particular inclusion may be close to the composition of the mafic magma.

In conclusion, the mineralogy and non-equilibrium textures, such as quartz rimmed with augite and overgrowths of sodic feldspar on plagioclase, of most of the inclusions support the interpretation that the inclusions are hybrid in origin and are the product of mechanical mixing of two partially crystalline liquids, one mafic and one silicic. The major element chemistry of the rhyolite and the inclusions offer further supportive evidence for this hypothesis as will be shown in the next section.

Petrology

Major element analyses and CIPW norms for 8 East Butte rhyolites, 2 hybrid inclusions, and 2 samples of basalt which erupted from the vent at the base of East Butte are given in Table 4. In terms of major oxides the rhyoite is quite different from that of Big Southern Butte, but normative compositions are very similar (Fig. 33). East Butte rhyolite is believed to have an origin similar to that of Big Southern Butte rhyolite.

The basalt is included in the analyses because during preliminary study of the origin of the inclusions it was modeled as the mafic magma which mixed with the rhyolite to produce the inclusions (Spear, 1979). However, additional chemical data has shown that model to be

All

TABLE 4. Major element analyses and CI

	EB-1	EB-2	EB-3[1]
SiO_2	74.7	74.7	74.31
TiO_2	.18	.15	.17
Al_2O_3	11.9	12.1	11.90
Fe_2O_3	.96	---	1.47
FeO	1.28	2.19*	.97
MnO	.06	.06	.05
MgO	.08	.15	.05
CaO	.92	1.34	.67
Na_2O	3.67	3.95	3.78
K_2O	5.18	4.80	5.13
P_2O_5	.03	.05	.02
H_2O^+	---	---	.71
CO_2	---	---	.00
Loss on ignition	1.12	1.14	---
TOTALS	100.1	100.6	99.23
Q	31.48	30.46	31.24
Or	30.59	28.17	30.57
AB	31.04	33.19	32.25
An	.70	1.10	.36
Di Wo	1.53	2.67	1.20
Di En	.17	.37	.08
Di Fs	1.52	1.86	1.25
Hy En	.03	---	.04
Hy Fs	.27	---	.68
Ol Fo	---	---	---
Ol Fa	---	---	---
Mt	1.15	1.17	1.24
Il	.34	.28	.33
Ap	.07	.12	.05

1,2, and 3 refer to a

incorrect. In particular, rare earth element abundances for the basalt, rhyolite and an inclusion (Fig. 34) show that the inclusion is greatly enriched in rare earths relative to the baslat or rhyolite and consequently could not have resulted from the mixing of those two magmas. It was interesting to discover that the rare earth element abundances of the inclusion were the same as those of the evolved tholeiite lavas. This may indicate more than coincidence as will be discussed later.

Sample EB-7 is the globular inclusion described in the previous section. If it originated from the intrusion of mafic magma into silicic magma and it underwent only minor mixing as suggested by the mineralogy and macroscopic features, then it may be a reasonable choice for the composition of the mafic magma which mixed with the rhyolite to produce the hybrid inclusions. The compositions of EB-7, a hybrid inclusion, and an average composition for the rhyolite of East Butte are plotted against SiO_2 in Figure 35. The diagram shows that for most oxides, the hybrid inclusion lies on mixing lines between the rhyolite and EB-7 in the proportion of approximately 14 percent rhyolite and 86 percent EB-7. Although some of the oxides do not lie exactly on mixing lines as ideally they should, the porphyritic nature of the samples, paucity of analyses, and the probability of some elemental diffusion, probably accounts for most of the discrepancies. Therefore, it is concluded that East Butte rhyolite mixed with an evolved tholeiite similar in composition to or more basic than EB-7 to produce the hybrid inclusions.

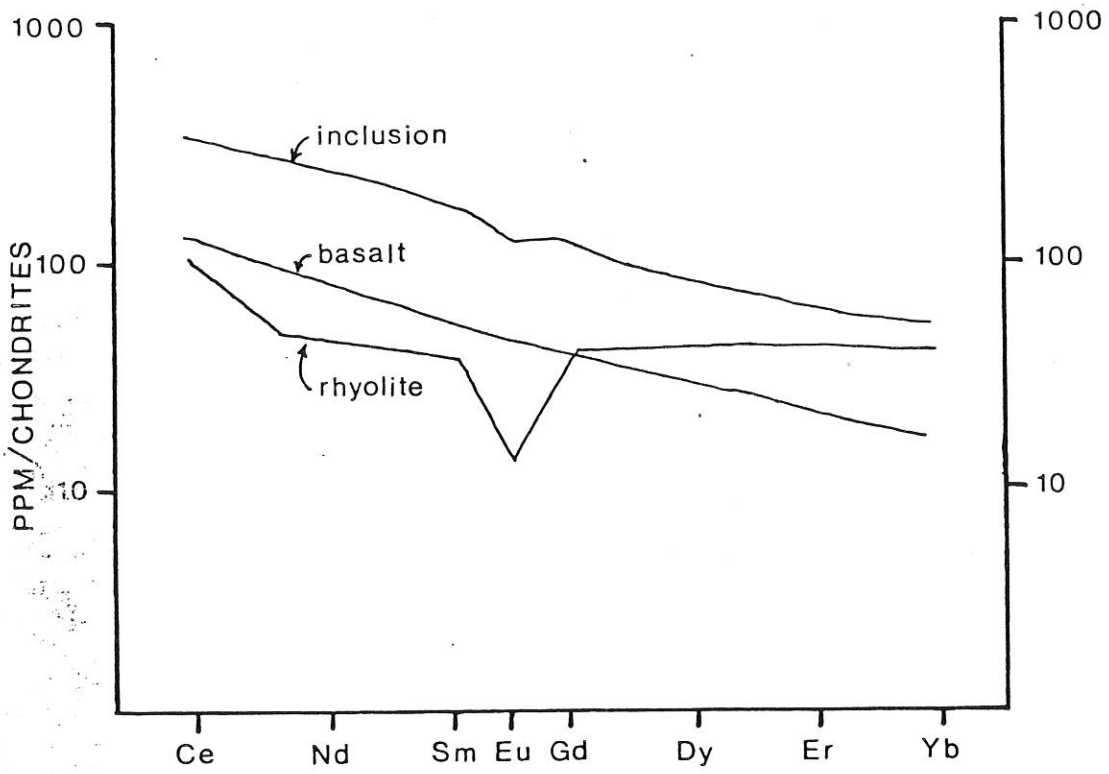


FIGURE 34. Rare earth element plot for East Buute rhyolite, hybrid inclusion, and the basalt which erupted from the vent at the base of East Butte.

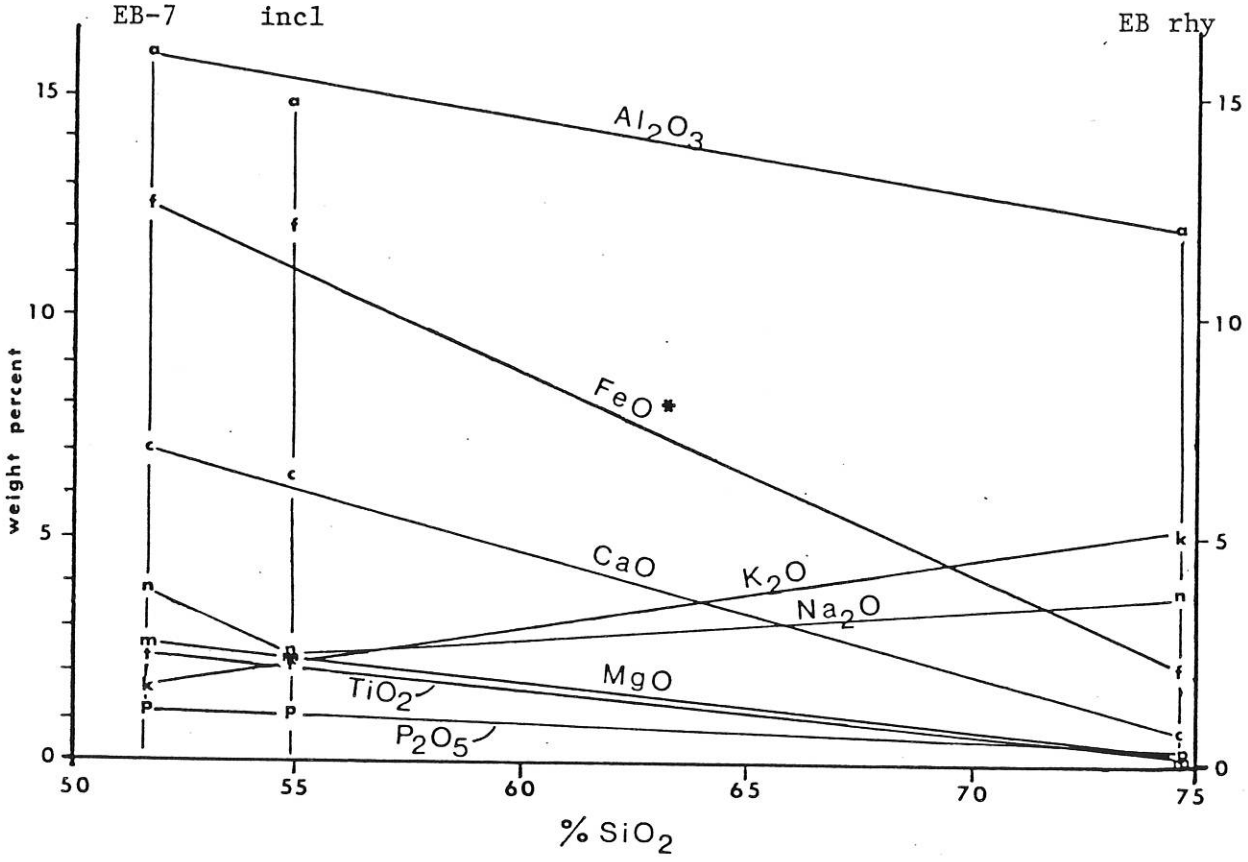


FIGURE 35. Mixing diagram for East Butte hybrid inclusions. Inclusion (incl) results from mixing 16% rhyolite (EB rhy) with 84% EB-7 (the globular inclusion).

MIDDLE BUTTE

Middle Butte, located 4 km west of East Butte, has a diameter of 2 km at its base and is 350 m high (Plate 2, Fig. 37). It is an upraised block of basalt flows which dips about 10^{o} to the south (Fig. 38). The slopes of Middle Butte are mantled by a thick accumulation of scree, particularly on the northern slope.

The two basalt flows capping Middle Butte are typical Snake River Plain olivine tholeiites. A sample from the more massive lower flow has phenocrysts of plagioclase ($An_{61} \pm 2$) and olivine ($Fo_{65} \pm 3$) which occur in about equal amounts and make up 10 percent of the rock. The groundmass is composed of plagioclase, pale-brown clinopyroxene, olivine, magnetite, ilmenite, and brown glass. Calcite fills vesicles and replaces some of the glass. Two chemical analyses are given in Table 5.

The mechanism responsible for elevating the block of basalt flows is believed to be the intrusion of viscous silicic magma. Schoen (1974) reports that interpretations of gravity data support a hypothesis that less dense rocks lie concealed beneath the basalt of Middle Butte. However, the most direct evidence is the presence of silicic domes nearby and the basalt elevated during the development of Big Southern Butte. These both demonstrate that such a mechanism is viable.

Origin of the Hybrid Inclusions

If the number of inclusions present in outcrop is representative of the total volume of inclusions, then the volume is small compared to that of the rhyolite. This implies that the mixing of the two magmas was minor, as might occur at an interface between them. Yoder (1973) showed experimentally that such an interface between rhyolitic and basaltic melts can be maintained for a short time.

Wager and others (1965) discussed a model for the origin of hybrid rocks on the Isle of Skye which seems applicable for the inclusions of East Butte. They proposed that a mafic magma emplaced in the crust undergoes differentiation and, if the residence time is long, partially melts the overlying country rocks to produce a granitic liquid. Because of differing densities in the two liquids, two separate systems of convection arise. At the interface between the two systems of currents, where they would be flowing in opposite direction, mechanical mixing of the two magmas would occur producing a hybrid rock (Fig. 36). Rice and Eichelberger (1976), in a discussion of a similar model, calculate that a rhyolitic magma need be only 10 m thick to convect. Therefore, if the conditions are right, even small volumes of rhyolite might produce hybrid rocks.

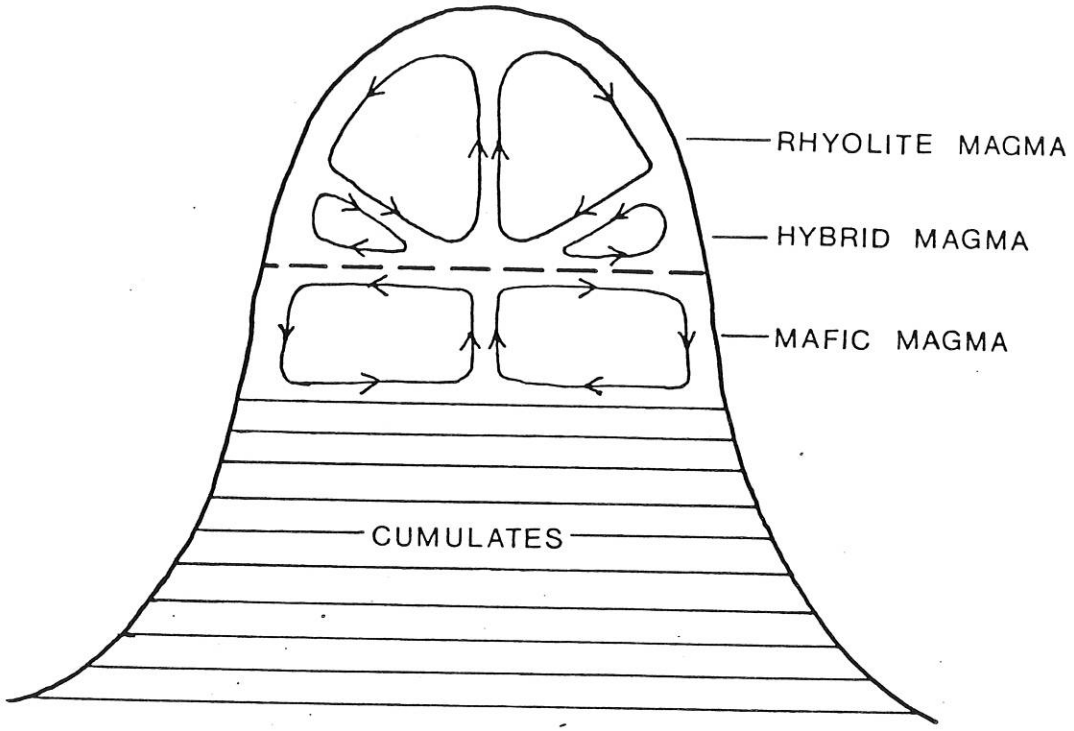


FIGURE 36. Digrammatic representation of cupola-shaped magma reservoir produced by melting of overlying granitic rock by convecting basic magma. Mechanical mixing produces hybrid rocks. (From Wager and others, 1965, p. 303, fig. 35b.)

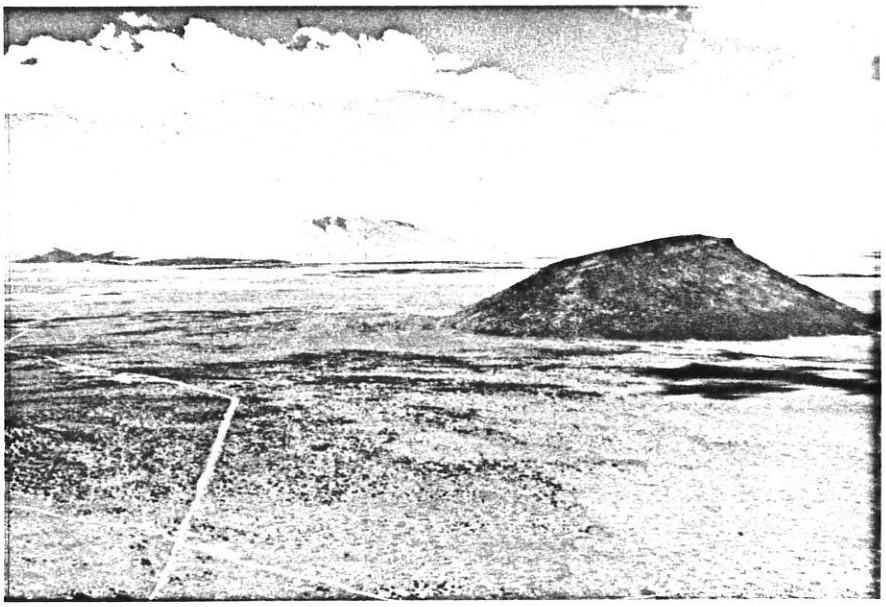


FIGURE 37. Photograph of Middle Butte from East Butte (4 km). View is to the southwest; Big Southern Butte is in the distance about 28 km.

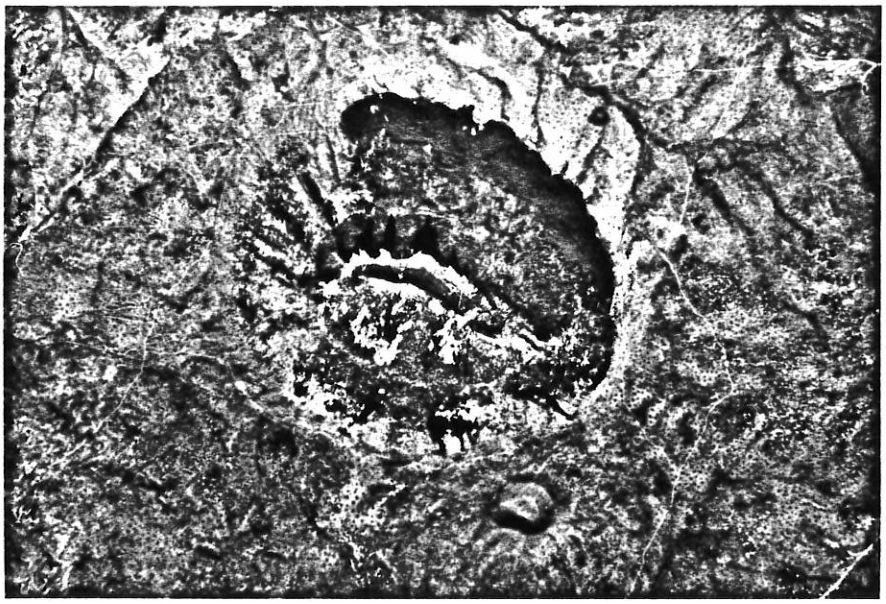


FIGURE 38. Aerial view of Middle Butte. The diameter of Middle Butte is about 2 km; north is at the top of the photo.

	MB-1	MB-2		MB-1	MB-2
SiO_2	47.1	47.00	Or	1.24	3.28
TiO_2	2.29	2.20	Ab	21.18	17.95
Al_2O_3	15.7	15.50	An	30.87	30.77
Fe_2O_3	--	.53	Di Wo	9.91	5.81
FeO	10.81*	11.40	Di En	6.05	3.34
MnO	.21	.18	Di Fs	3.31	2.21
MgO	9.23	8.66	Hy En	2.04	10.50
CaO	11.39	10.90	Hy Fs	1.12	6.94
Na_2O	2.51	2.14	Ol Fo	10.40	5.29
K_2O	.21	.56	Ol Fa	6.28	3.85
P_2O_5	.19	.48	Mt	2.27	2.48
H_2O^+	--	.27	Il	4.34	4.14
CO_2	--	.93	Ap	.45	1.13
Loss	.46	--			
TOTALS	100.10	100.74			

(MB-2 analysis from Leeman (1974))

*total iron

Note: norms calculated with $Fe^{3+}/Fe^{2+} = 0.15$

TABLE 5. Major element analyses and CIPW norms for Middle Butte samples.

OLD RHYOLITE DOME

One kilometer southwest of East Butte is an old rhyolite dome (1.42 m.y., K-Ar age determined by G.B. Dalrymple, U.S.G.S.; personal communication of M. Kuntz) which has been almost completely covered by basalt flows; only the top is still exposed (Plate 2, Fig. 39). A craterless basaltic vent lies just to the west of the exposed rhyolite. A drill hole about one-half kilometer north revealed rock similar in character to that of the dome beneath a cover of 120 m of basalt (D. Doherty, personal communication). It is present at least 250 m below the surface and may extend to approximately 550 m.

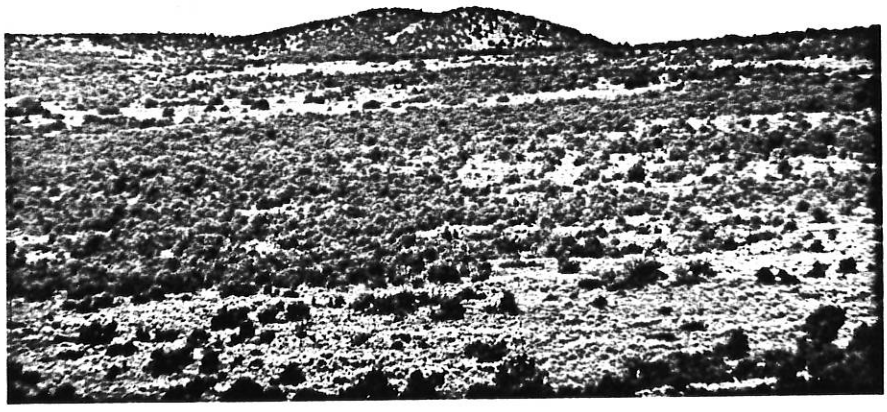


FIGURE 39. Photograph of old rhyolite dome located 1 km southwest of East Butte. The dome is almost completely covered by younger basalt flows.

In general, the rhyolite exposed in the dome is light gray to pinkish-gray and flow-layered. It is porphyritic with phenocrysts of sanidine, clinopyroxene, and Fe-Ti oxides set in a glassy to devitrified groundmass (Fig. 40). Small plagioclase laths occur together with partially altered olivine crystals in some sections. Fresh samples are not common and secondary calcite is abundant in the groundmass and in fractures within individual minerals.

An analysis of the rhyolite is presented in Table 6 along with the average composition of East Butte rhyolite for comparison.



FIGURE 40. Photomicrograph of rhyolite of the old dome. Large crystal on right is sanidine; next to it is a small clinopyroxene. Light colored crystal in northwest portion of photo is plagioclase and next to it are some altered olivines. More sanidine is seen in the southwest corner. Groundmass is devitrified. Field of view is 2.50 mm by 1.62 mm.

	OD-1	EB-AVG		OD-1	EB-AVG
SiO_2	75.1	74.65	Q	31.98	31.55
TiO_2	.15	.17	Or	29.99	29.90
Al_2O_3	12.1	12.10	Ab	33.13	32.43
FeO*	2.11	2.15	An	.75	1.07
MnO	.03	.04	Di Wo	.48	1.00
MgO	.15	.06	Di En	.09	.09
CaO	.43	.72	Di Fs	.42	1.02
Na_2O	3.88	3.81	Hy En	.29	.06
K_2O	5.03	5.03	Hy Fs	1.35	.76
P_2O_5	.04	.02	Mt	1.14	1.17
H_2O^+	---	.58	Il	.29	.33
CO_2	---	.00	Ap	.10	.05
Loss	1.36	---			
TOTALS	100.4	99.33			

*total iron

Note: norms calculated with $Fe^{3+}/ Fe^{2+} = 0.50$

TABLE 6. Comparison of old dome rhyolite with East Butte rhyolite.

CEDAR BUTTE

Cedar Butte is a unique volcanic center in the map area. Its prominent vent area and the composition of its lavas distinguish it from all other volcanoes. Cedar Butte is equal to or more than 400,000 years old (K-Ar age by G.B. Dalrymple, U.S.G.S.; in Kuntz, 1978) and apparently had a long eruptive history. It covers an area of approximately 31 km^2 and is surrounded by younger basalt flows on all sides (Fig. 41). Cedar Butte lava in the tilted block of lava flows at Big Southern Butte and its presence inferred from a well log and cuttings obtained from a water well 5 km to the southeast, document an originally greater areal extent.

The lavas of Cedar Butte are Craters of the Moon type evolved tholeiites which form a differentiated suite ranging from 54% SiO_2 to 67% SiO_2. A small amount of rhyolite (72% SiO_2) is also present but it is not considered to be part of the differentiated suite. Prior to the recognition of evolved lavas at Cedar Butte, all occurrences of evolved lavas were thought to occur only at the margins of the Snake River Plain.

Geology

The most conspicuous feature of Cedar Butte is its large, complex vent area consisting of a circular pyroclastic cone over 100 m high and 1.2 km in diameter and an elongate arcuate vent 1 km long and 30 to 60 m high which extends north-northwest from the base of the pyroclastic cone (Fig. 42). Field and petrologic evidence show that this feature is

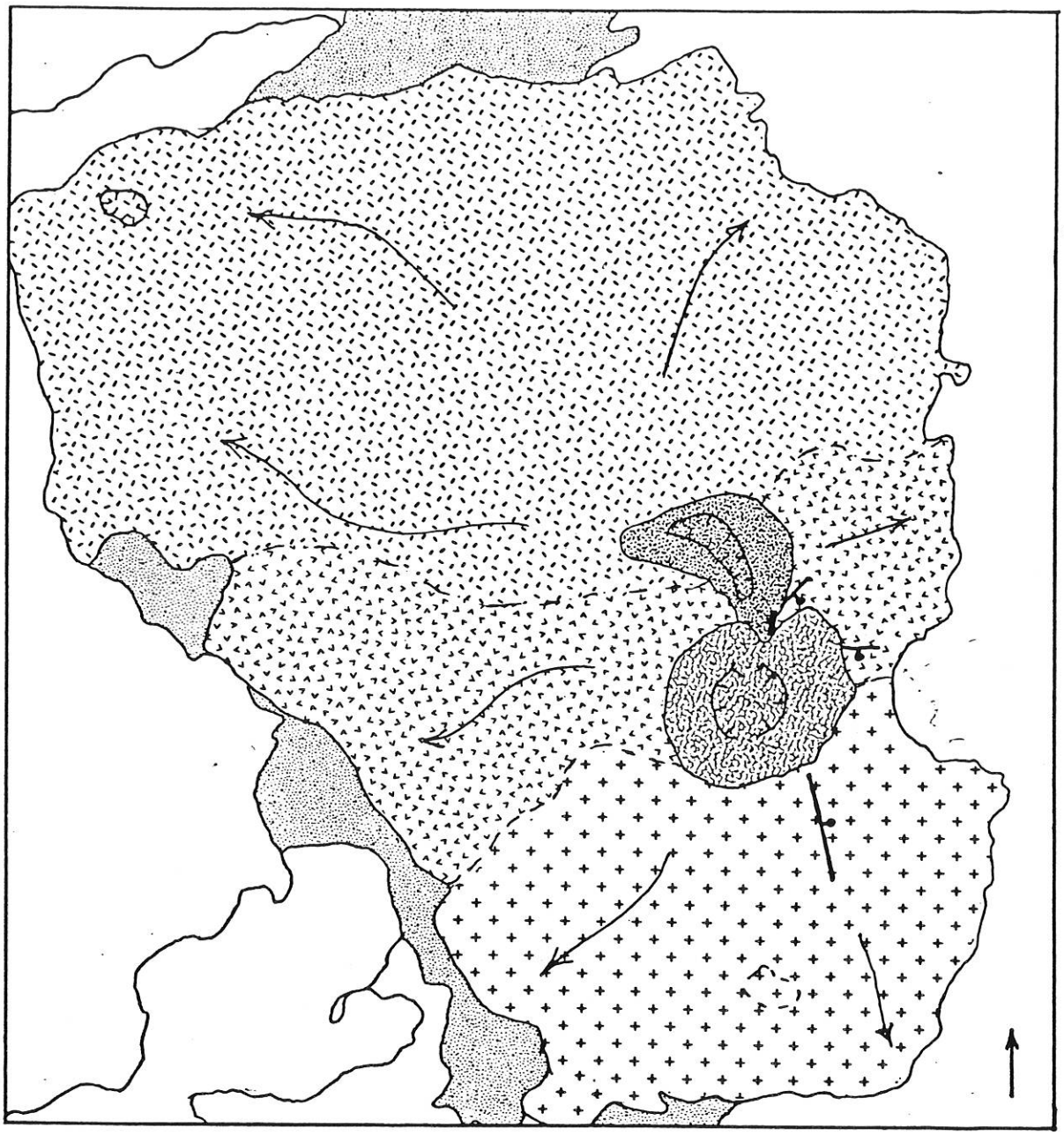


FIGURE 41. Geologic sketch map of Cedar Butte.

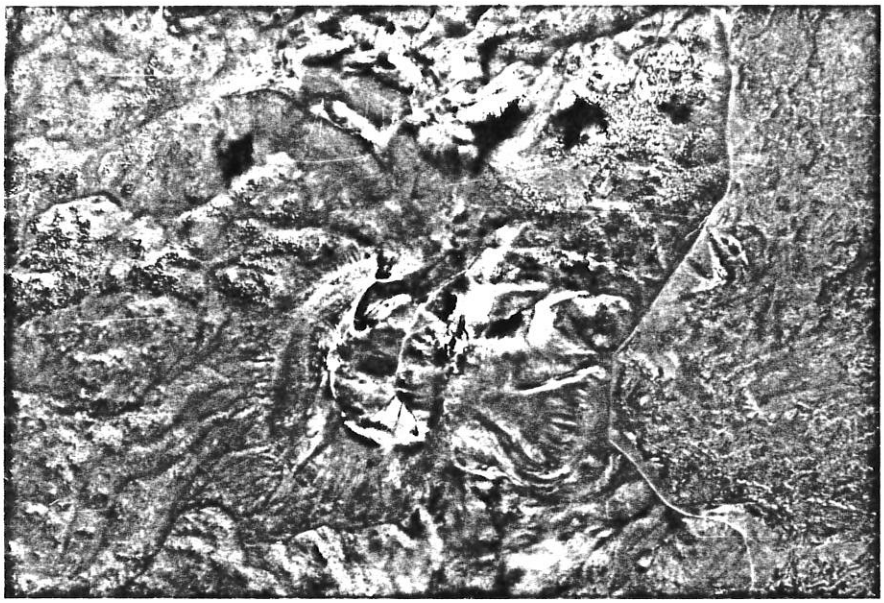


FIGURE 42. Aerial photo of Cedar Butte showing the vents area. North is at the top of the photo and the width of the photo is approximately 4 km.

actually two separate vents which were active at different times in the history of Cedar Butte. The pyroclastic cone is composed of buff-colored cinders and pumice, agglutinate, and minor amounts of gray, red, and black glass, some exhibiting small scale flow banding. Although no lava flows were extruded from this vent, it may overlie a slightly older vent from which the most silicic lavas were extruded. Stratigraphic position and composition of the glass (67% SiO_2) document that the development of this cone heralded the finaleruptive phase of Cedar Butte. The arcuate vent area to the north is composed of lava more basic in composition (58% SiO_2) and was active during an earlier phase in the evolution of Cedar Butte.

There is a V-shaped notch in the northern side of the pyroclastic cone which extends to its base. A dike 20 m long, 2 m wide, and a few meters high occurs in this notch; it trends N 8^{o} E and dips 85^{o} to the east (Fig. 43). The dike is composed of finely vesicular dark gray rock similar to that of the arcuate vent. A small amount of light-gray to gray-green rhyolite is exposed in a small prospect hole in the dike. In the samples studied the contact between the rhyolite and the mafic lava is well-defined in some places and gradational in others (Fig. 44). Fragments of the mafic rock within the rhyolite show similar relations. In thin section plagioclase and forsteritic olivine occur in dark, fine-grained patches within the rhyolite which is composed of a few phenocrysts set in an altered groudmass of alkali feldspar and quartz fragments. All evidence is consistent with an interpretation of the co-mingling of two partially crystalline magmas, such as have been described at Gardiner River in Yellowstone National Park (Fenner, 1938; Wilcox, 1944).



FIGURE 43. Dike at Cedar Butte. View is to the southwest; width of the dike is about 2 m.

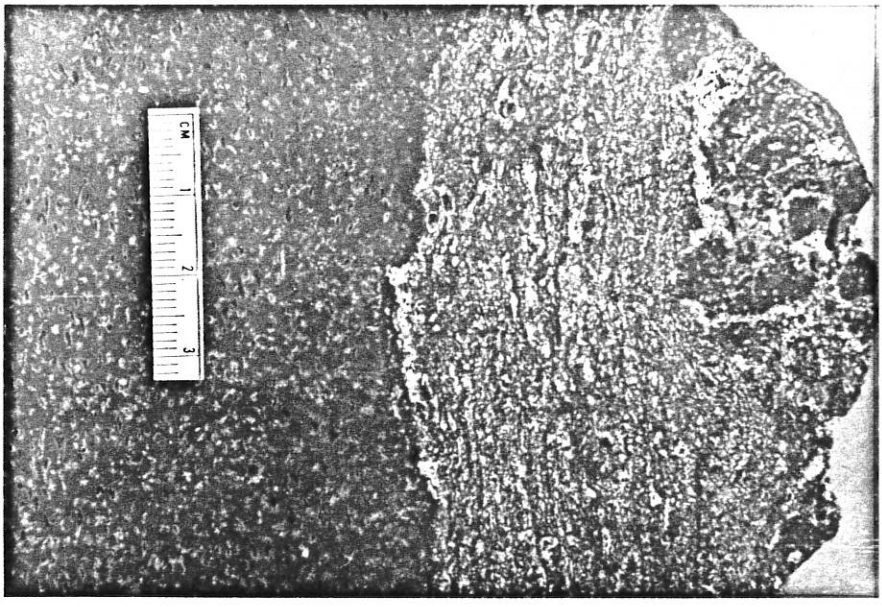


FIGURE 44. Contact between dike rock (on left) and rhyolite (on right) exposed in a prospect hole in the dike. Although this photo shows a fairly distinct contact, it sometimes appears completely gradational.

In section 17 close to the northwestern margin of the exposed lavas of Cedar Butte is a small crater, 240 m long, 120 m wide, and 25 m deep. It is aligned along a N 45° W trend. This crater does not have an elevated rim, evidence for extrusive activity, or explosion debris. It is interpreted to be a pit crater resulting from collapse. Its localization may be related to a lava tube system or more likely a buried fracture zone as is common in Hawaii. A major zone of fractures, the Arco rift zone (Kuntz, 1977), trends approximately N 45° W and terminates in the vicinity of Cedar Butte.

Petrography

The lavas of Cedar Butte are dark gray to black, very fine-grained, and contain 1 to 2 percent small (<2 mm) phenocrysts. Vesicles are abundant, comprising up to 30 percent of the rock, and attest to the high volatile content. The vesicles are characteristically stretched.

Texturally the rocks are hyalopilitic to intersertal; 10 to 30 percent of the groundmass is brown glass. Minerals present as phenocrysts include plagioclase, olivine, clinopyroxene, alkali feldspar, magnetite, apatite, and zircon. All of the minerals are not present throughout the range of lavas. The groundmass is composed of stubby laths of feldspar (usually flow-aligned), magnetite, olivine, clinopyroxene, glass and traces of apatite and zircon.

Feldspars occur as phenocrysts and are the dominant groundmass mineral throughout the suite. Plagioclase forms euhedral phenocrysts and stubby groundmass laths in the more mafic lavas; compositions range from $\sim An_{30}$ to $\sim An_{15}$. Many of the phenocrysts are partly resorbed and

the percentage of such phenocrysts increases with decreasing An content. In the more silicic lavas (>61% SiO_2) euhedral sanidine is the dominant phase. In the latite glass most of the sanidine crystals display evidence of reaction with the host liquid, such as rounded and embayed crystal faces, a condition probably due to a sudden decrease in pressure during eruption.

Olivine is present as phenocrysts throughout the suite and as groundmass grains in the more mafic lavas. Phenocrysts are typically euhedral; they increase in size but decrease in number as SiO_2 increases. Compositons are estimated to range from about Fo_{55} to Fo_5. The color of the olivine changes from pale yellow-green to pale golden-amber with increasing iron-magnesium ratio of the rock.

Clinopyroxene occurs in all rocks as phenocrysts and as groundmass grains, but phenocrysts are rare in the most mafic lavas. Throughout the compositional range the clinopyroxene exhibits a striking color transition from a non-pleochroic, almost colorless variety in the mafic lavas, through a slightly pleochroic, greenish-brown type, to a pleochroic, grass-green variety in the latite glass. This probably is related to an increase of iron and sodium in the pyroxene.

Magnetite is present as phenocrysts and groundmass grains in all rocks. Apatite occurs with magnetite phenocrysts and as groundmass grains throughout the suite, although it is rare in the more silicic lavas. Zircon is also present as a microphenocryst phase in the most silicic lavas (>64% SiO_2). Figure 45 summarizes the mineralogical data for the lavas of Cedar Butte. Representative textures are shown in Figure 46.

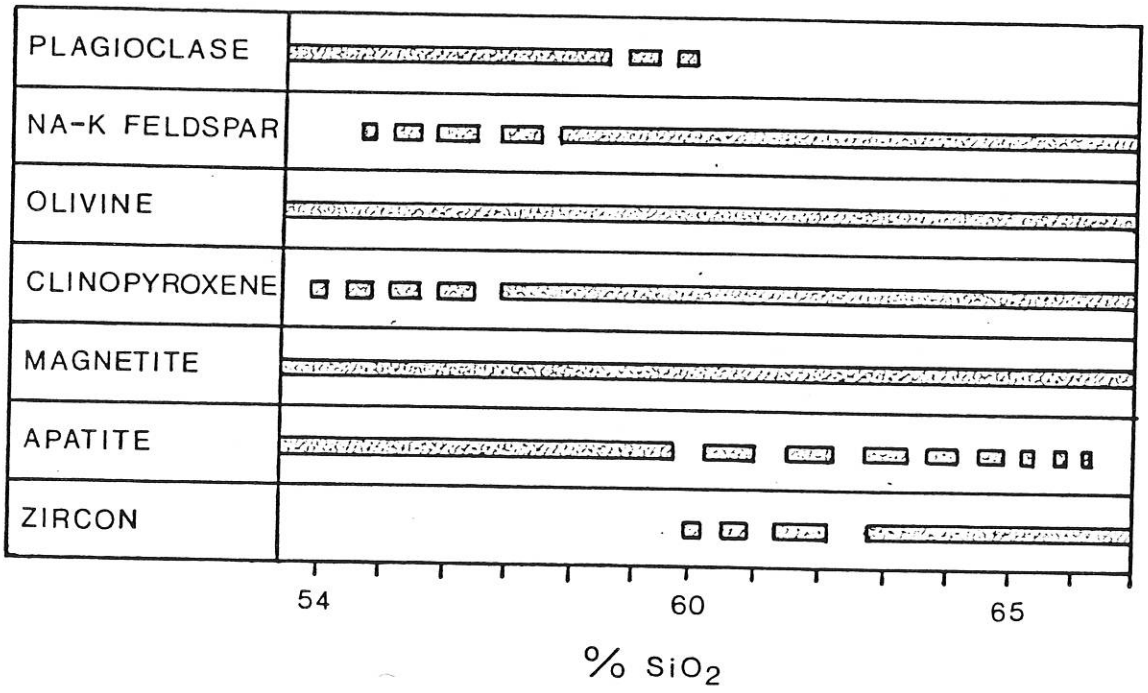


FIGURE 45. Phenocryst assemblages of Cedar Butte lavas relative to percent SiO_2.

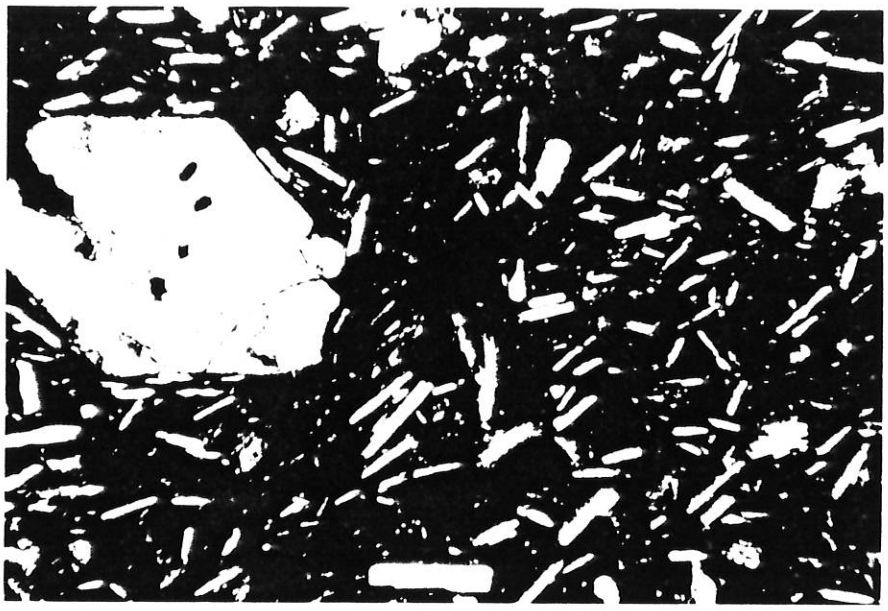


FIGURE 46a. Photomicrograph of Cedar Butte lava. Large crystal in northwest corner is olivine; laths are plagioclase. Groundmass is mostly glass. Field of view is 2.50 mm by 1.62 mm.



FIGURE 46b. Photomicrograph of Cedar Butte lava. Large euhedral plagioclase crystals (light-colored) and intergrown clinopyroxene. Groundmass is primarily glass and plagioclase laths. Field of view is 2.50 mm by 1.62 mm.

Petrology

Volcanic rocks from Cedar Butte form a suite spanning the range of intermediate to rhyolitic compositions. Chemical analyses and CIPW norms for 16 samples are presented in Table 7. Sample locations and brief petrographic descriptions are given in Appendix C.

Major element compositons vary smoothly with increasing SiO_2: total iron, TiO_2, MgO, CaO, and P_2O_5 decrease, Na_2O and K_2O increase, and Al_2O_3 remains relatively constant throughout (Fig. 47). Compositions of Cedar Butte lavas plotted on an AFM diagram (Fig. 48) demonstrate the characteristic iron enrichment and strong alkali enrichment. All observed major element trends can be produced by fractional crystallization of phases present as phenocrysts. An example of fractionation calculations using the method of Bryan and others (1969) is given in Table 8. Phenocryst compositions were determined by optical methods or estimated from analyses of minerals by Leeman (1974) from Craters of the Moon National Monument.

Comparison of rare earth element abundances (Table 9) throughout the suite provides additional evidence in support of fractional crystallization. The rare earths show a steady increase in total abundance and in relative enrichment of the light rare earths (Fig. 49). A negative Eu anomaly characterizes the more evolved members of the suite. The rhyolite does not follow the pattern and has lower overall abundances relative to the latite glass; this and the fact that there are no phases present which could produce the pattern leads to the conclusion that the rhyolite is not related to the lavas of Cedar Butte by fractional crystallization.

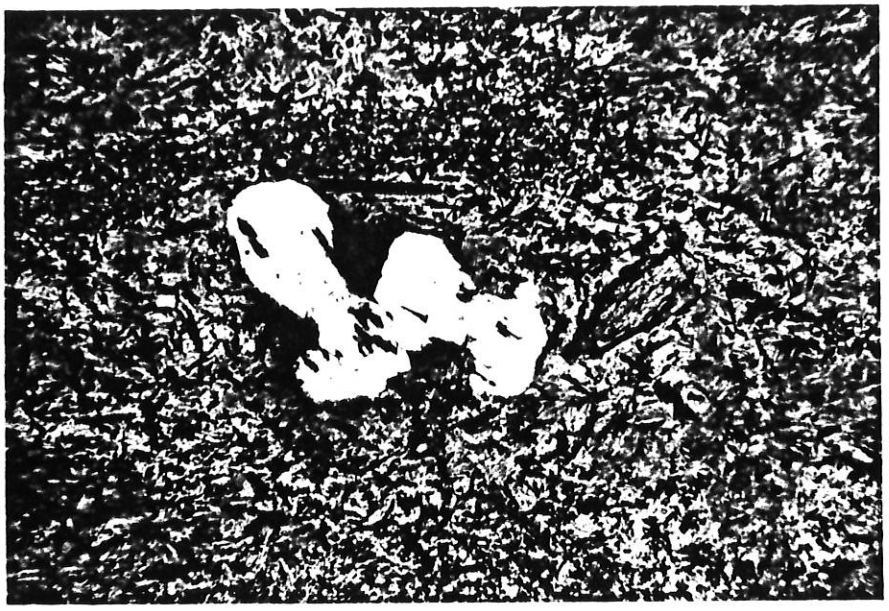


FIGURE 46c. Photomicrograph of Cedar Butte latite glass from pyroclastic cone. Embayed sanidine crystals and clinopyroxene (right of sanidine) with fayalite overgrowths are set in a glassy matrix. Field of view is 2.50 mm by 1.62 mm.

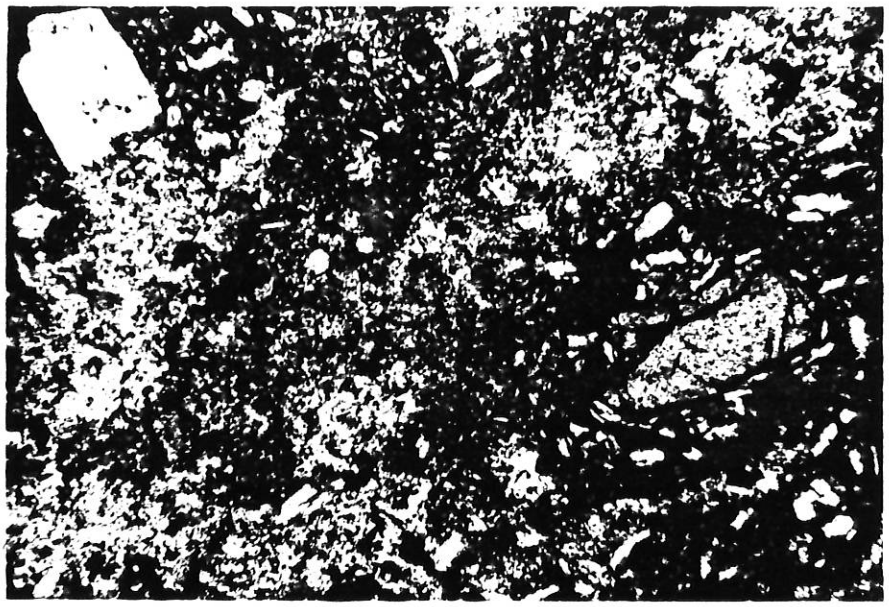


FIGURE 46d. Photomicrograph of rhyolite found at Cedar Butte. Sanidine crystal is seen in northwest corner; groundmass is devitrified and altered. Dark patch in southeast corner is part of mafic dike rock. Large crystal is olivine which is surrounded by plagioclase laths and magnetite granules. Note absence of sharp boundary between rhyolite and dike rock. Field of view is 2.50 mm by 1.62 mm.

A11

TABLE 7. Major element analyses and CIPW nor

	FLOWS		DIKE	
	CB-1[1]	CB-2	CB-3	K-CB[2]
SiO_2	54.32	56.5	58.4	56.9
TiO_2	1.88	1.67	1.53	1.6
Al_2O_3	13.64	13.4	13.3	13.9
Fe_2O_3	1.67	---	---	1.8
FeO	11.90	12.44*	12.09*	10.4
MnO	.38	.31	.31	.27
MgO	1.74	1.60	1.22	1.3
CaO	5.66	6.14	4.47	4.7
Na_2O	3.75	3.55	3.86	3.9
K_2O	3.14	3.17	3.27	3.3
P_2O_5	.76	.63	.54	.46
H_2O^+	.54	---	---	.69
CO_2	.29	---	---	.02
Loss on ignition	---	1.09	.54	---
TOTALS	99.68	100.5	99.5	99.2
Q	3.00	6.55	8.35	5.97
Or	18.62	18.61	19.38	19.60
Ab	31.84	29.84	32.75	33.17
An	11.15	11.19	9.33	10.73
Di Wo	4.26	4.81	3.91	3.99
Di En	.91	1.02	.68	.74
Di Fs	3.64	4.13	3.55	3.56
Hy En	3.44	2.94	2.37	2.51
Hy Fs	13.79	11.95	12.42	11.99
Mt	2.82	2.59	2.55	2.62
Il	3.58	3.15	2.91	3.05
Ap	1.81	1.48	1.28	1.10

NOTE: Norms calculated with $Fe^{3+}/Fe^{2+} = 0$

1 and 2 refer to analysts; see Appendix C.

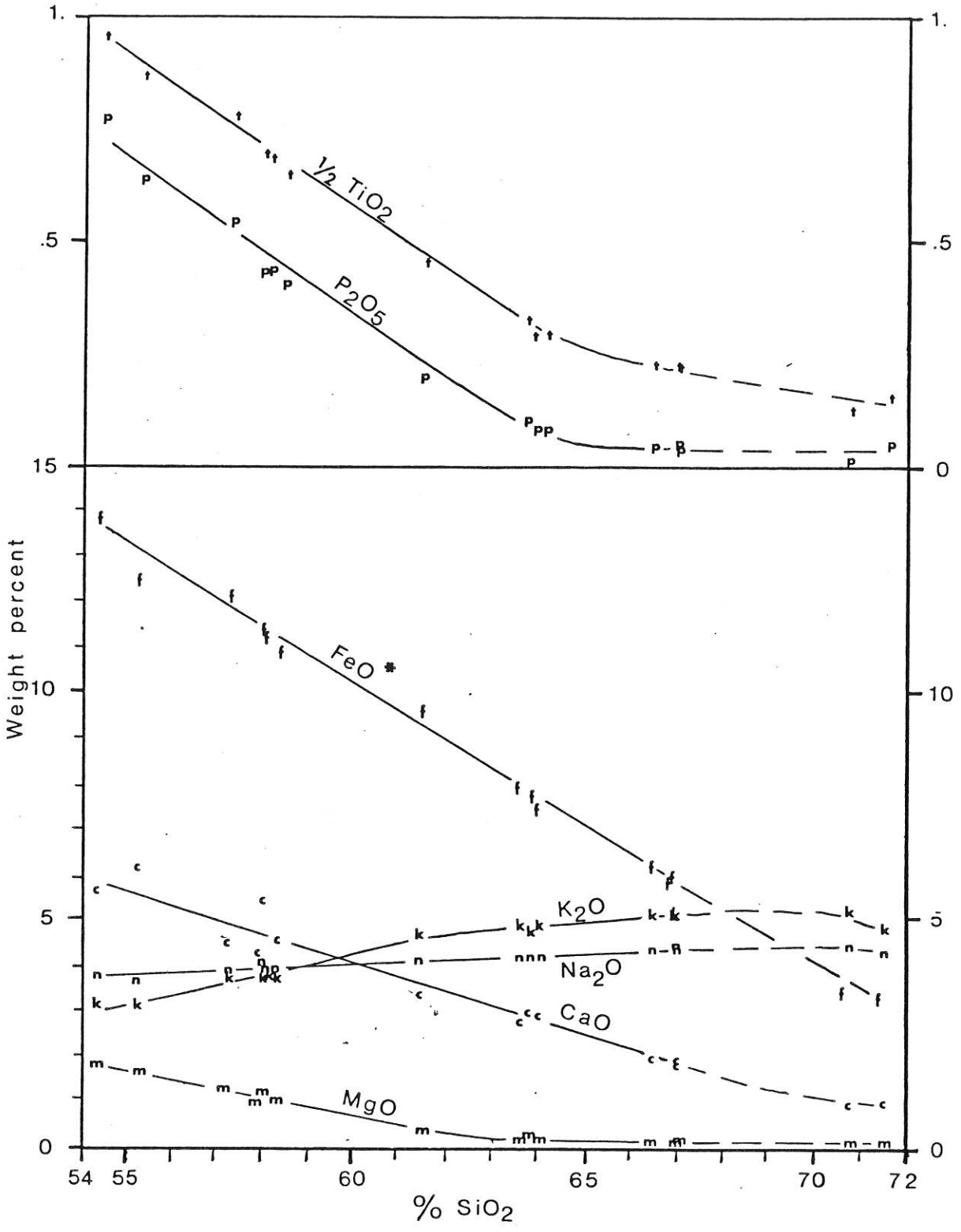


FIGURE 47. Major element variation diagram for Cedar Butte lavas. FeO* is total iron determined as FeO.

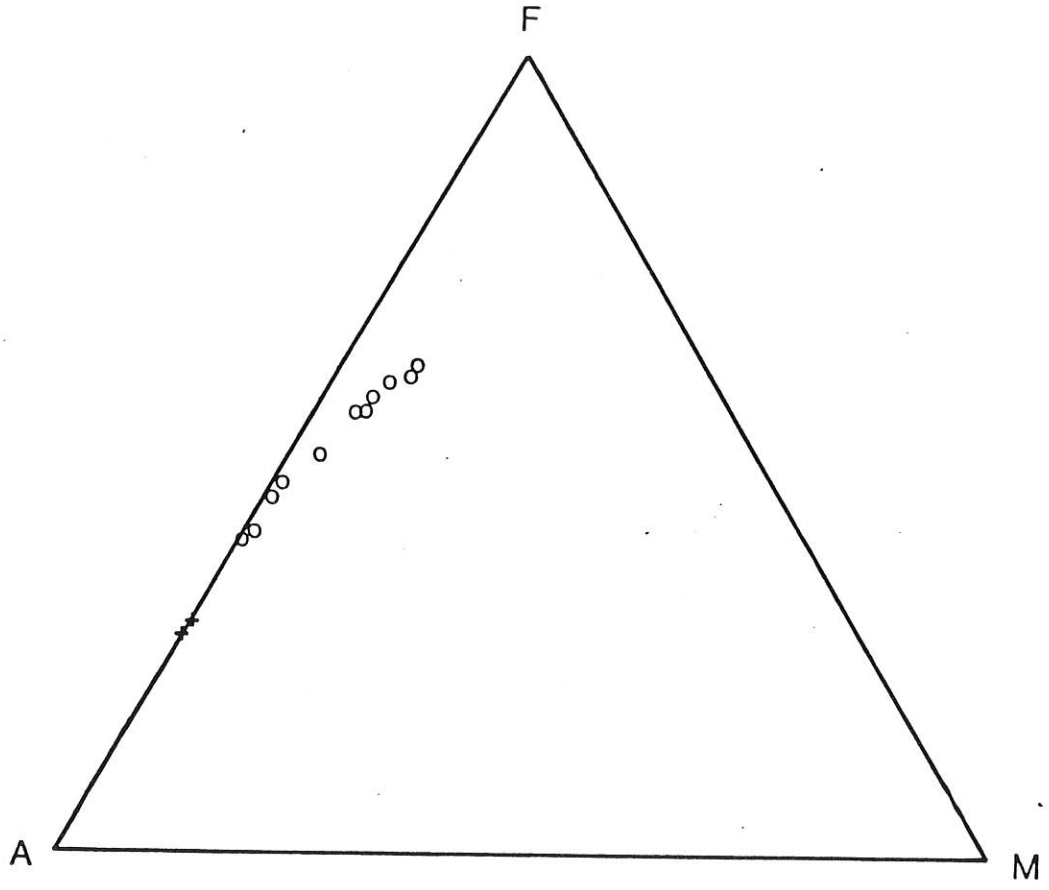


FIGURE 48. AFM diagram for Cedar Butte lavas (circles) and rhyolite which occurs at Cedar Butte (crosses).

PARENT	DAUGHTER	MINERALS					F	Σr^2
CB-1	CB-6	Pl_{41}	Ol_{61}	Mt	Cpx	Ap	0.803	0.265
		0.10	0.021	0.048	0.018	0.008		
CB-6	CB-8	Pl_{41}	Ol_{61}	Mt	Cpx	Ap	0.805	0.146
		0.082	0.015	0.015	0.077	0.007		
CB-8	CB-11	Pl_{35}	Ol_{61}	Mt	Cpx	Ap	0.093	0.328
		0.064	0.008	0.03	0.02	0.03		
CB-11	CB-14	Pl_{35}	Ol_5	Mt	Cpx	Ap	0.882	0.302
		0.066	0.023	0.009	0.014	0.005		

Mineral compositions used:

	Pl_{41}	Pl_{35}	Ol_{61}	Ol_5	Cpx	Mt	Ap
SiO_2	56.8	59.87	35.41	30.56	47.54	.52	.41
TiO_2	.01	.04	.08	.72	.59	24.66	.01
Al_2O_3	25.6	24.91	.30	.09	1.81	2.29	.02
FeO*	.58	.63	33.14	60.9	26.17	66.64	1.00
MnO	---	---	.49	3.43	.44	.77	.01
MgO	.05	.02	29.58	3.47	4.82	2.75	.41
CaO	8.11	7.35	.35	1.13	18.10	.26	54.70
Na_2O	6.04	6.74	---	---	.48	---	---
K_2O	.82	1.15	---	---	---	---	---
P_2O_5	---	---	---	---	---	---	42.00

TABLE 8. Example of crystal fractionation model for Cedar Butte lavas.

	CB-1	CB-3	CB-6	CB-8	CB-11	CB-14	CB-16
Ce	369.9	410.6	363.9	427.8	527.0	797.3	386.0
Nd	259.4	249.0	240.0	273.9	334.8	467.3	211.4
Sm	164.5	161.4	156.3	172.0	200.9	260.2	159.0
Eu	137.5	130.2	130.8	136.6	101.1	86.5	28.6
Dy	90.1	94.1	90.5	90.7	111.9	130.3	124.8
Er	85.1	84.5	80.4	86.5	99.9	115.6	112.4
Yb	74.2	79.5	76.9	87.5	97.8	109.8	101.0

TABLE 9. Rare earth element contents of samples from Cedar Butte (Fountain and Spear, in preparation).

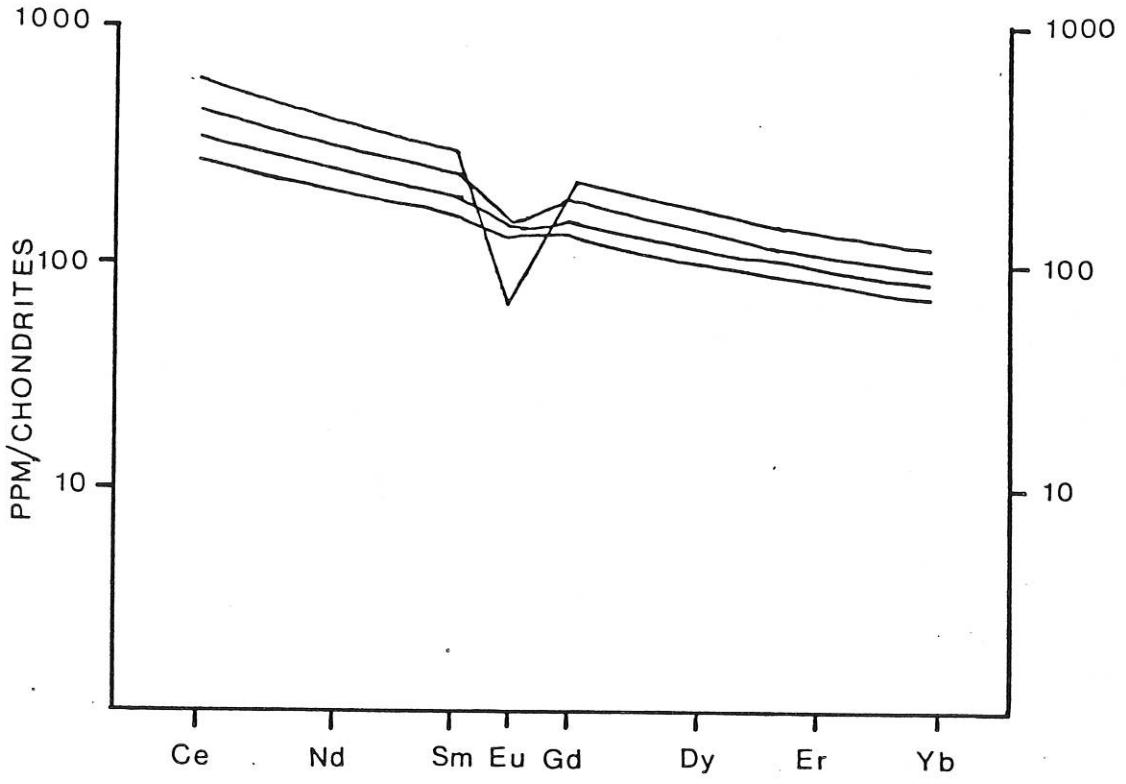


FIGURE 49. Rare earth element diagram for Cedar Butte evolved tholeiite lavas. With increase in differentiation there is an increase in total abundance of rare earths; the negative Eu anomaly also becomes more pronounced. The rhyolite found at Cedar Butte does not follow the pattern seen above and is not included; it is not a member of the Cedar Butte evolved tholeiite suite.

Origin of Cedar Butte Magma

Evolved tholeiite magma of Cedar Butte is believed to have originated through fractional crystallization of an olivine tholeiite parent magma. This conclusion is based on results of experimental studies of similar lavas by Tilley and Thompson (1970), Thompson (1972), and Leeman (1974).

There are, however, restrictions on just how and where the evolved magma can develop. Stone (1970) and Tilley and Thompson (1970) showed that the gap between the olivine tholeiites and the evolved tholeiites cannot be bridged by fractional crystalliztion of phenocryst phases in the olivine tholeiites, namely olivine and plagioclase. Thompson (1972) demonstrated that a link could be made if clinopyroxene was present on the liquidus with olivine and plagioclase and showed that there are only two pressures, 8 kbar and 26 kbar, when these three phases are on the liquidus for both magmas. He determined that the interstitial liquid formed during crystallization at 8 kbar very nearly matched the composition of the evolved tholeiites, whereas that which formed at 26 kbar did not. Thompson (1972) therefore concluded that the iron-rich andesine-normative evolved tholeiite lavas of the Snake River Plain originated by partial (50%) crystallization of a hydrous olivine tholeiite magma at a pressure of approximately 8 kbar. Leeman and others (1976) arrived at basically the same conclusion from their study of Craters of the Moon lavas.

Another feature of evolved tholeiites is their apparent contamination by crustal material. Leeman and others (1976) showed that the Sr^{87}/Sr^{86} ratios increase from 0.708 to 0.712 with increasing differ-

entiation in the Craters of the Moon lavas. However, as documented by fractionation calculations for Cedar Butte lavas in Table 8 and those of Leeman (1974) for Craters of the Moon lavas, most of the changes in major element chemistry within a suite can be accounted for by fractional crystallization of the phases present as phenocrysts. Consequently, contamination may have been minor or selective. Strontium isotopic studies have not been conducted on Cedar Butte lavas but a hypothesis of contamination is consistent with the patterns seen on AFM and variation diagrams. Note in Figures 47 and 48 that the more evolved lavas of Cedar Butte and the rhyolites in the study area fall on mixing lines. This may suggest that the rhyolites have somehow been involved during the evolution of the Cedar Butte magma. This idea will be developed in a later section.

In conclusion, Cedar Butte magma is believed to have developed through fractional crystallization of an olivine tholeiite magma at a pressure of approximately 8 kbar. The magma was emplaced at some depth beneath Cedar Butte where it underwent further differentiation and minor progressive contamination by crustal material. Subsequent eruptions produced the lavas which make up the large volcanic shield.

BASALTIC VOLCANISM

Within the map area 25 olivine tholeiite basalt lava fields of varying areal extent have been mapped (Plate 3). Rather than discuss each flow separately, a general discussion of eruptive style and the petrology of the flows within the study area will be presented. Significant features or characteristics of individual flows are noted on the geologic map.

Eruptive Style

The eruptive style of the basaltic volcanism of the eastern Snake River Plain has its own unique characteristics. The combination of the features of basaltic flood eruption such as the Columbia River area and major shield-building eruptions typified by Hawaii and Iceland, led Greeley (1976) to propose the term basaltic plains for this intermediate type of volcanism. Basaltic plains volcanism is therefore characterized by extensive outpouring of very fluid lavas from low shield volcanoes. Individual eruptive centers have a relatively short life span, probably on the order of a few years or less. The present surface of the Snake River Plain is envisioned by most workers to have developed through the overlapping of numerous such eruptive centers much in the manner proposed by Rutten (1964) for parts of Iceland (Fig. 50).

Lava Flows. Pahoehoe flows are the dominant flow-type in the map area and are typically characterized by relatively smooth surfaces. Small scale surface features such as ropy pahoehoe are common on fresh flows (Fig. 51). Thicknesses average about 10 m, although localized

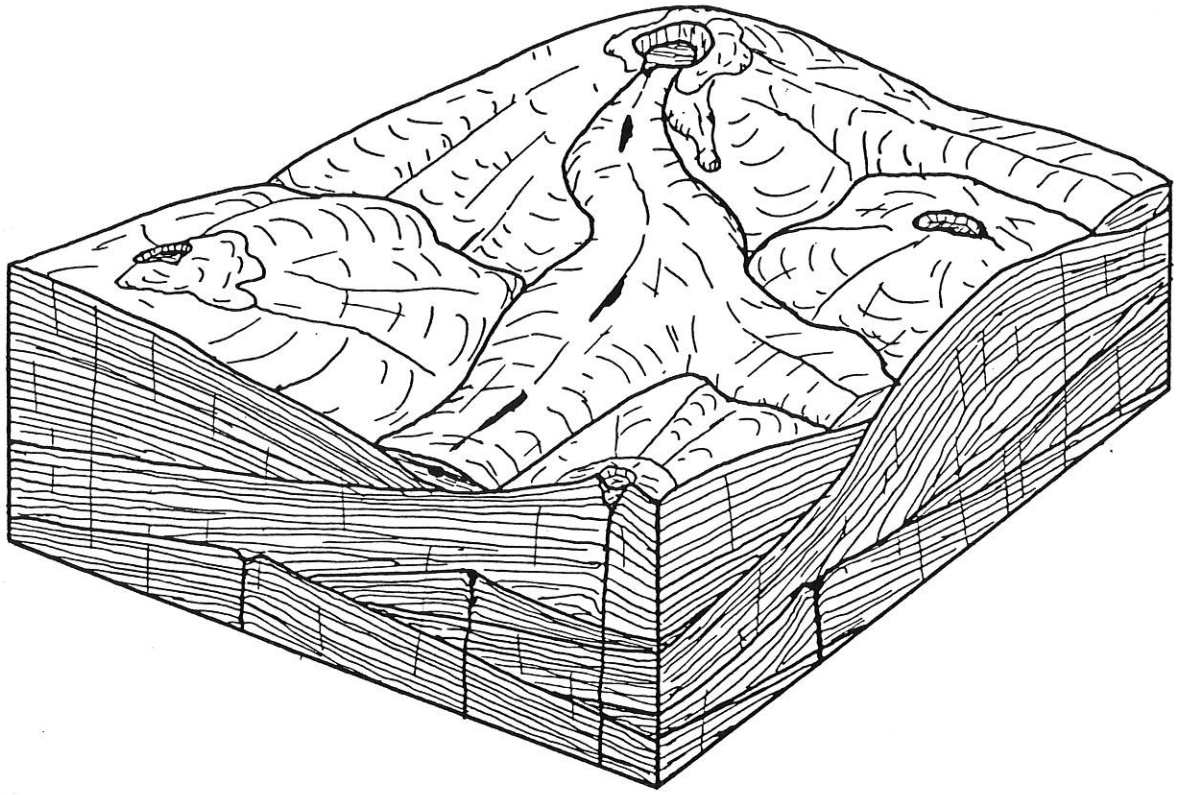


FIGURE 50. Hypothetical development of surface of the Snake River Plain through basaltic plains style volcanism (after Greeley, 1977).



FIGURE 51. Example of ropy pahoehoe on the Cerro Grande Flow.

areas of flows may be as much as three times the average. Exposures in pressure ridges and collapse depressions away from vent areas show that the flows are composed of a number of flow units 0.5 to 5 m thick. Overlapping flow units are separated by a time interval ranging from minutes to perhaps more than a year and are the result of coalescing pahoehoe toes and/or pulses of magma. Walker (1972) classifies flows made up of flow units as compound flows and relates their development to a low rate of extrusion and a low viscosity.

Lava tubes have played an important, but poorly understood, role in the emplacement of many of the pahoehoe flows. Tubes or channels are present in 8 of the 25 flow fields; the total number is probably greater but may are no longer recognizable due to loess cover. Greeley's

estimate (1977) that roughly one-fifth of all flows of the Snake River Plain have tubes or channels is a little low for the flows within the study area. Perhaps the lack of detailed mapping throughout most of the Snake River Plain may account for the difference.

Fresh pahoehoe surfaces, such as those on the Cerro Grande Flow, have as much as 10 m of local relief produced by primary features such as collapse depressions (Fig. 52) and pressure ridges (Fig. 53). With time most of these features become obscured by the accumulation of loess resulting in a smoothing of the topography

Examples of aa lava are not common within the boundaries of the map area. A few localized occurrences are present on the Cerro Grande Flow and the surfaces of two small flows, North Robbers and in paricular South Robbers (Fig. 54). Greeley (1977) interpreted the South Robbers Flow as having been emplaced as pahoehoe but transformed into aa during the final stages of flow. He reports that such transformations have been observed during the emplacement of flows on Mount Etna.

Volcanoes. A wide variety of basaltic constructs, such as shield volcanoes, lava cones, pyroclastic cones, and phreatomagmatic cones, occur within the area; their distribution is noted on the geologic map. The dominant type of construct is the broad, low shield volcano from which most flows were extruded. The slopes of this type of volcano are generally low, ranging from 1^{o} to 10^{o}, and most terminate with a summit crater (Fig. 55).

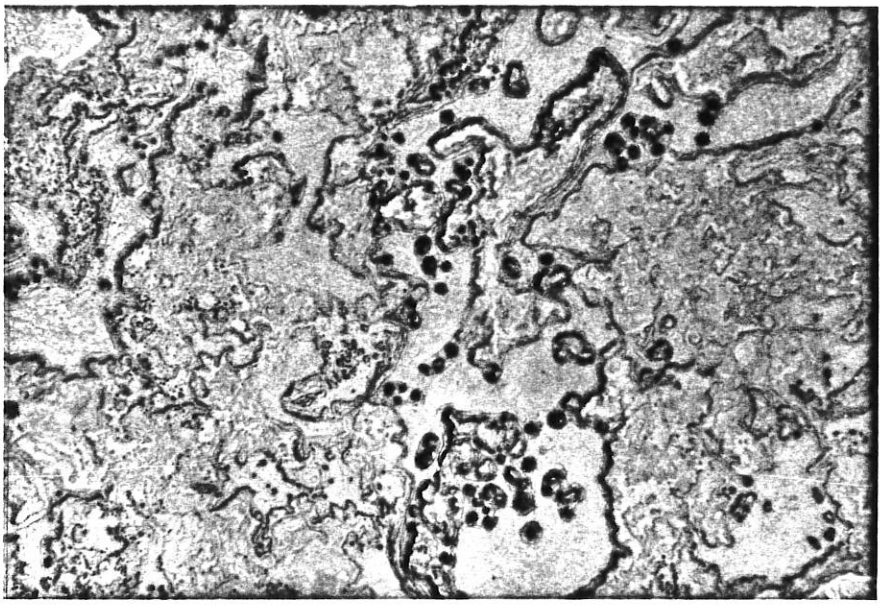


FIGURE 52. Collapse depressions of the Cerro Grande Flow. Width of photo is about 600 m.

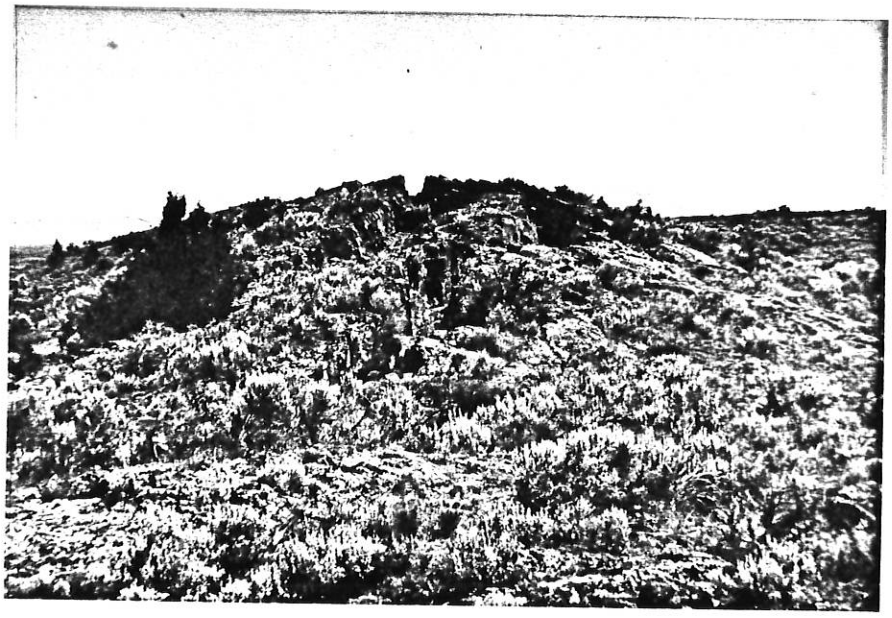


FIGURE 53. Pressure ridge on the Cerro Grande Flow (~2 m high).

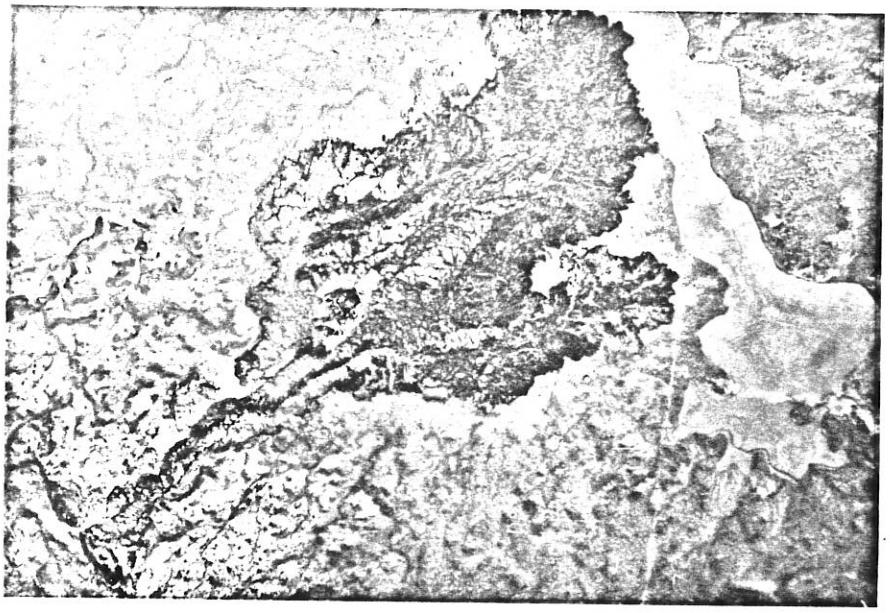


FIGURE 54. Aerial view of the South Robbers Flow showing the dark aa lava surface. Width of photo is approximately 3 km; north is at top of photo.

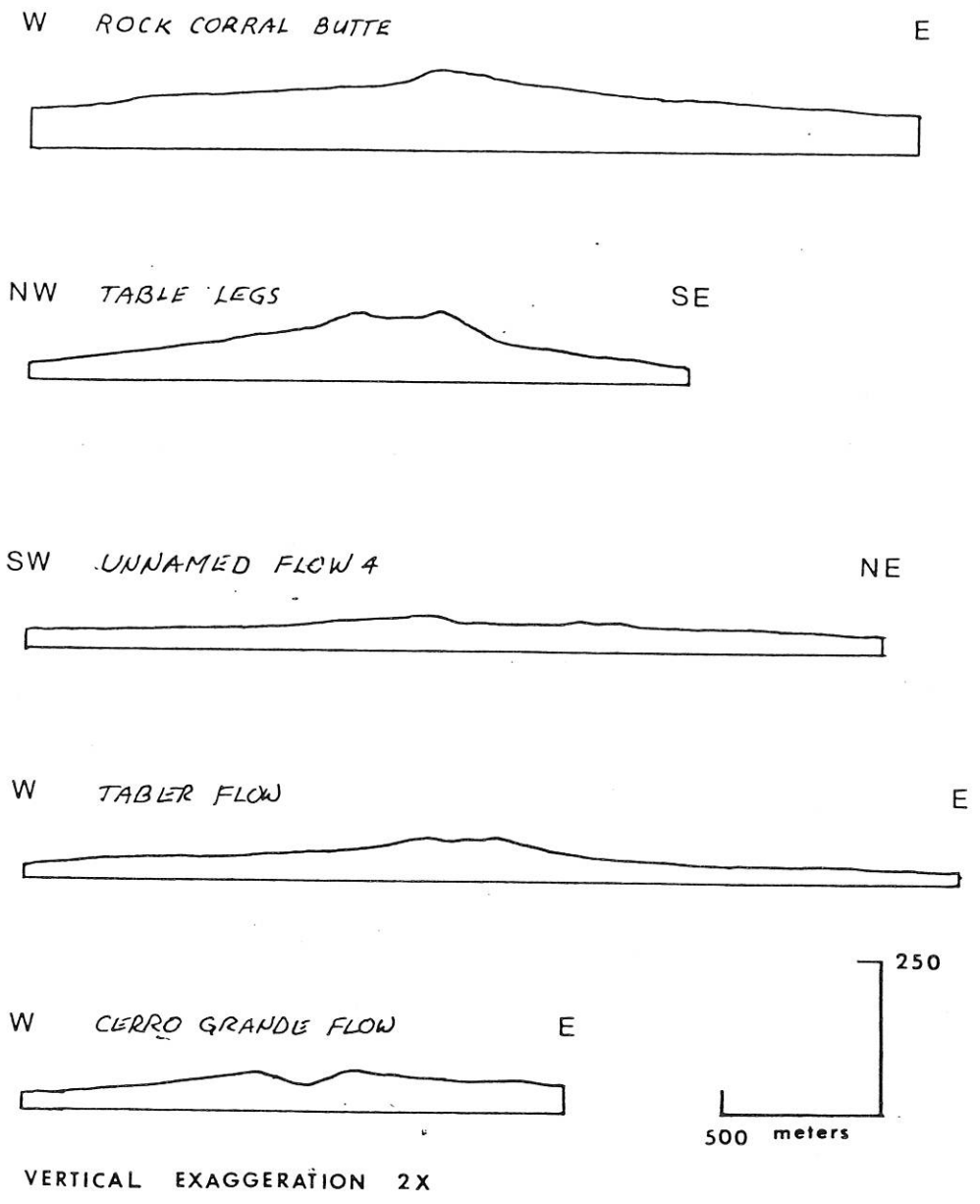


FIGURE 55. Topographic profiles of typical shield volcanoes from the Snake River Plain.

Flow Stratigraphy

The surface morphology of the eastern Snake River Plain has developed through extrusions of fluid basaltic lavas and the deposition of wind blown silt (loess). By combining the overlap relations of the basalt flows with the estimated amount of loess cover, a relative stratigraphy can be established. Although the assumption that loess deposition has been a continuous process throughout the Pleistocene may be tenuous, it does permit a working chronology to be developed until a systematic dating program is conducted.

The criteria which were used for the grouping of flows in the map area are summarized in Table 10. The schemes developed by other mappers in the Snake River Plain (LaPoint, 1977; Karlo, 1977; Kuntz, 1978) were consulted in order to maintain conformity necessary for comparisons of different areas. The relative stratigraphic sequence developed for the map area is presented on the geologic map. Characteristics of individual flows are also included.

Petrology

Petrography. Over 200 samples from all flows present in the map area were examined with a binocular microscope and 120 were selected for thin sections.

The basalts are all dark gray to black in color and are characteristically vesicular. All samples studied were porphyritic with olivine and plagioclase as the phenocrysts, although not always occurring together. The phenocrysts commonly comprise 5 to 20 percent of the total rock (less vesicles) with plagioclase the dominant phase. Small

GROUP	CHARACTERISTICS
A	Fresh, unweathered flow surfaces; less than 10 percent of the surface masked by a thin cover of loess.
B	10 to 40 percent of flow surface obscured by loess accumulating up to 1 m locally; primary flow features such as pressure ridges and flow fronts are distinct.
C	40 to 70 percent of flow surface is covered by loess, up to 3 m locally; flow fronts and pressure ridges are subdued but identifiable; intermittent streams are present on most flow surfaces.
D	At least 70 percent of flow surface heavily loess covered, commonly more than 3 m thick; outcrops are not common; flow fronts are identifiable only as inditinct topographic rises, other primary flow features are generally absent.

TABLE 10. Criteria used to establish relative stratigraphy in addition to overlap relations.

cubic spinel crystals occur as inclusions in many of the olivine phenocrysts. The groundmass of most samples is composed of plagioclase, olivine, clinopyroxene, magnetite, ilmenite, a trace of apatite, and brown glass. Most vesicles are filled with secondary calcite and some by chalcedony or opal.

A variety of textures are present in the samples studied. They range from subophitic to ophitic in samples collected from massive flow interiors to hyalopilitic to intersertal in samples collected from flow surfaces. Because of the varied textures within one flow and the lack of mineralogical variation between all flows, an intangible quality called "overall appearance in hand sample" proved to be the most reliable means of correlation.

As has been observed in all other studies of Snake River Plain basalts (see Stone, 1967; Leeman, 1974; Karlo, 1977), the mineralogy is remarkably similar throughout. Detailed mineralogical studies were not conducted in this study, but a number of universal stage determinations of olivine and plagioclase compositions were made as a means of comparison with the more detailed studies of others. The compositions are noted, where applicable, in the descriptions of the flows on the geologic map. The mineralogical characteristics of Snake River Plain basalts established through this study and from the investigations of Stone (1967) and Leeman (1974) are summarized in Table 11.

Major Element Compositions. Major element analyses and CIPW norms for 19 basalts representing 12 different flows are reported in Table 12. The norms were calculated after setting the ratio $Fe^{3+}/Fe^{2+} = 0.15$; this eliminates the effects of secondary oxidation present in some

	PHENOCRYST MINERALS
PLAGIOCLASE	Euhedral tabular and lath-shaped crystals; some show oscillatory zoning; may contain inclusions of olivine of spinel; oftern occurs with olivine in glomeroporphyritic clusters; compositions normally range from An54 to An 72; sizes range serially up to 3 cm with 5 mm about average; comprises 30 to 90% of total phenocrysts.
OLIVINE	Euhedral equant crystals, slthough most are fragments; often contain small opaque spinel inclusions; partial to complete alteration to iddingsite is common; often occurs with plagioclase in glomeroporphyritic clusters; sizes range from 1 to 3 mm; compositions range from Fo70 to Fo85; makes up 20 to 100% of total phenocrysts with 40% about average.
	GROUNDMASS MINERALS
PLAGIOCLASE	Seriate euhedral lath-shaped crystals averaging 0.3 mm; composition of groundmass grains range from labradorite to calcic andesine; total plagioclase (phenocrysts + groundmass) averages 52% of total rock.
OLIVINE	Small equant crystals averaging 0.1 to 0.2 mm; compositions range from Fo50 to Fo70; total olivine (including phenocrysts) accounts for 10 to 20% of rock (by volume).
CLINOPYROXENE	Calcium-poor augite to calcium-poor ferroaugite; tan to purplish, weakly pleochroic; occurs as subhedral to anhedral ophitic to intergranular crystals.
MAGNETITE	Occurs as equant anhedral to subhedral crystals; identified as titanomagnetite.
ILMENITE	Characteristically occurs as elongate tabular or acicular crystals; identified as ilmenite-hematite solid solution.
MINOR MINERALS AND MESOSTASIS	Apatite is common in all basalts; glassy residium often comprises 10 to 13% of well-crystallized samples and is commonly brown to opaque depending on the amount of inclusions.

TABLE 11. Summary of mineralogy of Snake River Plain basalts (data from this study; Stone, 1967; and Leeman, 1974).

STRUCTURAL CONTROL OF VOLCANISM

Volcanism in the study area is localized by two dominant structural trends. One is NE-SW and parallels the longitudinal axis of the ESRP; the other is NW-SE, more or less perpendicular to the axis (Fig. 58). Although these two trends are the major ones, a N-S trend may be important in the southern part of the map area. The surface expression of the two major trends differs considerably. The NE-SW trend is distinguished by the concentration of volcanic constructs, including Big Southern Butte, East Butte, and Middle Butte, along the axis of the Plain. NE-SW lineaments are evident in aerial photos but most are believed to be related to aeolian processes; open fractures are rare. The Ne-SW trend may be due to a broad, gentle arching of the Snake River Plain producing longitudinal fractures and/ or a high thermal input concentrated along the axis at depth.

The NW-SE trend is marked by numerous open fractures, elongated craters, alignment of vents, and sites of fissure eruptions. The concentration of these features in narrow zones constitute volcanic rifts (Prinz, 1970; Greeley and King, 1975). One such volcanic rift is the Arco rift zone (Kuntz, 1977) which extends from Arco at the northern margin of the Plain southeastward into the map area terminating in the vicinity of Cedar Butte. Other rift zones identified by Kuntz (1978) for the eastern Snake River Plain are shown in Figure 59.

Many workers have noticed that when rift zones reach the margin of the Plain (particularly on the north) they are aligned with Basin and Range faults in the bordering ranges. This correlation has led to the interpretation that the rift zones are extensions of Basin and Range

TABLE 12. Major element analyses and CIPW norms of basalts within the study area.

	B-1	B-2	B-3	B-4	B-5	B-6	B-7	B-8	B-9	B-10	B-11	B-12	B-13	B-14	B-15	EB-9#	EB-10#	MB-1&	MB-2&
SiO_2	45.75	45.30	47.0	44.82	46.3	46.5	45.6	46.9	46.5	45.0	44.2	45.3	46.40	46.4	47.1	44.5	45.8	47.1	47.00
TiO_2	2.27	3.41	2.3	3.11	2.75	3.2	2.15	3.48	3.7	3.14	2.91	2.32	2.77	3.7	2.1	2.82	2.32	2.29	2.20
Al_2O_3	15.00	15.70	15.5	14.76	15.4	14.5	14.3	15.6	14.3	15.1	14.8	15.3	15.10	14.9	15.2	15.1	14.9	15.7	15.50
Fe_2O_3	1.87	2.12	3.7	2.03	---	2.4	---	---	3.4	---	---	---	2.50	2.1	1.9	---	---	---	.53
FeO	11.25	12.73	9.2	12.58	13.60*	11.6	12.55*	13.68*	11.9	14.13*	13.49*	12.15*	10.80	13.2	10.2	13.81*	12.33*	10.81*	11.40
MnO	.21	.25	.16	.22	.21	.17	.19	.19	.17	.22	.19	.19	.21	.18	.15	.19	.20	.21	.18
MgO	8.82	7.04	8.8	6.91	7.10	6.8	10.37	5.40	6.1	6.60	7.21	7.96	6.83	6.6	8.3	6.84	7.04	9.23	8.66
CaO	10.52	9.85	10.1	9.43	10.03	8.9	10.63	9.84	10.1	9.77	11.38	10.57	10.02	9.4	10.7	10.58	10.71	11.39	10.90
Na_2O	2.67	2.52	2.6	2.95	2.72	2.8	2.40	2.87	2.6	2.83	2.74	2.60	2.88	2.5	2.5	2.55	2.76	2.51	2.14
K_2O	.48	.68	.43	.85	.63	.89	.31	.64	.70	.75	.71	.75	.65	.49	.44	.65	.55	.21	.56
P_2O_5	.62	1.03	.67	1.18	.57	1.4	.44	.69	.09	.91	.84	.47	.71	.81	.55	.99	.78	.19	.48
H_2O^+	.22	.26	.23	.38	---	.45	---	---	.48	---	---	---	---	.49	.36	---	---	---	.27
CO_2	.08	.00	.00	.04	---	.02	---	---	.04	---	---	---	---	.01	.00	---	---	---	.93
Loss on ignition	---	---	---	---	.11	---	.39	.00	---	.61	1.11	1.14	---	---	---	1.17	.84	.46	---
TOTALS	99.76	100.89	100.7	99.26	99.4	99.6	99.3	99.3	100.1	99.1	99.6	98.8	98.87	100.8	99.5	100.2	99.2	100.1	100.74
Or	2.84	3.98	2.53	5.06	3.76	5.28	1.83	3.78	4.14	4.43	4.21	4.48	3.89	2.87	2.65	3.85	3.33	1.24	3.28
Ab	22.25	21.14	21.89	25.15	23.22	23.79	20.28	24.28	22.01	23.93	18.85	21.74	24.63	20.99	21.52	21.64	23.92	21.18	17.95
An	27.59	29.26	29.20	24.70	28.19	24.47	27.30	27.79	25.29	26.26	26.08	28.16	26.67	27.77	29.46	28.74	25.90	30.87	30.77
Ne	.22	---	---	---	---	---	---	---	---	---	2.39	.27	---	---	---	---	---	---	---
Di Wo	8.42	5.22	6.80	6.01	7.62	4.41	9.40	6.90	10.02	6.22	9.49	8.17	7.91	5.51	6.20	7.01	5.07	9.91	5.81
Di En	4.71	2.63	3.87	3.00	3.97	2.26	5.62	3.26	4.77	3.08	4.95	4.54	4.08	2.70	3.50	3.52	4.27	6.05	3.34
Di Fs	3.38	2.47	2.65	2.88	3.43	2.04	3.28	3.55	5.12	3.02	4.27	3.31	3.62	2.71	2.44	3.33	3.16	3.31	2.21
Hy En	---	4.26	4.96	.51	2.79	8.57	2.29	6.63	3.22	3.24	---	---	2.39	9.23	9.28	1.99	1.72	2.04	10.50
Hy Fs	---	4.00	3.40	.49	2.41	7.77	1.34	7.24	3.46	3.18	---	---	2.13	9.27	6.47	1.34	1.45	1.12	6.94
Ol Fo	12.13	7.35	9.09	9.68	7.76	4.34	12.53	2.50	15.05	7.08	9.16	10.86	7.53	3.07	5.78	8.67	7.83	10.40	5.29
Ol Fa	9.59	7.60	6.86	10.27	7.37	4.33	8.05	3.00	5.98	7.65	8.70	8.74	7.36	3.40	4.44	9.04	7.27	6.28	3.85
Mt	2.72	3.05	2.63	3.05	2.78	2.90	2.59	2.86	3.15	2.97	2.85	2.58	2.77	3.15	2.55	2.91	2.66	2.27	2.48
Il	4.32	6.42	4.35	5.95	5.27	6.10	4.08	6.61	7.03	5.96	5.55	4.45	5.32	6.97	4.06	5.37	4.51	4.34	4.14
Ap	1.47	2.42	1.58	2.82	1.36	3.30	1.04	1.63	.21	2.15	1.93	1.13	1.70	1.90	1.33	2.35	1.89	.45	1.13

NOTE: Norms calculated with $Fe^{3+}/Fe^{2+} + 0.15$. For analysts see Appendix D.

- also included in Table 4.
& - also included in Table 5.

samples and facilitates comparisons among samples. Sample locations and brief petrographic descriptions are given in Appendix D.

Based on olivine and hypersthene in the norm, the basalts are classified as olivine tholeiites according to the classification of Yoder and Tilley (1962). A plot of the samples on an AFM diagram shows that they fall within the field of other analyzed basalts from the Snake River Plain. The characteristic iron enrichment trend is evident.

The minor diversity within the basalts is due to low-pressure fractionation of olivine and plagioclase. Tilley and Thompson (1970) experimentally showed that these two phases are near-liquidus phases up to 8 kbar; above 8 kbar clinopyroxene becomes stable and dominates the differentiation. The absence of clinopyroxene as a phenocryst phase and the strong olivine and plagioclase control demonstrated in Figure 57 support the hypothesis of low-pressure fractionation. Leeman and Vitaliano (1976) conclude from their study of the McKinney basalt that the parental magma (and by implication all Snake River Plain olivine tholeiite magmas) was formed by partial melting of spinel lherzolite or aluminous pyroxene peridotite mantle at depths of 50 to 60 km. They also suggest that the magma rose quickly from that depth and underwent little high-pressure fractionation.

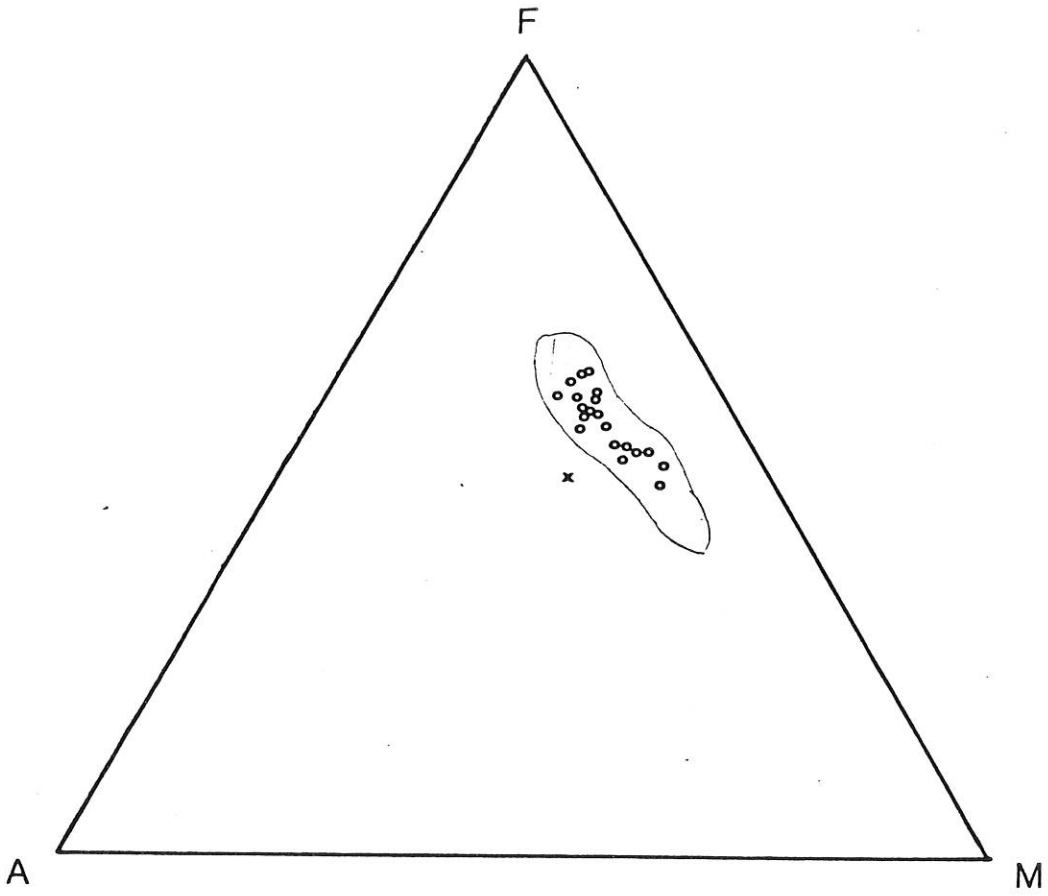


FIGURE 57. AFM plot of basalts in study area. Cross is the quartz-normative tholeiite from Big Southern Butte.

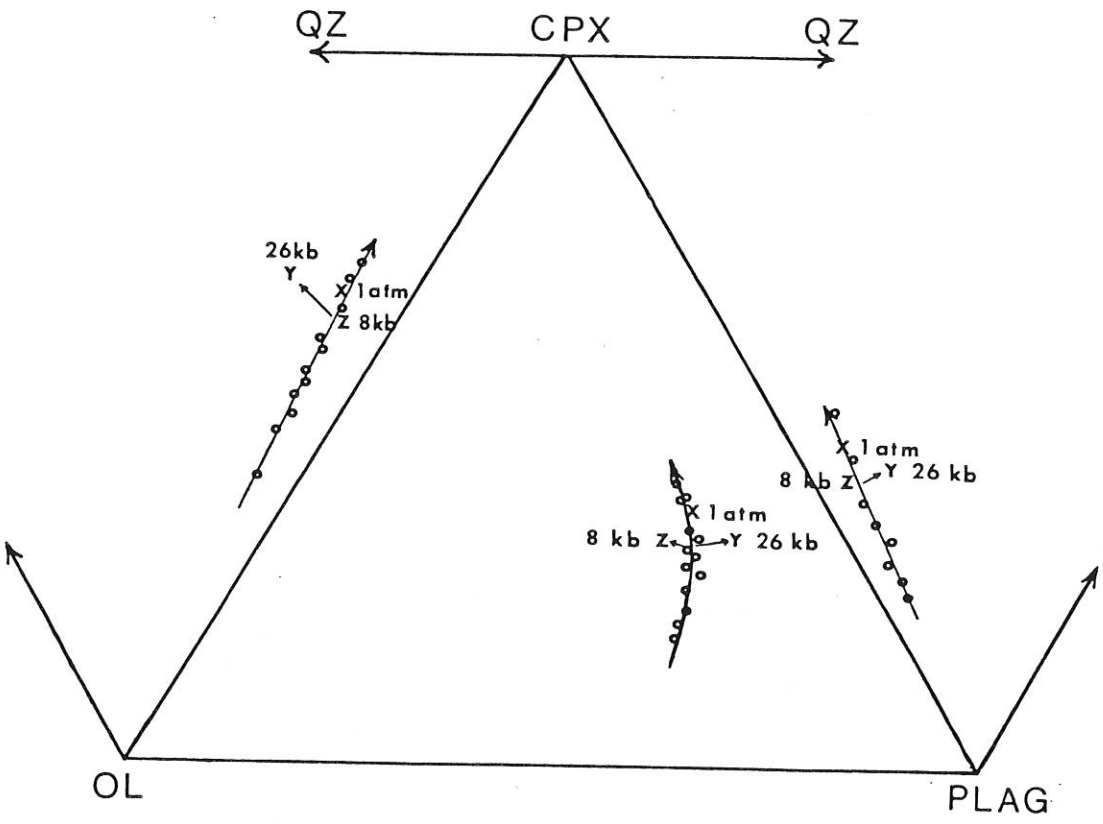


FIGURE 57. Olivine - plagioclase control diagram demonstrating that thses two phases dominate the low-pressure fractionation of olivine tholeiite magmas from the Snake River Plain (from Leeman, 1974, p. 44).

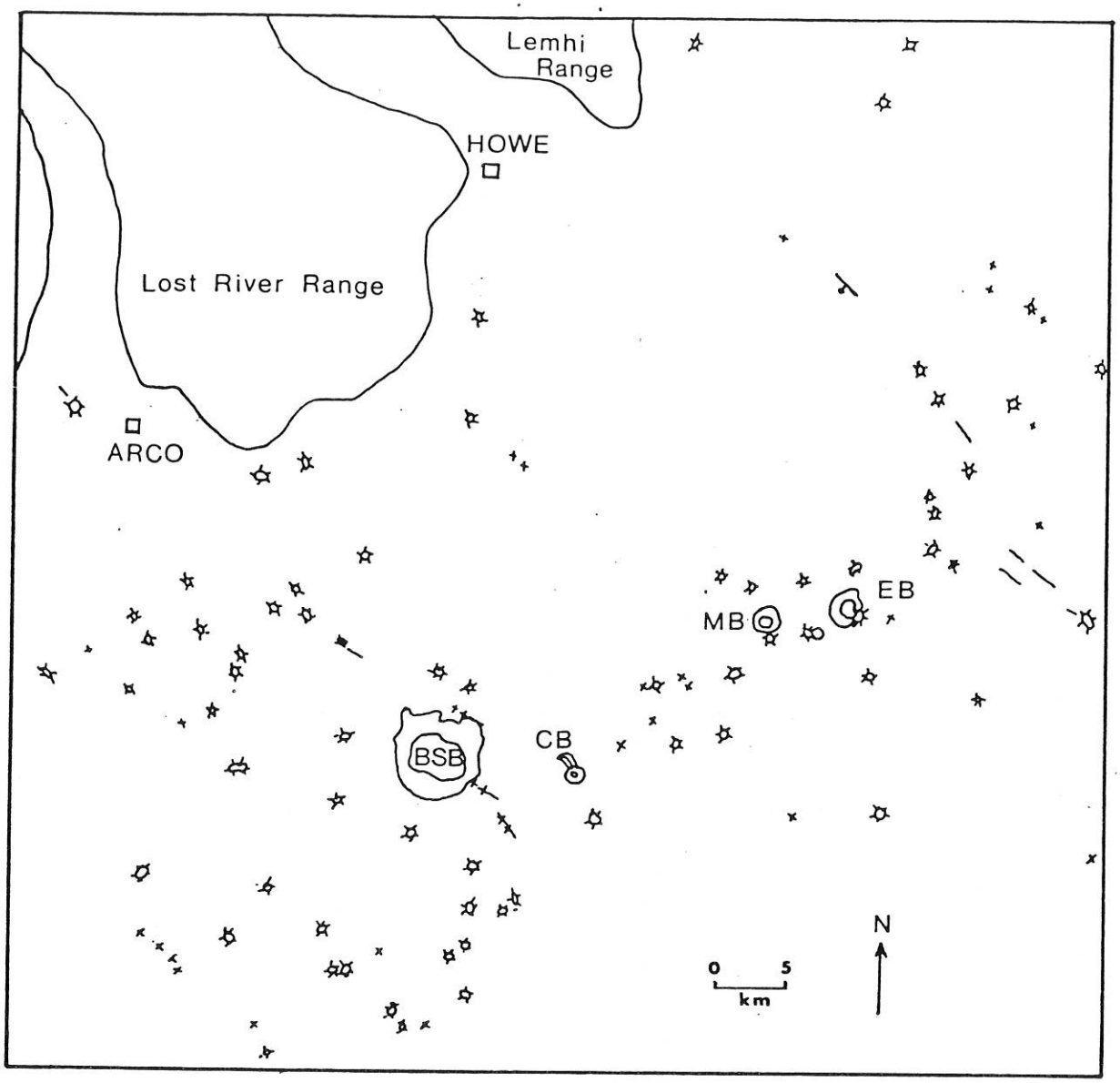


FIGURE 58. Localization of volcanism in part of the eastern Snake River Plain in the vicinity of Big Southern Butte (BSB), Middle Butte (MB), East Butte (EB), and Cedar Butte (CB). Two dominant structural trends, NE-SW and NW-SE, are defined by the concentration of volcanoes and surface fractures (NW-SE).

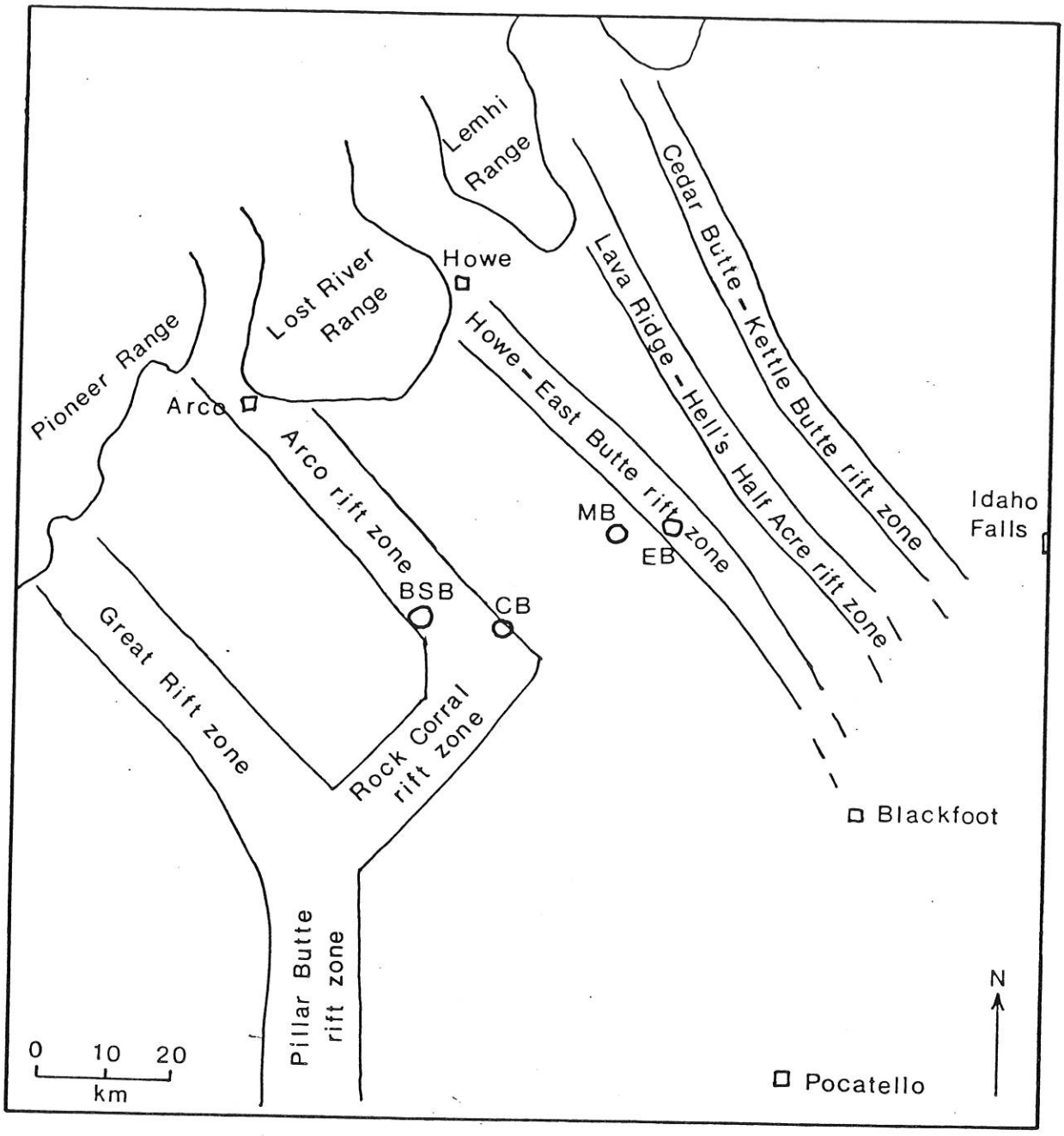


FIGURE 59. Rift zones of the central eastern Snake River Plain identified by Kuntz (1978). BSB - Big Southern Butte; CB - Cedar Butte; MB - Middle Butte; EB - East Butte.

structure onto the Snake River Plain. Aeromagnetic data (Zietz and others, 1978) show distinct highs and lows coinciding with the extensions onto the Plain; the fact that the magnetic anomalies cross the margins of the Plain adds support for the interpretation.

VOLCANIC HISTORY WITHIN THE MAP AREA

There is a dual purpose in mapping and describing the geology of an area. Besides documenting observations and establishing temporal and spatial relationships, it provides the framework for interpretation of the processes involved in producing the geology. This section will investigate the relationship of the buttes to the overall volcanic development of the Snake River Plain within the map area.

From the discussions of Big Southern Butte, East Butte, and Cedar Butte, one common feature emerged. Evolved tholeiitic rocks occur with rhyolite. At Big Southern Butte evolved tholeiite lavas preceded the emplacement of the rhyolite, at Cedar Butte they are in direct contact with and partially mixed with a small amount of rhyolite, and at East Butte an evolved tholeiite magma coexisted with a rhyolite magma long enough for minor mixing to occur and hybrid rocks formed. Because of these common occurrences it seems reasonable to infer some relationship between the rhyolite of the buttes and the evolved tholeiites.

It has been established that the rhyolites originated through fractional crystallization. This interpretation was based on the very low abundances of Sr and Ba and the large Eu anomalies for all the rhyolites analyzed. It was further noted that, based on rare earth element abundances, the rhyolites are not the end product of fractional crystallization of an olivine tholeiite (or evolved tholeiite) parent. It was therefore concluded that the rhyolites of the buttes originated from magmas produced by partial melting of crustal rocks. Pressures under which the rhyolites evolved may have been in the range of 3 to 5

kbar which is roughly equivalent to a depth of 10 to 16 km.

The origin of the evolved tholeiite magma is believed to be due to fractional crystallization of an olivine tholeiite magma under a pressure of approximately 8 kbar which corresponds to a depth near the base of the crust. It was also noted that the evolved tholeiites have undergone some minor crustal contamination.

The interpretations just summarized can be combined with other geologic and geophysical data for the Snake River Plain to propose a possible relationship between the different types of volcanism and to illustrate the development of the Snake River Plain within the boundaries of the map area. The following synopsis is offered as a working hypothesis to be evaluated as additional geologic data become available. Only the volcanism will be considered; tectonic models for the origin of the Snake River Plain will not be presented.

Concurrent with the initial development of the Snake River Plain, basaltic magmas were generated at depths of 50 to 60 km. They rose rapidly from the site of origin, undergoing little fractionation en route, and were emplaced at the base of the crust in a linear zone along the long axis of the Plain. The crust acted as a barrier to further ascent for most magmas and consequently extrusive volcanism was minor at this time. Figure 60a diagrammatically illustrates this stage in the volcanic history.

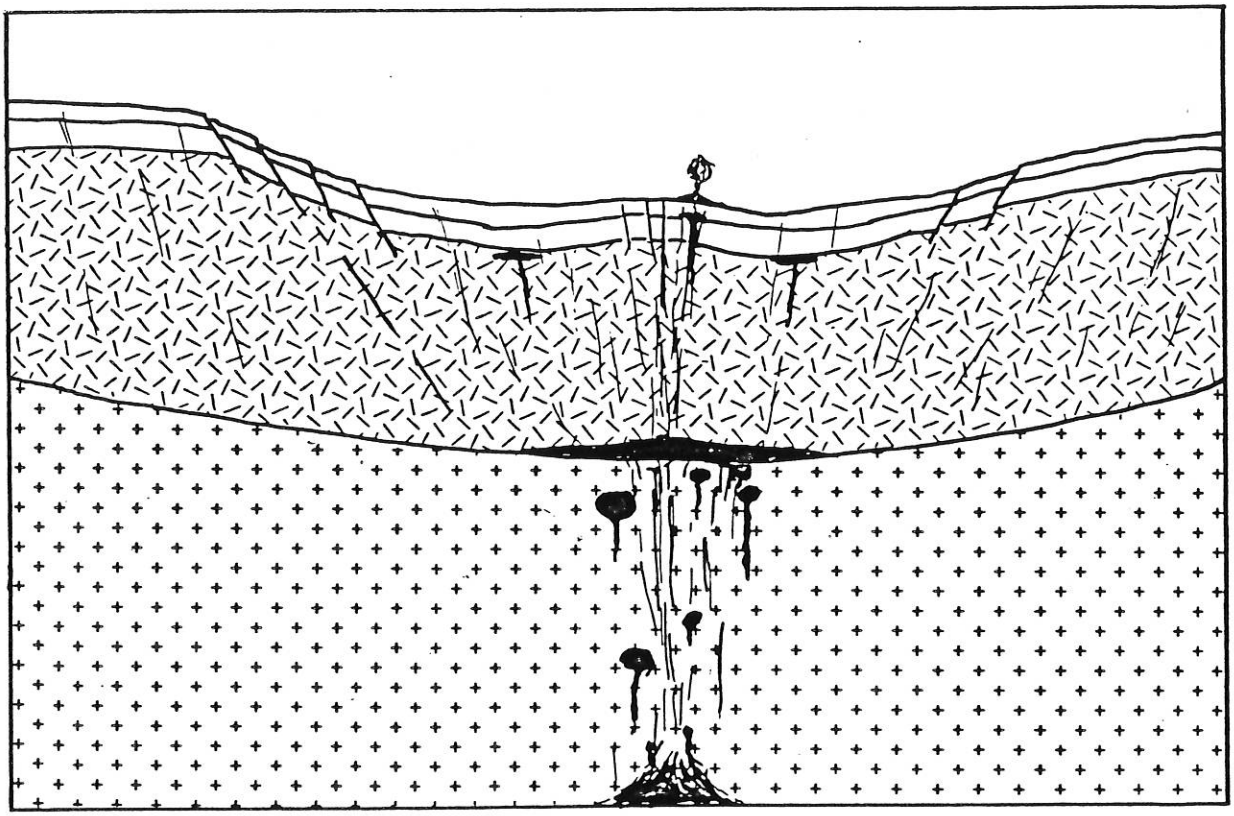


FIGURE 60a. Early stage in the development of the Snake River Plain. Basaltic magmas generated at depths of 50 to 60 km rise rapidly through the upper mantle to be trapped at the base of the crust.

The influx of hot mantle magmas raised the geotherms in the crust inducing partial melting of the crustal rocks forming silicic melts. The unmelted material (restite) acted as a barrier to the basaltic magmas beneath and therefore little or no mixing occurred between the silicic and mafic magmas. Both magmas, silicic and basaltic, subsequently underwent differentiation producing rhyolite and evolved tholeiite magma respectively. Figure 60b summarizes this pre-calsera stage.

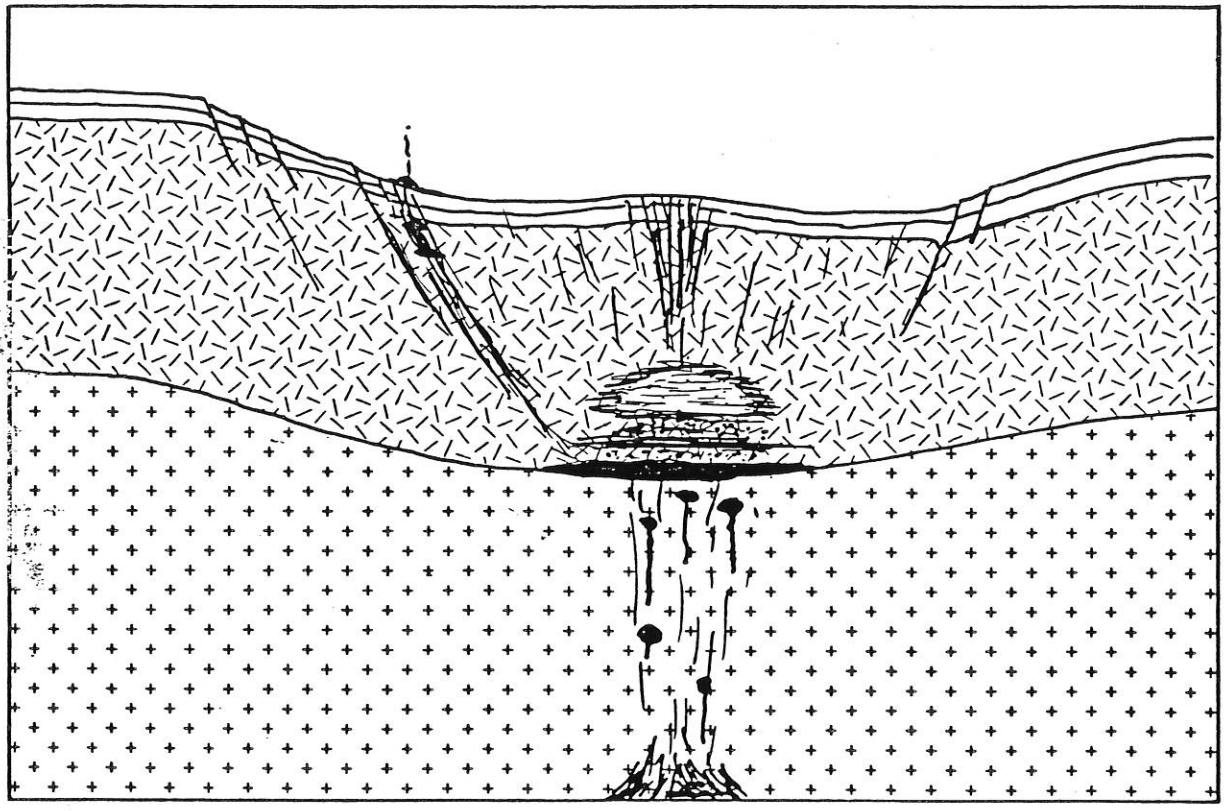


FIGURE 60b. Pre-caldera stage. Hot basaltic magmas trapped at the base of the crust induced melting of the overlying rocks. Large silicic magma reservoirs formed.

The formation of the large silicic magma reservoirs culminated in the eruption of voluminous, gas-charged ash-flows. The overall result of the formation and eruption of the silicic magmas was to thin the crust some 4 to 7 km, as indicated by the geophysical interpretations of Mabey (1978), and to allow basaltic magmas access to the surface. Thus commenced the stage of predominantly basaltic volcanism. The emptying of the crustal reservoirs also permitted the evolved tholeiite magmas to migrate to higher levels in the crust. Some were erupted at this time as evidenced by the evolved lavas low in the section of mafic lavas at Big Southern Butte. The caldera stage in the volcanic history is illustrated in Figure 60c.

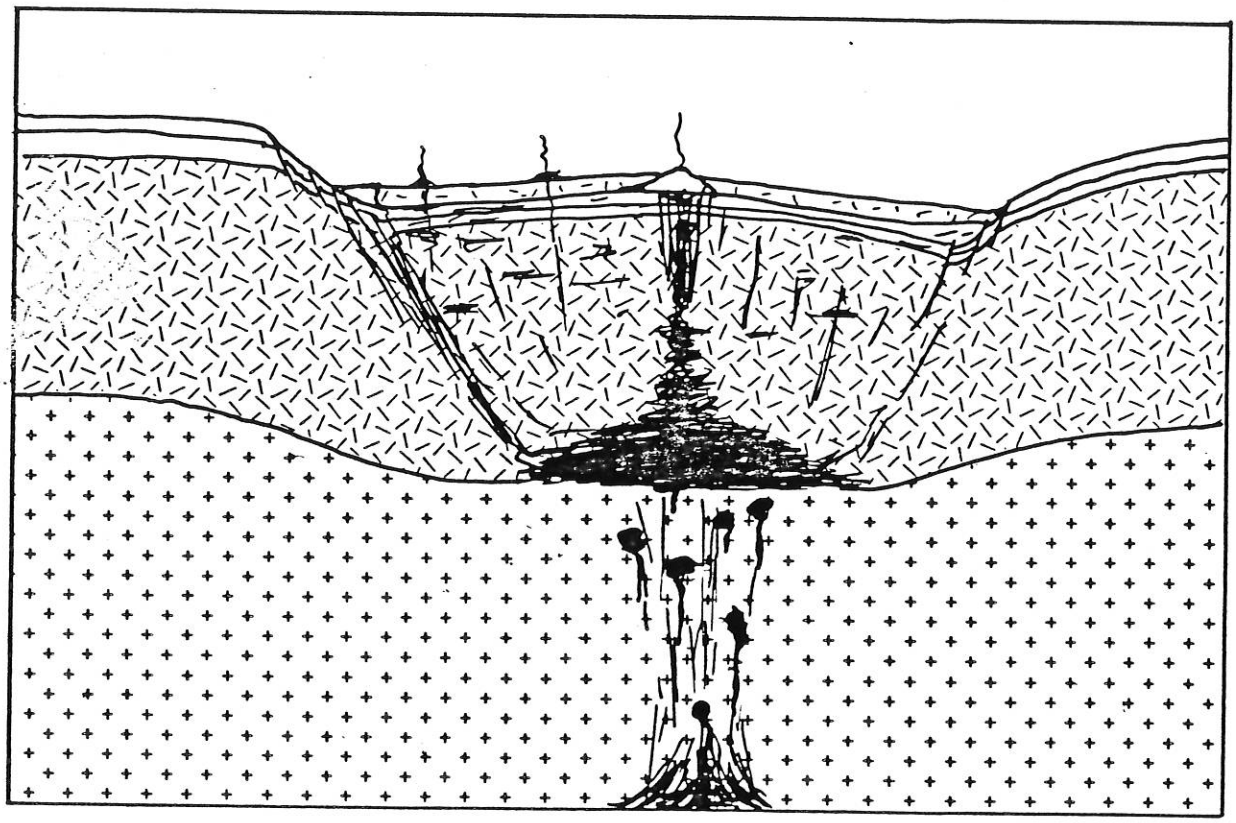


FIGURE 60c. Caldera stage. Eruption of voluminous, gas-charged ash-flows followed by basaltic volcanism.

Although the dominant volcanism at this time was basaltic, either pockets of silicic magma still existed in the crust or the potential for them to form was high. The emplacement of evolved tholeiite magmas higher in the crust contributed to addition melting and small silicic chambers developed, perhaps at depths of 10 to 16 km. These magmas gave rise to the rhyolite domes of Big Southern, Middle, and East Buttes. The close association of the evolved tholeiites and the rhyolites promoted some mixing to occur and selective exchange of chemical components to effect an "equilibration" between magmas, thus accounting for their trends as seen on AFM and variation diagrams. The rhyolite magmas were emplaced concurrently with the dominant basaltic volcanism to produce the general volcanic features seen today (Fig. 60d.).

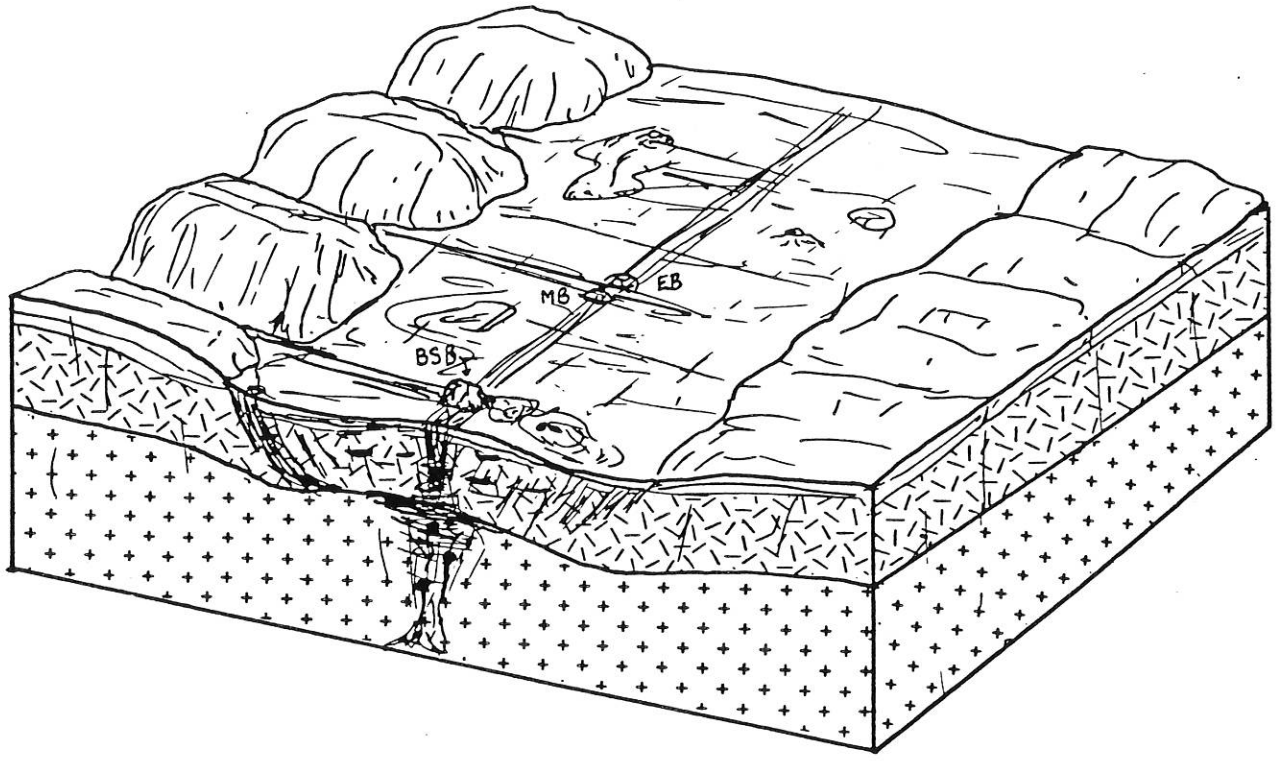


FIGURE 60d. Rhyolite domes were emplaced concurrently with the dominant basaltic volcanism producing the topography of the eastern Snake River Plain as seen today.

SUMMARY

Approximately 775 km^2 of volcanic terrain around and including Big Southern Butte, Middle Butte, and East Butte were mapped in order to document the geology of the area and to investigate the origin and localization of the buttes. Interpretations were based on detailed and reconnaissance mapping, petrography, major element chemistry, and rare earth element data.

Detailed mapping revealed that Big Southern Butte is a volcanic dome complex consisting of two coalesced cumulo domes and an elevated section of older basalt flows approximately 350 m thick. The occurrence of evolved tholeiite lavas within the basalt section was noted. The complex began its development as a laccolithic intrusion but because of its shallow emplacement broke through to the surface and continued its evolution by endogenous growth. The rhyolite of Big Southern Butte is aphyric and chemically mildly peralkaline. Low abundances of Sr and Ba and a large negative Eu anomaly were interpreted in light of available geologic data to indicate that the rhyolite originated by fractional crystallization from a silicic parent at depths in the range of 10 to 16 km. The parent magma was generated by partial melting of crustal rocks, probably intermediate to granitic in composition.

East Butte is interpreted to be a single cumulo dome which developed by endogenous growth. Phenocrysts of sanidine, quartz, and minor clinopyroxene set in a glassy to devitrified groundmass characterize the rhyolite. Reddish-brown inclusions, with a phenocryst assemblage of plagioclase, sanidine, forsteritic olivine, clinopyroxene, magnetite, and quartz rimmed with augite, are common in the rhyolite. They are

interpreted to be hybrid in origin and resulted from the mechanical mixing of a partially crystalline evolved tholeiite magma and the partially crystalline East Butte rhyolite magma. Geochemical data is consistent with the interpretation.

Middle Butte is an upraised block of basalt flows and is believed to have been elevated by the intrusion of viscous rhyolite still concealed beneath the butte. The basalt flows at Middle Butte are typical Snake River Plain olivine tholeiites.

Cedar Butte is a unique volcanic center in the map area; it is composed of a differentiated suite of evolved tholeiite lavas ranging from 54% SiO_2 to 67% SiO_2. A small amount of rhyolite (72% SiO_2) is also present but it is not part of the differentiated suite. Cedar Butte magma is thought to have formed by fractional crystallization of an olivine tholeiite magma at the base of the crust.

Twenty-five olivine tholeiite basalt flow fields of varying areal extent were delineated in the study area. The eruptive style characterizes basaltic plains volcanism, that is, extensive outpourings of very fluid lavas from low shield volcanoes. Pahoehoe is the dominant flow type.

The localization of volcanism in the study area is related to two dominant structural trends. One is NE-SW and coincides with the long axis of the ESRP; it is believed to be related to longitudinal fractures produced by the broad gentle arching of the Plain and/or a high thermal input along the axis at depth.

The common occurrence of rhyolite and evolved tholeiite lavas at Big Southern Butte, East Butte, and Cedar Butte was incorporated with other geologic data from the Snake River Plain to construct a model for

the volcanic history within the map area. The concentration of basaltic magmas at the base of the crust supplied heat to partially melt the overlying crustal rocks. This in turn led to the formation of large silicic reservoirs and eruption of voluminous ash-flows. The basalt magma trapped at the base of the crust differentiated to form the evolved tholeiite magma. The evolved tholeiite magmas migrated to higher levels in the crust where they encountered residual silicic melts and/or induced additional melting of crustal rocks of granitic composition. Some mixing of the two magmas also occurred, although this was not a major process. Ultimately the rhyolite domes formed from these small magma reservoirs. Their emplacement was concurrent with predominantly basaltic volcanism.

REFERENCES CITED

Armstrong, R.L., W.P. Leeman, and H.E. Malde, 1975, K-Ar dating, Quaternary and Neogene volcanic rocks of the Snake River Plain, Idaho: Amer. Jour. Sci., v. 275, p.225-251.

Arth, J.G., 1976, Behavior of trace elements during magmatic processes - a summary of theoretical models and their application: Jour. Research U.S. Geological Survey, v. 4, p. 41-47.

Axelrod, D.I., 1968, Tertiary flora and topographic history of the Snake River basin, Idaho: Geol. Soc. Amer. Bull., v. 79, p. 713-734.

Bryan, W.B., L.W. Finger, and F. Chayes, 1969, Estimating proportions in petrologic mixing equations by least squares approximation: Science, v. 163, p. 926-927.

Daly, R.A., 1925, The geology of Ascension Island: Proc. Amer. Acad. Arts and Sci., v. 60, n. 1, p. 1-80.

Eaton, G.P., R.L. Christiansen, H.M. Iyer, A.M. Pitt, D.R. Mabey, H.R. Blank, Jr., I. Zietz, and M.E. Gettings, 1975, Magma beneath Yellowstone National Park: Science, v. 188, p. 787-796.

Eichelberger, J.C., and R. Gooley, 1978, Evolution of silicic magma chambers and their relationship to basaltic volcanism: in The Earth's Crust, J.G. Heacock, ed., AGU Geophys. Monograph 20, p. 57-77.

Fenner, C.N., 1938, Contact relations between rhyolite and basalt on Gardiner River, Yellostone Park: Geol. Soc. Amer. Bull., v. 49, p. 1441-1484.

Fisher, R.V., 1966, Rocks composed of volcanic fragments and their classification: Earth-Science Reviews, v. 1, p. 287-298.

Gast, P.W., 1968, Trace element fractionation and the origin of tholeiitic and alkaline magma types: Geochim. Cosmochim. Acta, v. 32, p.1057-1086.

Greeley, R.C., 1977, Basaltic "plains" volcanism: in Greeley, R.C. and J.S. King, eds., Volcanism of the eastern Snake River Plain, Idaho: A comparative planetology guidebook, NASA CR-154621, 308 pp.

_____, 1976, Modes of emplacement of basaltic terrains and an analysis of mare volcanism in the Orientale Basin: Proc. Lunar Sci. Conf. 7th, p. 2747-2759.

_____ and J.S. King, 1975, Rift zones in the south-central Snake River Plain, Idaho (abs): Geol. Soc Amer. Abs. with Programs, v. 7, n. 5, p. 610-611.

Hamilton, W.C., 1965, Geology and petrogenesis of the Island Park Caldera of rhyolite and basalt, eastern Idaho: U.S. Geological Survey Prof. Paper 504-C, 37 pp.

Hildreth, W., 1979, The Bishop tuff: evidence for the origin of compositional zonation in silicic magma chambers: in Chapin, C.E., and W.E. Elston, eds., Ash-Flow Tuffs, Geol. Soc. Amer. Spec. Paper 180, in press.

Hill, D.P., 1963, Gravity and crustal structure in the western Snake River Plain, Idaho: Jour. Geophys. Res., v. 68, p. 5807-5819.

_____ , and L.C. Pakiser, 1967, Seismic refraction study of crustal structure between the Nevada Test Site and Boise, Idaho: Geol. Soc. Amer. Bull., v. 78, p. 685-704.

Karlo, J.F., 1977, The geology and bouguer gravity of the Hell's Half Acre area and their relation to volcano-tectonic processes within the Snake River Plain rift zone, Idaho: SUNY at Buffalo, Ph.D. dissertation, 152 pp.

Kirkham, V.R.D., 1931, Snake River downwarp: Jour Geology, V. 39, n. 5, p.456-487.

Kuntz, M.A., 1978a, Geologic map of the Arco-Big Southern Butte area, Butte, Blaine, and Bingham Counties, Idaho: U.S. Geological Survey Open-file Report 78-302.

_____ , 1978b, Geology of the Arco-Big Southern Butte area eastern Snake River Plain, and potential volcanic hazards to the radioactive waste management complex and other waste storage and reactor facilities at the Idaho National Engineering Laboratory, Idaho: U.S. Geological Survey Open-file Report 78-691.

_____ , 1977, Extensional faulting and volcanism along the Arco rift zone, eastern Snake River Plain, Idaho (abs): Geol. Soc. Amer. Abs. with Programs, v. 9, n. 6, p. 740-741.

LaPoint, P.J.I., 1977, Preliminary photogeologic map of the eastern Snake River Plain, Idaho: U.S. Geological Survey Map MF-850.

Leeman, W.P., 1974, Part I. Petrology of basaltic lavas from the Snake River Plain, Idaho and Part II. Experimental determination of partioning of divalent cations between olivine and basaltic liquid: Ph.D thesis, Univ. Oregon, 337 pp.

_____ and C.J. Vitaliano, 1976, Petrology of McKinney basalt, Snake River Plain, Idaho: Geol. Soc. Amer. Bull., v. 87, p. 1777-1792.

_____, C.J. Vitaliano, and M. Prinz, 1976, Evolved lavas from the Snake River Plain: Craters of the Moon National Monument, Idaho: Contr. Min. Petrol., v. 56, p. 35-60.

Mabey, D.R., 1978, Regional gravity and magnetic anomalies in the eastern Snake River Plain, Idaho: Jour. Research U.S. Geological Survey, v. 6, n. 5, p. 553-562.

_____ , 1976, Interpretation of a gravity profile across the western Snake River Plain, Idaho: Geology, v. 4, p. 53-55.

_____ , D.L. Peterson, and C.W. Wilson, 1975, Regional gravity and magnetic studies of the Snake River Plain (abs): Geol. Soc. Amer. Abs. with Programs, v. 7, n. 5, p. 624-625.

Malde, H.E., 1959, Fault zone along northern boundary of western Snake River Plain, Idaho: Science, v. 130, n. 3370, p. 272.

_____ , and H.A. Powers, 1962, Upper Cenozoic stratigraphy of western Snake River Plain, Idaho: Geol. Soc. Amer. Bull., v. 73, n. 10, p. 1197-1219.

_____ , _____ , and C.H. Marshall, 1963, Reconnaissance geologic map of west-central Snake River Plain, Idaho: U.S. Geological Survey Misc. Geol. Inv. Map I-373.

McIntyre, D.H., 1972, Cenozoic geology of the Reynolds Creek experimental water-shed, Owyhee County, Idaho: Idaho Bur. Mines and Geology Pamphlet 151, 115 pp.

Nichols J., and I.S.E. Carmichael, 1969, Peralkaline acid liquids-- a petrologic study: Contr. Min. Petrol., v. 20, p. 268-294.

Noble, D.C., M.K. Korringa, C.E. Hedge, and G.O. Riddle, 1972, Highly differentiated subalkaline rhyolite from glass mountain, Mono County, California: Geol. Soc. Amer. Bull., v. 83, n. 4, p. 1179-1184.

Norrish, K., and J.T. Hutton, 1969, An accurate x-ray spectrographic method for the analysis of a wide range of geologic samples: Geochim. Cosmochim. Acta, v. 33, p. 431-453.

Poldervaart, A., 1950, Correlation of physical properties and chemical composition in the plagioclase, olivine, and orthopyroxene series: Amer. Min., v. 35, p. 1067-1079.

Powers, H.A., 1960, A distinctive chemical characteristic of Snake River basalts of Idaho: U.S. Geological Survey Prof. Paper 400-B, p. 298.

Prinz, Martin, 1970, Idaho rift system, Snake River Plain, Idhao: Geol. Soc. Amer. Bull., v. 81, p. 941-948.

Reyer, E., 1888, Theoretische Geologie, Stutgart

Rice, A., and J.C. Eichelberger, 1976, Convection in rhyolite magma (abs): EOS Trans. AGU, v. 57, n. 12, p. 1024.

Ross, C.S., and R.L. Smith, Ash-flow tuffs: their origin, geologic relations, and identification: U.S. Geological Survey Prof. Paper 366, 81 pp.

Russell, I.C., 1902, Geology and water resources of the Snake River Plains of Idaho: U.S. Geological Survey Bull. 199, 192 pp.

Rutten, M.G., 1964, Formation of a plateau series from the example of Iceland: Bull. Volcanologique, v. 27, p. 93-111.

Schoen, R., 1974, III. Geology, in Robertson, J.B., R. Schoen, and J. Barraclough, Influence of liquid waste disposal on the geochemistry of water at the National Reactor Testing Station, Idaho: U.S. Geological Survey Open-file Report, IDO 22053, 231 pp.

Shapiro, L., 1975, Rapid analysis of silicate, carbonate, and phosphate rocks, revised edition: U.S. Geological Survey Bull. 1401, 76 pp.

Shaw, D.M., 1970, Trace element fractionation during anatexis: Geochim. Cosmochim. Acta, v. 34, p. 237-243.

Slemmons, D.E., 1962, Determination of volcanic and plutonic plagioclase using a three- or four-axis universal stage: Geol. Soc. Amer. Spec. Paper 69, 64 pp.

Spear, D.B., 1979, Evidence for mixing of rhyolite and basalt magmas at East Butte, eastern Snake River Plain, Idaho: Geol. Soc. Amer. Abs. with Programs, v. 11, n. 6, p. 303.

Stout, M.Z., 1975 Mineralogy and petrology of Quaternary lavas, Snake River Plain, Idaho and the cation distribution in natural titanomagnetite: Masters thesis, Univ. Calgary, 150 pp.

_____ , and J. Nicholls, 1977, Mineralogy and petrology of Quaternary lavas from the Snake River Plain, Idaho: Can. Jour. Earth Sci., v. 14, p. 2140-2156.

Stanley, W.D., J.E. Boehl, F.X. Bostick, and H.W. Smith, 1977, Geothermal significance of magnetotelluric sounding in the eastern Snake River Plain - Yellowstone region: Jour. Geophys. Res., v. 82, n. 17, p. 2501-2514.

Stearns, H.T., L.Crandall, and W.G. Steward, 1938, Geology and groundwater resources of the Snake River Plains in southeastern Idaho: U.S. Geological Survey Water Supply Paper 774, 268 pp.

Steiner, J.C., R.H. Jahns, and W.C. Luth, 1975, Crystallization of alkali feldspar and quartz in the haplogranite system $NaAlSi_3O_8$ - $KAlSi_3O_8$ - SiO_2 - H_2O at 4 Kb: Geol. Soc. Amer. Bull., v. 86, P. 83-98.

Stone, G.T., 1970, Highly evolved basaltic lavas in the western Snake River Plain, Idaho (abs): Geol. Soc. Amer. Abs. with Programs, v. 2, n. 7, p. 695-696.

_____ , 1967, Petrology of upper Cenozoic basalts of the western Snake River Plain, Idaho: Ph.D. dissertation, Univ. Colorado, 392 pp.

Thompson, R.N., 1972, Melting behavior of two Snake River lavas at pressures up to 35 Kb: Carnegie Inst. Wash. Yearbook, v. 75, p. 406-410.

Tilley, C.E., and R.N. Thompson, 1970, Melting and recrystallization relations of the Snake River basalts of southern Idaho, USA: Earth and Planetary Sci. Letters, v. 8, n. 1, p. 79-92.

Tröger, W.E., 1956, Optische Bestimmung der gesteinbildenden Minerale, Teil I Bestimmungstabellen, 3. Auflage: E. Schweizerbartische Verlagsbuchhandlung, 147 pp.

Tuttle, O.F., and N.L. Bowen, 1958, Origin of granite in light of experimental studies in the system NaAlSi308 - KAlSi308 - Si02 - H2O: Geol. Soc. Amer. Mem. 75, 153 pp.

Wager, L.R., E.A. Vincent, G.M. Brown, and J.D. Bell, 1965, Marscoite and related rocks of the western Red Hills complex, Isle of Skye: Phil. Trans. Roy. Soc. London, ser. A, v. 257, p. 273-307.

Walker, G.P.L., 1972, Compound and simple lava flows and flood basalts: Bull. Volcanologique, v. 35, p. 1-12.

Washington, H.S., 1926, Santorini eruption of 1925: Geol. Soc. Amer. Bull., v. 37, p. 349-384.

Wilcox, R.E., 1944, The rhyolite-basalt complex on Gardiner River, Yellowstone Park, Wyoming: Geol. Soc. Amer. Bull., v. 55, p. 1047-1080.

Williams, H.S., 1932, The history and character of volcanic domes: Univ. Calif. Dep. Geol. Sci. Bull., n. 21, p. 51-146.

Yoder, H.S., Jr., 1973, Contemporaneous basaltic and rhyolitic magmas: Amer. Min., v. 58, p. 153-171.

Zietz, I., F.P. Gilbert, and J.R. Kirby, Jr., 1978, Aeromagnetic map of Idaho: Color coded intensities: U.S. Geological Survey Geophysical Investigation Map GP-920.

APPENDIX A. Precision and accuracy of chemical analyses.

Major element data for this study was obtained by wet chemical rapid silicate analysis procedures (Shapiro, 1975) and x-ray fluorescence of fused sample disks (Norrish and Hutton, 1969). Most samples were run in duplicate and the average of the two runs reported. Some samples analyzed by the rapid method were used as secondary standards for the XRF analyses and as a check on accuracy. Also these secondary standards were used as a check between analysts.

In general both methods gave similar results for TiO_2, FeO^*, MnO, CaO, and K_2O; SiO_2 results from XRF were usually slightly lower than those obtained by the rapid method. Consequently the XRF SiO_2 were corrected relative to the rapid determinations. Owing to very low count rates for Al_2O_3 on XRF the data may or may not be accurate. Where possible Al_2O_3 data obtained by the rapid method were used as references for correction. All Na_2O and MgO results were obtained by atomic absorption and all P_2O_5 data by spectrophotometer. For the XRF analyses H_2O^+ and CO_2 were not determined, however the amount of volatiles can be related to the loss on ignition.

Analysis of sample BS-1 by the different methods.

	Rapid method					XRF				
	1[1]	2[2]	3[2]	mean	s.d.	1	2	3	mean	s.d.
SiO_2	76.22	75.94	76.02	76.06	.14	74.1	74.6	74.2	74.3	.2
TiO_2	.09	.10	.10	.10	.01	.09	.09	.09	.09	---
Al_2O_3	12.22	12.18	12.12	12.17	.05	11.7	12.2	11.8	12.2	.3
Fe_2O_3	1.17	1.31	1.24	1.24	.07	---	---	---	---	---
FeO	.72	.55	.63	.63	.09	1.72*	1.74*	1.75*	1.74*	.01
MnO	.04	.05	.05	.05	.01	.04	.04	.04	.04	---
MgO	.00	.00	.01	.00	.01	---	---	---	---	---
CaO	.47	.44	.48	.46	.02	.45	.48	.44	.46	.02
Na_2O	4.40	4.35	4.37	4.37	.03	---	---	---	---	---
K_2O	4.76	4.74	4.69	4.73	.04	4.73	4.75	4.74	4.74	.01
P_2O_5	.01	.00	.01	.01	.01					
H_2O^+	.30	.27	---	.29	.01					
CO_2	.01	.00	---	.01	.01					

Comparison of rapid method with XRF.

	R	XRF
SiO_2	76.06	74.3
TiO_2	.10	.09
Al_2O_3	12.17	12.2
FeO*	1.75	1.74
MnO	.05	.04
CaO	.46	.45
K_2O	4.73	4.74

1 - D. Borden analyst

2 - D. Spear analyst

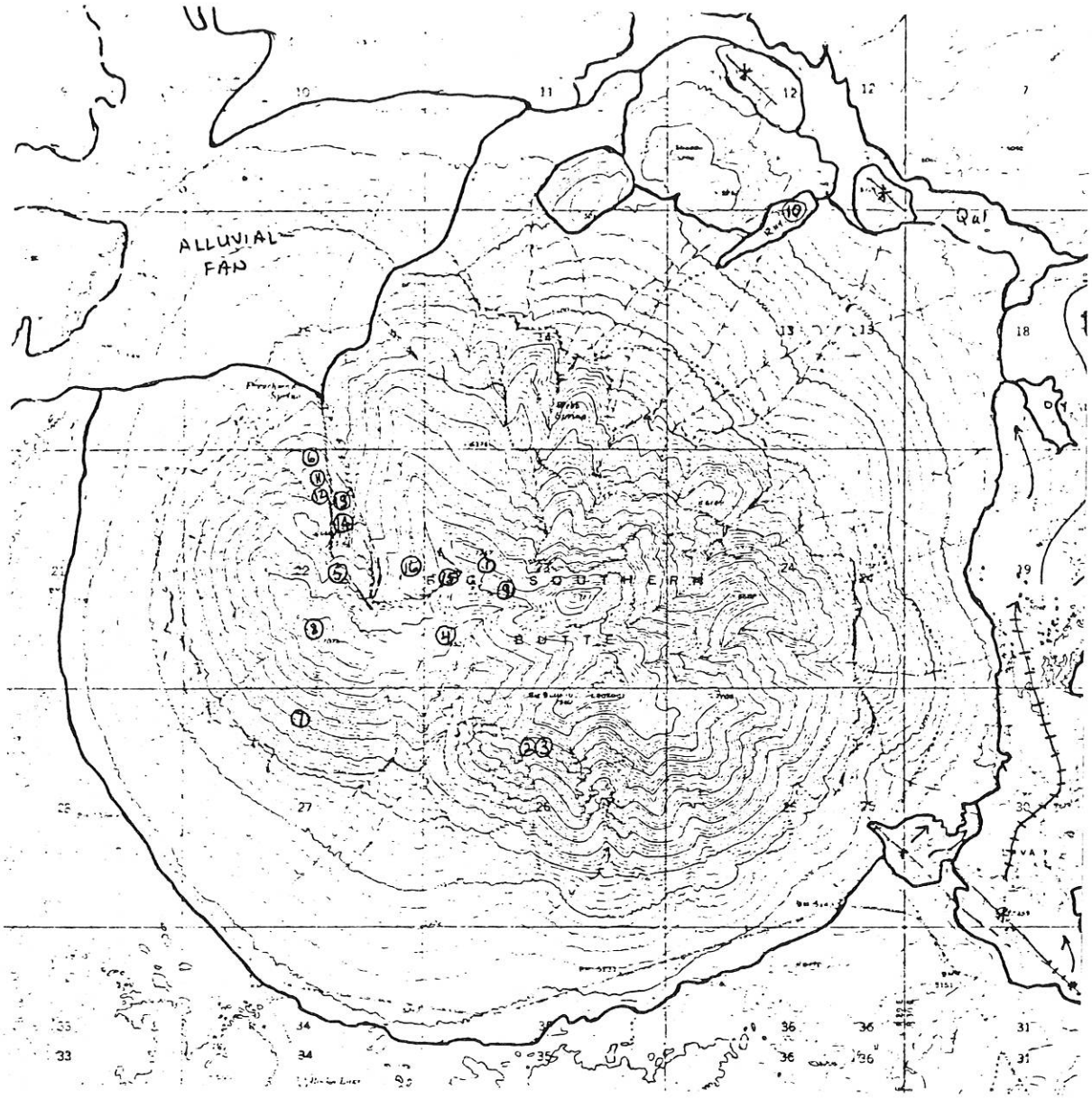
XRF - D. Spear analyst

APPENDIX B. Location and description of samples from Big Southern Butte.

SAMPLE	FIELD NO.	LOCATION AND DESCRIPTION	METHOD	ANALYST
BS-1	BS-OBS	see map; obsidian	Rapid	D. Borden
BS-2	76SBS15a	see map; sugary rhyolite	Rapid	D. Spear
BS-3	76SBS15b	see map; purple, flow-layered rhyolite	Rapid	D. Spear
BS-4	76SBS35	see map; pale purple massive rhyolite	Rapid	D. Spear
BS-5	76SBS37	see map; white sugary rhyolite	Rapid	D. Spear
BS-6	76SBS38	see map; white massive rhyolite	Rapid	D. Spear
BS-7	76SBS50	see map; white massive rhyolite	Rapid	D. Borden
BS-8	77SBS7	see map; white massive rhyolite	XRF	D. Spear
BS-9	77SBS21	dike in roadcut, see map; light gray massive rhyolite	Rapid	D. Borden
BS-10	77SMF27	see map; flow-layered rhyolite	XRF	D. Spear
BS-11	inc-1	see map; basaltic inclusion	XRF	D. Spear
BS-12	inc-2	see map; basaltic inclusion	XRF	D. Spear
BS-13	78SBS6	see map; dense, red evolved tholeiite lava	XRF	D. Spear
BS-14	78SBS5	see map; glassy, black evolved tholeiite lava	XRF	D. Spear
BS-15	78SBS2	see map; well-crystallized evolved tholeiite lava, olivine and plagioclase phenocrysts	XRF	D. Spear
BS-16	77SBS11	see map; basalt from near rhyolite dike in basalt section	XRF	D. Spear
NOB		location unknown; obsidian	Rapid	N. Hafty[2]
KFB	S75M188[1]	location unknown; flow-layered rhyolite	Rapid	Z. Hamlin[2]
K-S	S75M189[1]	location unknown; sugary rhyolite	Rapid	Z. Hamlin[2]

1 - Mel Kuntz, U.S.G.S.

2 - U.S.G.S.



Analysts from Table 4:

1. D. Borden
2. U.S.G.S. analysis (from Leeman, 1974)
3. Z. Hamlin, U.S.G.S.

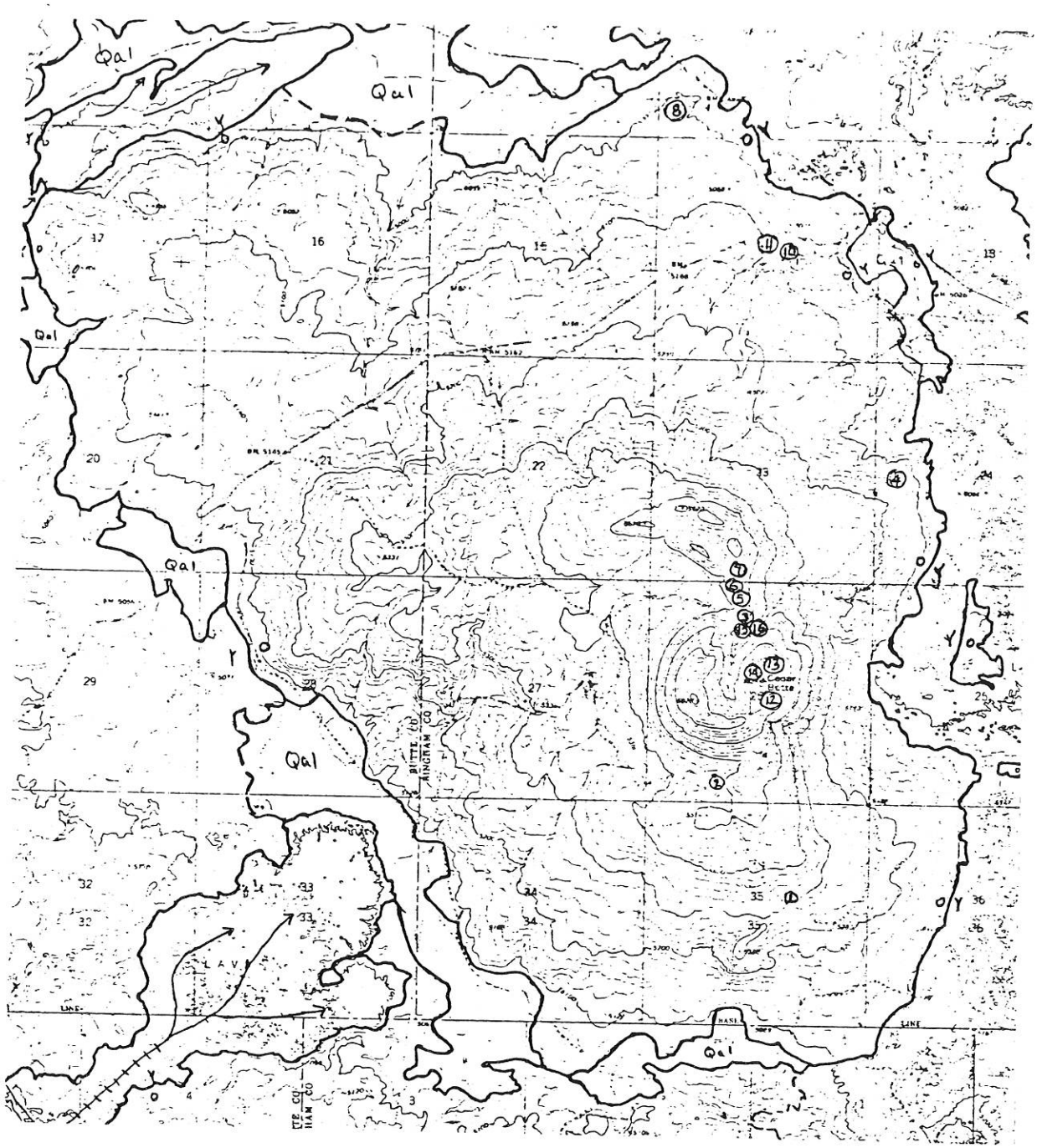
all others - D. Spear

APPENDIX C. Location and description of samples from Cedar Butte.

SAMPLE	FIELD NO.	DESCRIPTION AND LOCATION (map)	METHOD	ANALYST
CB-1	77SCB3	dense ferrobasalt, ol-pl-mt	Rapid	D. Borden
CB-2	78SCB12	ferrobasalt flow, ol-pl-mt-(cpx)	XRF	D. Spear
CB-3	78SCB6	dike rock; ol-pl-cpx-mt	XRF	D. Spear
CB-4	78SCB1	flow; ol-pl-cpx-mt	XRF	D. Spear
CB-5	77SCB1	arcuate vent; ol-feld(2)-cpx-mt	XRF	D. Spear
CB-6	77SCB2	arcuate vent; ol-feld(2)-cpx-mt	Rapid	D. Borden
CB-7	78SCB8	arcuate vent, ol-feld(2)-cpx-mt	XRF	D. Spear
CB-8	76SCB1	latite flow; fa-san-cpx-mt	Rapid	D. Borden
CB-9	78SBS24	from Big Southern Butte; fa-san-cpx-mt	XRF	D. Spear
CB-10	76SCB3	latite flow; fa-san-cpx-mt	XRF	D. Spear
CB-11	76SCB2	latite flow; fa-san-cpx-mt	Rapid	D. Borden
CB-12	78SCB2	latite glass; fa-san-cpx-mt	XRF	D. Spear
CB-13	78SCB3	latite glass; fa-san-cpx-mt	XRF	D. Spear
CB-14	78SCB13	latite glass; fa-san-cpx-mt	XRF	D. Spear
CB-15	78SCB5	rhyolite from dike, minor amounts of included mafic rock; san-qz	XRF	D. Spear
CB-16	78SCB4	similar to CB-15	XRF	D. Spear
K-CB	S75M172[1]	ol-pl-cpx-mt	Rapid	Z. Hamlin[2]

1 - Mel A. Kuntz, U.S.G.S.

2 - U.S.G.S.


Qal
Qal
Qal
Qal
Qal
Qal
BUTTE CO
KINGMAN CO
LINE
LINE

APPENDIX D. Location of basalt samples chosen for chemical analysis.

SAMPLE	FIELD NO.	LOCATION	METHOD	ANALYST
B-1	76SNR1	SE 1/4, sec. 5, T.1S, R.30E, Rock Butte quad; basalt from South Robbers vent area	Rapid	D. Spear
B-2	77SMF43	NE 1/4, sec. 31, T.1N, R.30E, Scoville quad; basalt from eastern margin of North Robbers flow	Rapid	D. Borden
B-3	S75M173[1]	basalt from South Robbers flow	Rapid	Z. Hamlin[2]
B-4	76SCG5	S 1/2, sec. 13, T.1N, R.30E; basalt from Cerro Grande vent area	Rapid	D. Spear
B-5	76SMF21	SW 1/4, sec. 15, T.2N, R.30E; Atomic City quad; basalt from the northern margin of Cerro Grande flow	XRF	D. Spear
B-6	S75M166a[1]	basalt from the Cerro Grande flow	Rapid	Z. Hamlin[2]
B-7	78SMF19	SE 1/4, sec. 21, T.1N, R.32E; olivine-rich basalt of Table Legs flow	XRF	D. Spear
B-8	78SMF23	NW 1/4 SW 1/4, sec. 7, T.1N, R.32E; plagioclase-rich basalt of Table Legs flow	XRF	D. Spear
B-9	S75M229a[1]	basalt of the Table Legs vent	Rapid	Z. Hamlin[2]
B-10	78SMF34	S 1/2, sec. 31, T.1S, R.30E; basalt of the Rock Corral Butte flow	XRF	D. Spear
B-11	78SMF37	SW 1/4, sec. 33, T.1S, R.30E; basalt from skylight of lava tube	XRF	D. Spear
B-12	77SMF18	T. 2N, R.31E, Sec. 36; Atomic City quad; dense basalt from old vent	XRF	D. Spear
B-13	WPL-88[3]	T.2N, R.30E, Sec.11	Micro-probe	W. Leeman
B-14	S75M225[1]	basalt from vent 1 km south of Middle Butte	Rapid	Z. Hamlin[2]

SAMPLE	FIELD NO.	LOCATION	METHOD	ANALYST
B-15	S75M223a[1]	basalt from Little Butte flow	Rapid	Z. Hamlin[2]
EB-9	76SMF17	NW 1/4, NE 1/4, sec. 13, T.2N, R.32E	XRF	D. Spear
EB-10	78SMF16	NE 1/4, SW 1/4, sec. 34, T.2N, R.32E	XRF	D. Spear
MB-1	76SMB-1	SW 1/4, sec. 17. T.2N, R.32E; very dense sample from Middle Butte	XRF	D. Spear
MB-2	70-35[3]	sample from Middle Butte	Rapid	U.S.G.S.

1 - Mel A. Kuntz, U.S.G.S.

2 - U.S.G.S.

3 - from Leeman (1974)

APPENDIX E. Trace element analyses of volcanic rocks within the study area.

	BSB		EB	CB	MB	B					
	KFB	KS	KEB	KCB	MB2	B-3	B-6	B-9	B13	B14	B15
Sr	4	2	9	230	262	190	240	280	340	250	260
Ba	8	10	110	1600	---	150	350	270	---	240	240
Nb	170	180	140	65	---	11	24	35	---	21	25
Zr	140	240	210	1700	209	110	150	180	267	180	140
Ni	---	---	---	5	160	64	56	55	57	41	65
Cr	---	---	---	3	---	230	170	100	189	110	170

Samples MB-2 and B-13 are from Leeman, 1974, Table 41 (SRU-17 and SRU-10 respectively); determined by XRF.

All other samples were determined by semiquantitative spectographic analysis, N. Rait analyst, U.S.G.S., 1977. These results were kindly made available to me by Mel A. Kuntz of the U.S.G.S.

Key to samples:

BSB - Big Southern Butte
EB - East Butte
CB - Cedar Butte
MB - Middle Butte
B - Basalts